Echoes of contamination: Investigating heavy metal exposure at Wadi Faynan 100, Jordan

by

Kasiah Ruddell

A thesis
presented to the University of Waterloo
in fulfillment of the
thesis requirement for the degree of
Master of Arts
in
Public Issues Anthropology

Waterloo, Ontario, Canada, 2024

© Kasiah Ruddell 2024

Author's Declaration

I hereby declare that I am the sole author of this thesis. This is a true copy of the thesis, including any required final revisions, as accepted by my examiners.

I understand that my thesis may be made electronically available to the public.

Abstract

Located in southern Jordan, Wadi Faynan was once a center for copper mining, smelting, and trade during the Early Bronze Age (EBA). The legacy of pollution in Wadi Faynan is visible in the contemporary landscape in the form of spoil tips and over 250 copper mines. The largest and possibly most significant EBA site in Wadi Faynan is Wadi Faynan 100 (WF100), which dates to EBA Ib (3300-3000 BCE) and has clear evidence of copper production including copper ores, slag, and copper casting molds. This research employed laser ablation-inductively coupled plasma-mass spectrometry (LA-ICP-MS) to measure trace element concentrations of lead (Pb), cadmium (Cd), and arsenic (As) in human enamel from WF100 to determine if copper production during EBA Ib introduced heavy metal toxicity into the population. The sample consisted of 29 human teeth divided into three groups representative of different early life stages: first molars, premolars, and third molars. Although seven samples were excluded from the main analysis, the others all had trace amounts of Pb, Cd, and As. The samples were categorized into four different groupings for Pb based on their pattern of exposure across the growth layers of enamel: stable exposure, variable exposure, increasing exposure, and decreasing exposure. For Cd and As, each sample was identified as having concentrations above or below their limit of detections. Examination of the distribution of these heavy metals revealed inter- and intra-individual variation in exposure providing insight into participation in copper production activities and possible mobility patterns practiced at WF100.

Acknowledgements

Moving to another country for a short sixteen months to complete this program has been one of the most challenging and rewarding adventures of my life. I would not have been able to finish this program without the support and guidance of my professors, friends, and family. First and foremost, I would like to thank my fantastic advisor, Dr. Alexis E. Dolphin who has helped guide me through my research. Thank you for answering all my questions and being patient with me as I learned something entirely new.

Thank you to the Barqa Landscape Project (BLP) and its Director Dr. Russell Adams for the opportunity to work on the Wadi Faynan 100 materials, which are on loan from the BLP to the ACE Biolab. The Barqa Project was funded by SSHRC Insight grant 435-2018-0944 and was conducted under permits (2019 and 2023) to Dr. Adams from the Department of Antiquities of Jordan. Thanks also to the staff and student excavators of the Barqa Project for their hard work and dedication in the recovery of these remains, and to Department of Antiquities staff in supporting this essential work.

Thank you to the Department of Earth and Environmental Sciences for allowing me to use the LA-ICP-MS instrument. I extend my deepest gratitude to Dr. Chris Yakymchuk for working his magic with the laser.

To my committee member, Dr. Alexis E. Dolphin, Dr. Chris Yakymchuk, and Dr. John Grattan, I appreciate the time and effort you put into the feedback on my research. Thank you for helping me improve my thesis and do the Wadi Faynan 100 individuals justice.

To the Department of Anthropology and Dr. Seçil Dağtaş, Dr. Jennifer Liu, and Dr. Alexis E. Dolphin, thank you for helping me navigate the coursework, learn new things, and all the invigorating class discussions. Thank you, Jeffrey Coffin, for teaching me how to prepare my samples and always being willing to answer my thousands of questions as I sorted through bags and bags of teeth.

I am thankful for the financial support provided by the Faculty of Arts and Department of Anthropology through the International Master's Award of Excellence and Anthropology Graduate Scholarship. I would like to express my heartfelt gratitude for the generous support provided by the family of Iris Yuzdepski through the Iris Yuzdepski Memorial Entrance Scholarship and the Iris Yuzdepski Graduate Memorial Award. I also extend my gratitude to the family of Sally Weaver for granting me the Sally Weaver Award. The financial support I have received over the course of the last 16 months had a profound impact on my ability to complete my master's degree.

To my partner, forever adventure companion, and best friend, Kevin Russell, I would never have been able to do this without you. Through your love and unwavering belief in me, I have been able to do something I thought was forever out of reach. Thank you for doing the hard things so that I could pursue my passion. I love doing life with you and am excited for our next adventure.

To my father-in-law, William Russell, and mother-in-law, Michelle Russell whose love and support allowed my family and I to live internationally for sixteen months. Thank you for being my family and helping me follow my dreams.

Finally, I extend the utmost gratitude to the Wadi Faynan 100 individuals, who were the focus of my research. Without you, this research would not have been possible. Thank you for allowing me to tell part of your story.

Table of Contents

Author's Declaration ii

Abstract iii

Acknowledgements iv

List of Figures ix

List of Tables xx

Chapter 1: Introduction 1

1.1 | Research Purpose, Scope, and Theoretical Foundations 1

1.2 | Working with Human Remains: Public Issues and Ethical Considerations 6

Chapter 2: Background 11

2.1 | Trace Element Analysis 11

2.1.1 | Trace Elements and the Body 12

2.1.1.1 | Heavy Metals and the Body 13

2.1.2 | Human Dentition 15

2.1.2.1 | Tooth Growth and Development 16

2.1.2.2 | Chemical Composition of Dental Tissues 18

2.1.3 | LA-ICP-MS Methodology 20

2.1.3.1 | Benefits 21

2.1.3.2 | Limitations 22

2.1.4 | Diagenesis 23

2.2 | Social and Archaeological Context 24

2.2.2 | Early Bronze Age Society and Copper Production 25

2.2.1 | Legacies of Pollution 27

2.2.3 | Wadi Faynan 100 Site Description 30

Chapter 3: Materials and Methods 33

3.1 | Sample Selection and Preparation 33

3.2 | LA-ICP-MS Instrumentation 35

3.3 | Data Reduction and Analysis 36

3.4 | Analysis of Diagenesis 37

Chapter 4: Results **41**

4.1 | Analysis of Diagenesis **41**

4.2 | Temporal Variation of Lead Exposure During Early Life **43**

4.2.1 | First Molars **46**

4.2.1.1 | Temporal Variation of Lead (~30 weeks in utero - ~3 years old) *46*

4.2.2 | Premolars **51**

4.2.2.1 | Temporal Variation of Lead (~1.8-2.8 to ~5-6 years old) *51*

4.2.3 | Third Molars **54**

4.2.3.1 | Temporal Variation of Lead (~8 years to ~11 years old) *54*

4.3 | Temporal Variation of Cadmium and Arsenic Exposure During Early Life **59**

4.3.1 | Temporal Variation of Cadmium and Arsenic in First Molars (~30 weeks *in utero* to ~3 years old) **61**

4.3.2 | Temporal Variation of Cadmium and Arsenic in Premolars (~1.8-2.8 to ~5-6 years old) **69**

4.3.3 | Temporal Variation of Cadmium and Arsenic in Third Molars (~8 to ~11 years old) **75**

Chapter 5: Discussion **85**

5.1 | Patterns of Variation Over Time **85**

5.1.1 | Stable Exposure Over Time **85**

5.1.2 | Variable Exposure Over Time **86**

5.1.3 | Increasing Exposure Over Time **86**

5.1.4 | Decreasing Exposure Over Time **86**

5.1.5 | Cadmium and Arsenic Exposure Over Time **87**

5.2 | Previous Studies in Wadi Faynan **87**

5.3 | Inter- and Intraindividual Variation Across Time **92**

5.2 | Limitations and Future Directions **94**

Chapter 6: Conclusion **96**

References **97**

Appendix A: Heavy Metals and the Body **111**

A.1 | Lead and the Body **111**

A.2 | Cadmium and the Body **112**

A.3 | Arsenic and the Body **113**

Appendix B: Dentine Development and Chemical Composition 115

Appendix C: Dental Pathology and Non-Metrics 118

C.1 | Dental Pathology 118

C.1 | Non-Metric Traits 119

Appendix D: Early Bronze Age Society and Copper Production 122

List of Figures

Figure 1 | The southern Levant (above) and the location of Wadi Faynan in relation to other significant archaeological sites in the region (below) (Barker et al. 2007: 228). 2

Figure 2 | General structure of teeth (Hillson 2012: 9). 16

Figure 3 | Diagram of a LA-ICP-MS instrument (Barbosa and Sussulini 2019: 48). 21

Figure 4 | Location of Wadi Faynan between Wadi 'Arabah and the Mountains of Edom and in relation to other significant archaeological sites in the Faynan region (Barker et al. 2007: 229). 25

Figure 5 | Egyptian depiction of smelting using a crucible and blowpipes from above. Saqqara, tomb of Mereruka, 6th dynasty, 2450-2350 BCE (Hauptmann 2007: 220). 27

Figure 6 | Site plan of Wadi Faynan 100 (Adams et al. 2023: 2). 32

Figure 7 | M101 after LA-ICP-MS. Rectangle indicates an area identified as affected by interference from the Crystalbond adhesive and/or epoxy resin that corresponds to the simultaneous fluctuation of Pb, U, La, Cu, and Mn that occurs at ~1050 days in Figure 8. 39

Figure 8 | Concentrations of Pb, U, La, Cu, and Mn along ablation transect of M101. Areas highlighted in light gray represent potential postmortem alteration. MTC for U = 0.05 ppm; MTC for La = 0.01 ppm. 40

Figure 9 | Concentrations of Pb, U, La, Cu, and Mn along ablation transect of M309. Areas highlighted in light gray represent potential postmortem alteration. MTC for U = 0.05 ppm; MTC for La = 0.01 ppm. 42

Figure 10 | Concentration of Pb along ablation transect of M111 enamel. Maximum concentration indicated. Classified as (1) stable over time. Areas highlighted in light gray represent potential postmortem alteration and are excluded from analysis. 47

Figure 11 | Concentration of Pb along ablation transect of M101 enamel. Maximum concentration indicated. Classified as (2) variable over time. Areas highlighted in light gray represent potential postmortem alteration and are excluded from analysis. 47
Figure 12 | Concentration of Pb along ablation transect of M102 enamel. Maximum concentration indicated. Classified as (2) variable over time. Areas highlighted in light gray represent potential postmortem alteration and are excluded from analysis. 48
Figure 13 | Concentration of Pb along ablation transect of M103 enamel. Maximum concentration indicated. Classified as (2) variable over time. Areas highlighted in light gray represent potential postmortem alteration and are excluded from analysis. 48
Figure 14 | Concentration of Pb along ablation transect of M104 enamel. Maximum concentration indicated. Classified as (4) decreasing over time. Areas highlighted in light gray represent potential postmortem alteration and are excluded from analysis. 49
Figure 15 | Concentration of Pb along ablation transect of M106 enamel. Maximum concentration indicated. Classified as (4) decreasing over time. Areas highlighted in light gray represent potential postmortem alteration and are excluded from analysis. 49
Figure 16 | Concentration of Pb along ablation transect of M108 enamel. Maximum concentration indicated. Classified as (4) decreasing over time. Areas highlighted in light gray represent potential postmortem alteration and are excluded from analysis. 50
Figure 17 | Concentration of Pb along ablation transect of M109 enamel. Maximum concentration indicated. Classified as (4) decreasing over time. Areas highlighted in light gray represent potential postmortem alteration and are excluded from analysis. 50

Figure 18 | Concentration of Pb along ablation transect of PM01 enamel. Maximum concentration indicated. Classified as (2) variable over time. Areas highlighted in light gray represent potential postmortem alteration and are excluded from analysis. 51
Figure 19 | Concentration of Pb along ablation transect of PM03 enamel. Maximum concentration indicated. Classified as (3) increasing over time. Areas highlighted in light gray represent potential postmortem alteration and are excluded from analysis. 52
Figure 20 | Concentration of Pb along ablation transect of PM02 enamel. Maximum concentration indicated. Classified as (4) decreasing over time. Areas highlighted in light gray represent potential postmortem alteration and are excluded from analysis. 52
Figure 21 | Concentration of Pb along ablation transect of PM05 enamel. Maximum concentration indicated. Classified as (4) decreasing over time. Areas highlighted in light gray represent potential postmortem alteration and are excluded from analysis. 53
Figure 22 | Concentration of Pb along ablation transect of PM06 enamel. Maximum concentration indicated. Classified as (4) decreasing over time. Areas highlighted in light gray represent potential postmortem alteration and are excluded from analysis. 53
Figure 23 | Concentration of Pb along ablation transect of M301 enamel. Maximum concentration indicated. Classified as (1) stable over time. Areas highlighted in light gray represent potential postmortem alteration and are excluded from analysis. 54
Figure 24 | Concentration of Pb along ablation transect of M303 enamel. Maximum concentration indicated. Classified as (1) stable over time. Areas highlighted in light gray represent potential postmortem alteration and are excluded from analysis. 55

Figure 25 | Concentration of Pb along ablation transect of M306 enamel. Maximum concentration indicated. Classified as (1) stable over time. Areas highlighted in light gray represent potential postmortem alteration and are excluded from analysis. 55
Figure 26 | Concentration of Pb along ablation transect of M311 enamel. Maximum concentration indicated. Classified as (1) stable over time. Areas highlighted in light gray represent potential postmortem alteration and are excluded from analysis. 56
Figure 27 | Concentration of Pb along ablation transect of M304 enamel. Maximum concentration indicated. Classified as (2) variable over time. Areas highlighted in light gray represent potential postmortem alteration and are excluded from analysis. 56
Figure 28 | Concentration of Pb along ablation transect of M308 enamel. Maximum concentration indicated. Classified as (2) variable over time. Areas highlighted in light gray represent potential postmortem alteration and are excluded from analysis. 57
Figure 29 | Concentration of Pb along ablation transect of M310 enamel. Maximum concentration indicated. Classified as (2) variable over time. Areas highlighted in light gray represent potential postmortem alteration and are excluded from analysis. 57
Figure 30 | Concentration of Pb along ablation transect of M302 enamel. Maximum concentration indicated. Classified as (4) decreasing over time. Areas highlighted in light gray represent potential postmortem alteration and are excluded from analysis. 58
Figure 31 | Concentration of Pb along ablation transect of M312 enamel. Maximum concentration indicated. Classified as (4) decreasing over time. Areas highlighted in light gray represent potential postmortem alteration and are excluded from analysis. 58

Figure 32 | Concentration of Cd along ablation transect of M101 enamel. LOD indicated by blue line. Areas highlighted in light gray represent potential postmortem alteration and are excluded from analysis. 61
Figure 33 | Concentration of Cd along ablation transect of M102 enamel. LOD indicated by blue line. Areas highlighted in light gray represent potential postmortem alteration and are excluded from analysis. 62
Figure 34 | Concentration of Cd along ablation transect of M103 enamel. LOD indicated by blue line. Areas highlighted in light gray represent potential postmortem alteration and are excluded from analysis. 62
Figure 35 | Concentration of Cd along ablation transect of M104 enamel. LOD indicated by blue line. Areas highlighted in light gray represent potential postmortem alteration and are excluded from analysis. 63
Figure 36 | Concentration of Cd along ablation transect of M106 enamel. LOD indicated by blue line. Areas highlighted in light gray represent potential postmortem alteration and are excluded from analysis. 63
Figure 37 | Concentration of Cd along ablation transect of M108 enamel. LOD indicated by blue line. Areas highlighted in light gray represent potential postmortem alteration and are excluded from analysis. 64
Figure 38 | Concentration of Cd along ablation transect of M109 enamel. LOD indicated by blue line. Areas highlighted in light gray represent potential postmortem alteration and are excluded from analysis. 64

Figure 39 | Concentration of Cd along ablation transect of M111 enamel. LOD indicated by blue line. Areas highlighted in light gray represent potential postmortem alteration and are excluded from analysis. 65
Figure 40 | Concentration of As along ablation transect of M101 enamel. LOD indicated by blue line. Areas highlighted in light gray represent potential postmortem alteration and are excluded from analysis. 65
Figure 41 | Concentration of As along ablation transect of M102 enamel. LOD indicated by blue line. Areas highlighted in light gray represent potential postmortem alteration and are excluded from analysis. 66
Figure 42 | Concentration of As along ablation transect of M104 enamel. LOD indicated by blue line. Areas highlighted in light gray represent potential postmortem alteration and are excluded from analysis. 66
Figure 43 | Concentration of As along ablation transect of M106 enamel. LOD indicated by blue line. Areas highlighted in light gray represent potential postmortem alteration and are excluded from analysis. 67
Figure 44 | Concentration of As along ablation transect of M108 enamel. LOD indicated by blue line. Areas highlighted in light gray represent potential postmortem alteration and are excluded from analysis. 67
Figure 45 | Concentration of As along ablation transect of M109 enamel. LOD indicated by blue line. Areas highlighted in light gray represent potential postmortem alteration and are excluded from analysis. 68

Figure 46 | Concentration of As along ablation transect of M111 enamel. LOD indicated by blue line. Areas highlighted in light gray represent potential postmortem alteration and are excluded from analysis. 68
Figure 47 | Concentration of As along ablation transect of M103 enamel. LOD indicated by blue line. Areas highlighted in light gray represent potential postmortem alteration and are excluded from analysis. 69
Figure 48 | Concentration of Cd along ablation transect of PM01 enamel. LOD indicated by blue line. Areas highlighted in light gray represent potential postmortem alteration and are excluded from analysis. 70
Figure 49 | Concentration of Cd along ablation transect of PM06 enamel. LOD indicated by blue line. Areas highlighted in light gray represent potential postmortem alteration and are excluded from analysis. 70
Figure 50 | Concentration of Cd along ablation transect of PM06 enamel. LOD indicated by blue line. Areas highlighted in light gray represent potential postmortem alteration and are excluded from analysis. 71
Figure 51 | Concentration of Cd along ablation transect of PM06 enamel. LOD indicated by blue line. Areas highlighted in light gray represent potential postmortem alteration and are excluded from analysis. 71
Figure 52 | Concentration of Cd along ablation transect of PM06 enamel. LOD indicated by blue line. Areas highlighted in light gray represent potential postmortem alteration and are excluded from analysis. 72

Figure 53 | Concentration of As along ablation transect of PM01 enamel. LOD indicated by blue line. Areas highlighted in light gray represent potential postmortem alteration and are excluded from analysis. 72
Figure 54 | Concentration of As along ablation transect of PM02 enamel. LOD indicated by blue line. Areas highlighted in light gray represent potential postmortem alteration and are excluded from analysis. 73
Figure 55 | Concentration of As along ablation transect of PM03 enamel. LOD indicated by blue line. Areas highlighted in light gray represent potential postmortem alteration and are excluded from analysis. 73
Figure 56 | Concentration of As along ablation transect of PM05 enamel. LOD indicated by blue line. Areas highlighted in light gray represent potential postmortem alteration and are excluded from analysis. 74
Figure 57 | Concentration of As along ablation transect of PM06 enamel. LOD indicated by blue line. Areas highlighted in light gray represent potential postmortem alteration and are excluded from analysis. 74
Figure 58 | Concentration of Cd along ablation transect of M301 enamel. LOD indicated by blue line. Areas highlighted in light gray represent potential postmortem alteration and are excluded from analysis. 75
Figure 59 | Concentration of Cd along ablation transect of M302 enamel. LOD indicated by blue line. Areas highlighted in light gray represent potential postmortem alteration and are excluded from analysis. 76

Figure 60 | Concentration of Cd along ablation transect of M303 enamel. LOD indicated by blue line. Areas highlighted in light gray represent potential postmortem alteration and are excluded from analysis. 76
Figure 61 | Concentration of Cd along ablation transect of M304 enamel. LOD indicated by blue line. Areas highlighted in light gray represent potential postmortem alteration and are excluded from analysis. 77
Figure 62 | Concentration of Cd along ablation transect of M306 enamel. LOD indicated by blue line. Areas highlighted in light gray represent potential postmortem alteration and are excluded from analysis. 77
Figure 63 | Concentration of Cd along ablation transect of M308 enamel. LOD indicated by blue line. Areas highlighted in light gray represent potential postmortem alteration and are excluded from analysis. 78
Figure 64 | Concentration of Cd along ablation transect of M310 enamel. LOD indicated by blue line. Areas highlighted in light gray represent potential postmortem alteration and are excluded from analysis. 78
Figure 65 | Concentration of Cd along ablation transect of M311 enamel. LOD indicated by blue line. Areas highlighted in light gray represent potential postmortem alteration and are excluded from analysis. 79
Figure 66 | Concentration of Cd along ablation transect of M312 enamel. LOD indicated by blue line. Areas highlighted in light gray represent potential postmortem alteration and are excluded from analysis. 79

Figure 67 | Concentration of As along ablation transect of M301 enamel. LOD indicated by blue line. Areas highlighted in light gray represent potential postmortem alteration and are excluded from analysis. 80
Figure 68 | Concentration of As along ablation transect of M302 enamel. LOD indicated by blue line. Areas highlighted in light gray represent potential postmortem alteration and are excluded from analysis. 80
Figure 69 | Concentration of As along ablation transect of M304 enamel. LOD indicated by blue line. Areas highlighted in light gray represent potential postmortem alteration and are excluded from analysis. 81
Figure 70 | Concentration of As along ablation transect of M308 enamel. LOD indicated by blue line. Areas highlighted in light gray represent potential postmortem alteration and are excluded from analysis. 81
Figure 71 | Concentration of As along ablation transect of M310 enamel. LOD indicated by blue line. Areas highlighted in light gray represent potential postmortem alteration and are excluded from analysis. 82
Figure 72 | Concentration of As along ablation transect of M311 enamel. LOD indicated by blue line. Areas highlighted in light gray represent potential postmortem alteration and are excluded from analysis. 82
Figure 73 | Concentration of As along ablation transect of M312 enamel. LOD indicated by blue line. Areas highlighted in light gray represent potential postmortem alteration and are excluded from analysis. 83

Figure 74 | Concentration of As along ablation transect of M303 enamel. LOD indicated by blue line. Areas highlighted in light gray represent potential postmortem alteration and are excluded from analysis. 83
Figure 75 | Concentration of As along ablation transect of M306 enamel. LOD indicated by blue line. Areas highlighted in light gray represent potential postmortem alteration and are excluded from analysis. 84

List of Tables

Table 1 | Intrauterine tooth formation timing sequence (Hillson 2024: 160-162). 17

Table 2 | Postnatal tooth development timing sequence (Hillson 2024: 162-164). 17

Table 3 | Sample inventory. 34

Table 4 | LA-ICP-MS operating parameters provided by Dr. Chris Yakymchuk, Department of Earth and Environmental Science, University of Waterloo. 36

Table 5 | Minimum and maximum concentrations of U and La found in enamel not identified as diagenetically altered. (*) = excluded from main analysis for potential postmortem alteration based on criteria outlined in Chapter 3. 43

Table 6 | Minimum and maximum concentrations and patterns of exposure for Pb in each tooth not identified as diagenetically altered. (*) = excluded from main analysis for potential postmortem alteration based on criteria outlined in Chapter 3. 46

Table 7 | Minimum and maximum concentrations for Cd and As found in each tooth and an indication of concentrations as above or below each heavy metal's LOD. 60

Table 8 | Summary of previous trace element studies using human skeletal remains from Wadi Faynan. 91

Table 9 | Minimum and maximum concentrations of Pb, Cd, As, U, and La found along ablation transect of dentine for all samples. 117

Table 10 | Dental pathology for all samples. All pathology was evaluated macroscopically and recorded as present or absent. 118

Table 11 | Dental non-metric traits for maxillary premolars. 119

Table 12 | Dental non-metric traits for mandibular premolars. 119

Table 13 | Dental non-metric traits for maxillary molars. 120

Table 14 | Dental non-metric traits for mandibular molars. 121

Chapter 1: Introduction

1.1 | Research Purpose, Scope, and Theoretical Foundations

For centuries, beginning with the development of mining and metalworking, humans have been entangled with metals and metal pollution (Nriagu 1996). Intensifying this relationship by creating more demand, mining and trading of craft products and mineral resources became central elements in ancient economic systems (Knabb et al. 2016; Nriagu 1996). Approximately 50 km southeast of the Dead Sea in southern Jordan lies one of the oldest, most extensive, and best-preserved industrial landscapes in the world, Wadi Faynan (Figure 1). This landscape represented the most important copper resource area in the southern Levant (Levy et al. 2002) and was a center for copper mining, smelting, and trade with peaks during the Early Bronze Age (EBA), Iron Age, and Roman Period (Beherec et al. 2016; Pyatt et al. 2005). The largest and possibly most significant EBA site in the Faynan region is Wadi Faynan 100 (WF100), which dates to EBA Ib (3300-3000 BCE) and has clear evidence of copper production including copper ores, slag, hammer-stones, copper awls, and copper casting molds (Adams et al. 2019; Barker et al. 2007; Wright et al. 1998). This research utilizes trace element analysis of human dental tissues to investigate possible environmental exposure to heavy metals stemming from metallurgical activities during the EBA Ib at WF100.

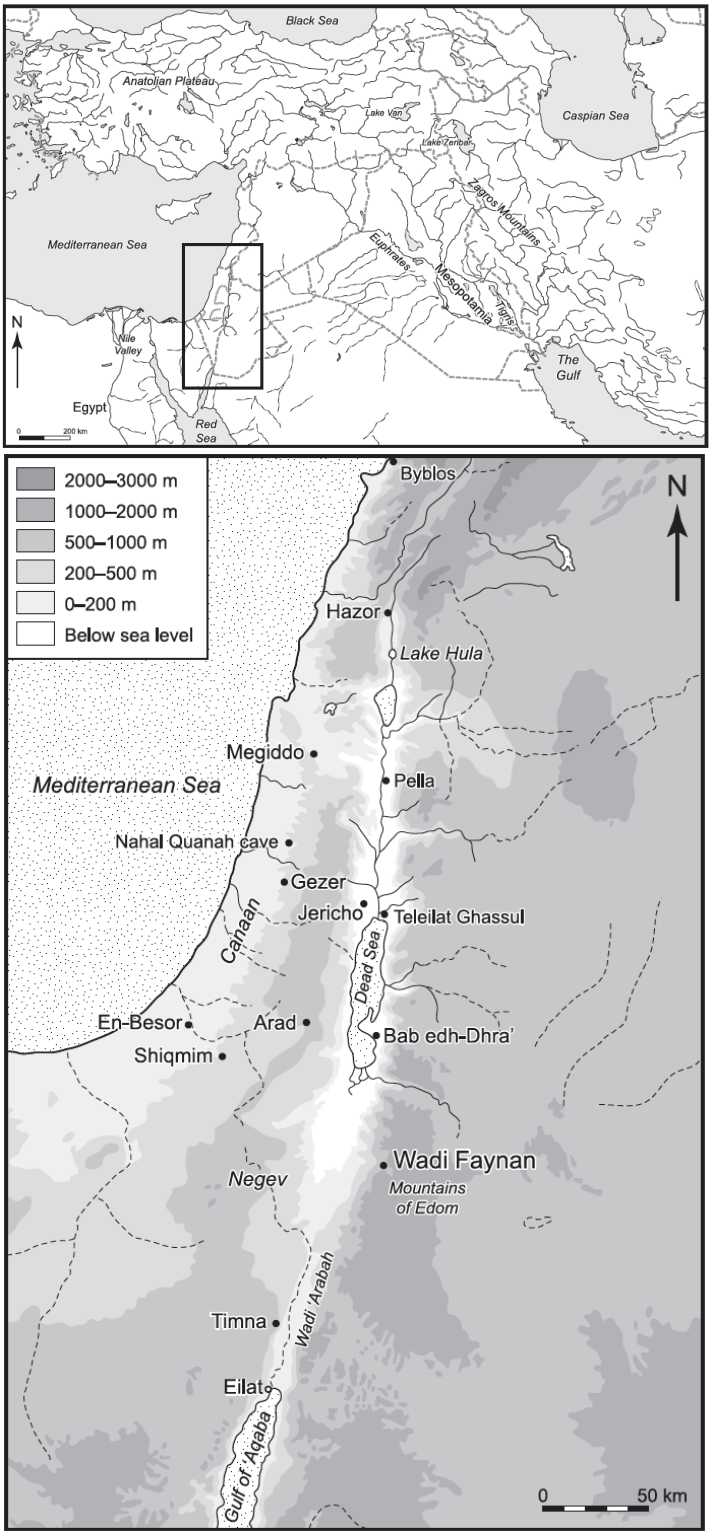


Figure 1 | The southern Levant (above) and the location of Wadi Faynan in relation to other significant archaeological sites in the region (below) (Barker et al. 2007: 228).

Within Faynan lies a vast ore field that covers an area of about 500 km^2 and holds an estimated 19.8 million metric tons of copper (Palmer et al. 2007). This ore field has been exploited for ~9,000 years beginning in the Pre-Pottery Neolithic (8500-6000 BCE), during which brightly colored copper ores were used for ornamental and cosmetic purposes (Hauptmann 2007; Hunt and el-Rishi 2012; Hunt et al. 2007). Increasing exploitation of natural resources often has lasting effects. The remnants of ancient metallurgical practices are visible in the contemporary landscape in the form of spoil tips containing an estimated several hundred thousand tons of black slag and over 250 copper mines in the valleys and tributaries of Faynan (Grattan et al. 2005; Hunt et al. 2007; Knabb 2019; Pyatt et al. 2000). Both contemporary and ancient copper production has been shown to deposit heavy metals into the environment, including but not limited to copper (Cu), zinc (Zn), lead (Pb), cadmium (Cd), arsenic (As), and mercury (Hg) (Bech et al. 1997; Chen et al. 2022; Christou et al. 2017; Filimon et al. 2021; Ghaderian and Ravandi 2012; Kerfoot et al. 2016; Knabb 2019; Knabb et al. 2016; Nassiri et al. 2023; Wilson and Pyatt 2007). Heavy metals exist naturally in the earth's crust and can neither be created nor destroyed; thus, once released and distributed, they remain in the environment until broken down or transported by natural forces (Knabb 2019; Pyatt et al. 2000). The visible leftover mining waste in Faynan is thought to still be undergoing weathering and erosional processes, continually releasing heavy metals into the environment (Pyatt et al. 2000), which has consequences for the people that occupy the region today.

All over the world, anthropogenic activities, such as copper mining and smelting, expose humans to heavy metals, which can have deleterious effects on their health (Asaduzzaman et al. 2017; Balali-Mood et al. 2021). Pb, Cd, and As are some of the most common heavy metals known to cause heavy metal poisoning or toxicity which has both acute and chronic effects,

posing a significant risk to human health (Balali-Mood et al. 2021; Jayamurali et al. 2021). Exposure can occur through food, water, or air and effects can vary based on dosage levels. Additionally, exposure to two or more heavy metals simultaneously can have cumulative health effects (Balali-Mood et al. 2021). Public health studies have shown that heavy metal toxicity can include kidney, gastrointestinal, nervous, and immune system dysfunction; skin lesions; birth defects; cancer; and vascular damage (Balali-Mood et al. 2021; Engwa et al. 2019; Tchounwou et al. 2012; Ufelle and Barchowsky 2019). Current understandings about how heavy metals impact the human body provide this research with deeper context and potential insight into daily life during the Early Bronze Age.

Anthropogenic activities, such as looting and expansion of agriculture, have caused extensive damage to archaeological sites in Wadi Faynan, actively erasing archaeological evidence in the area (Adams et al. 2019; Adams et al. 2023; Barqa Landscape Project 2023; Wright et al. 1997). With approval from the Jordanian Department of Antiquities, the Barqa Landscape Project (BLP) research team began excavating the WF100 cemetery in 2019 and continued in 2023 to preserve what is left of the population that could otherwise be destroyed by increasing agricultural activities (Adams et al. 2019; Adams et al. 2023). This study utilizes teeth recovered during the BLP 2019 and 2023 field seasons and is one of the first to examine human remains recovered from WF100.

The purpose of this thesis is to determine if copper production during the EBA Ib introduced heavy metals into the WF100 population. Trace element concentrations of Pb, Cd, and As were measured using laser ablation-inductively coupled plasma-mass spectrometry (LA-ICP-MS), a minimally invasive yet highly sensitive technique with low detection limits and the ability to simultaneously detect multiple elements. These concentrations were then used to

examine variation in exposure within the population, providing insights into differences in environmental pollutant exposure, and variation in exposure across different life stages, revealing fluctuations in frequency and/or timing of individual exposure.

This research is situated within the biocultural paradigm and uses the theoretical frameworks of embodiment and the life course in the interpretation of results. While there are various definitions of the biocultural paradigm, they center around the same core theme: humans, simultaneously biological and cultural beings, are products of the dynamic relationship between their biology and socio-cultural and physical environments. In other words, external factors, either socio-cultural or environmental, can affect human biology and health (Zuckerman and Martin 2016). Additionally, according to this paradigm, human variation is a function of phenotypic plasticity resulting from elements within the socio-cultural and physical environments in which humans exist that both create and facilitate each other (Zuckerman and Martin 2016). Human skeletal chemistry can provide insight into the physical and socio-cultural environments that an individual existed in and their biological response to said environments. In the case of this research, it is hypothesized that the socio-cultural and economic practice of copper production at WF100 caused heavy metals to leach into the environment which, in turn, accumulated in the dental tissues of the human population.

Within the biocultural paradigm, the theory of embodiment is the biological incorporation of an individual's environment into the physical body (Agarwal 2016; Schrader and Torres-Rouff 2021). Through this framework, the body is seen as a "material tool" that is used to experience the world (Wesp 2017, 106). Therefore, human development is not totally dependent on genetic factors but is shaped by the socio-cultural and physical environment that an individual finds themselves in (Wesp 2017). Importantly, embodiment cannot be understood outside of a life

course perspective, which includes “all approaches that view the individual at any point in time as the sum of previous life experiences” (Agarwal 2016, 131). Embodiment occurs constantly throughout the life course of an individual. At its foundations, this thesis assumes that the social activities surrounding copper production were embodied by WF100 individuals during their early life course, as evidenced by the presence of heavy metals in their teeth.

This research broadly contributes to reconstructions of ancient life in Jordan during the EBA Ib, specifically furthering understandings of how socio-cultural and economic activities of copper production affected the health of the WF100 population. Not only will it illuminate how early metallurgy affected the ancient population, but it will also contribute to the understanding of how heavy metals affect human biology and health in general. Furthermore, following the biocultural nature of anthropological inquiry, this research demonstrates the utility of trace element analysis in examining the dynamic relationship between human biology, cultural activities, and the physical environment.

1.2 | Working with Human Remains: Public Issues and Ethical Considerations

Public issues anthropology refers to the practice of applying anthropological concepts, methodologies, and epistemologies and engaging with various publics to examine and address contemporary human social issues (Hedican 2016; Martin et al. 2013). Anthropologists who embrace public issues anthropology aim to make their research accessible and relevant to diverse communities, policymakers, and the broader public (Hedican 2016; Scheper-Hughes 2009; Stojanowski and Duncan 2015). The publics or stakeholders that anthropologists engage with include descendant and local communities, governmental and non-profit organizations, other academics, and the public at large. For bioarchaeological research, public issues anthropology is

especially important because it involves the scientific study of human remains, which can have significant impact on descendant communities, cultural heritage, and public understandings of the past (DeWitte 2015; Gregoricka 2023; Martin et al. 2013; Walker 2008). Therefore, the relevance of bioarchaeological research is dependent on engagement with various publics and contemporary social issues through which bioarchaeologists can ensure their research is conducted ethically, informs policy and decision-making, and contributes to a greater public awareness of humanity's shared history (Hedican 2016; Martin et al. 2013; Stojanowski and Duncan 2015).

This research embraces a public issues approach in investigating the environmental pollution in Faynan that continues to impact the local environment and communities in the region (Grattan et al. 2013; Grattan et al. 2003b; Grattan et al. 2002; Hunt and el-Rishi 2010; Pyatt et al. 2002b; Pyatt et al. 2002a; Pyatt et al. 2000; Pyatt et al. 1999). Within the context of this thesis and the excavations at WF100, the various publics include local Bedouin communities, the Jordanian Department of Antiquities, the interdisciplinary researchers who have been conducting work in the region for decades, and anyone else who holds an interest in the research that is conducted there. With the aim of publishing this research to make it accessible in the public domain and amongst other academics, it has the potential to raise awareness and inform public perception of the longstanding legacies of pollution in the region and its long-term health impacts. Additionally, this research is relevant to other disciplines such as public health and environmental science and could contribute to a more comprehensive understanding of past and present heavy metal health effects. Finally, in the future, this thesis could help drive further research into how it affects the contemporary communities in Wadi Faynan and inform environmental regulations and discussions surrounding remediation efforts.

Future research could entail biomonitoring heavy metal exposure in contemporary humans living in Wadi Faynan, which could provide better understanding of current exposure to heavy metals. This could entail the collection of blood or urine, which would reflect recent exposures; hair or fingernails, which would reflect exposure that occurred within months to years prior to collection; or deciduous teeth, which could provide insight into exposure occurring during early development (Arruda-Neto et al. 2010; Asaduzzaman et al. 2017; Goodman et al. 2003). If future researchers could collect deciduous teeth from the local populations, the results of this thesis could be used as comparative data. Coupled with demographics such as age and sex and health information, determining heavy metal concentrations within these bodily tissues could illuminate the extent to which the longstanding legacies of pollution affect contemporary communities living in the region.

The excavation and scientific study of human remains raises several ethical issues (De Witte 2015; Gregoricka 2023; Martin et al. 2013; Walker 2008). Following a public issues approach requires the continual consideration of the ethical implications of working with human remains. As such, bioarchaeological research should only be conducted if the researcher has valid research questions that can be answered by empirical data from the study material and adequate justification for the research (Martin et al. 2013; Squires et al. 2019). This is especially true when conducting trace element analysis using laser ablation-inductively coupled plasma-mass spectrometry (LA-ICP-MS) because, although minimally destructive, this technique still destroys part of the skeletal sample.

The preservation ethic states that "human remains present such an invaluable material archive of human history that it is ethically imperative to preserve this information for future generations" (Zuckerman et al. 2014, 513-514). This ethic was established under the assumption

that skeletal remains provide a material memory or direct evidence of the lived experiences of past peoples. Thus, it is essential that they be preserved as much as possible for future generations to learn from, especially as analytical techniques and theoretical perspectives improve (Walker 2008). Bulk sampling strategies used for trace element analysis usually entail dissolution of a whole tooth or large portions of a tooth (Alomary et al. 2006; Dolphin 2012; Webb 2005). One of the major benefits of using LA-ICP-MS is that it does not require dissolution because laser ablation directly samples from the tooth surface. Additionally, the sample size from laser ablation is microscopic, leaving most of the dental tissue intact for future study. However, preparation of a tooth for laser ablation requires sectioning of the tooth, effectively cutting it in half to access the interior tissue for analysis. Thus, there still needs to be adequate justification for altering the tooth.

Squires et al. (2019) suggested that microspatial analyses of teeth have the potential to provide a much broader range of answers than the analysis of a tooth's morphology by itself, such as insights into diet, mobility and geographic origin, and environmental exposure. Bearing this in mind, the samples in this study were thoroughly documented by photography and recording of non-metric traits and pathological markers prior to preparation for laser ablation. Furthermore, the burials at WF100 consisted of highly commingled assemblages and selection of samples from such makes typical osteological assessment difficult if not impossible. The analysis of the chemical composition of dental tissues has the potential to reveal significant information about the WF100 population that would otherwise never be ascertained.

Aligning with a core objective of a public issues approach, Walker (2008) states that the only justification for the analysis of human remains is that the research should benefit contemporary people in some way. The intention behind this research is to deepen

understandings of the consequences of anthropogenic resource extraction and heavy metal pollution on human health, specifically how dental tissues permanently incorporate heavy metals. In addition, this research supports the use of enamel as a bioindicator of environmental pollution. Zuckerman (2014) adds another dimension to justification of the analysis of human remains by asserting that there are also benefits for the deceased, specifically those who cannot tell their stories: "bodies tell 'stories' about the biological and social conditions of their existence…and bodies therefore tell stories that people cannot or will not tell, either because they are unable to, forbidden to, or choose not to" (514). The EBA in the southern Levant currently lacks any evidence of writing systems, therefore reconstructions are based on the material evidence people left behind, including burials. Furthermore, there is a gap in knowledge about life during EBA Ib due to a dearth of comparative skeletal samples from other sites in the region. As this research is one of the first to study human remains at WF100, it will contribute to both the understanding of life during this period and a deeper comprehension of the interplay between human biology and socio-cultural, economic, and environmental aspects at the site.

Chapter 2: Background

2.1 | Trace Element Analysis

Analysis of trace elements accumulated in human skeletal remains has the potential to further understandings about past diet and health (Arnay-De-La-Rosa et al. 2011; Bianchi et al. 2017; Blakely and Beck 1981; Bocca et al. 2018; Guede et al. 2017), mobility and geographic origin (Balasse 2002; Bataille and Bowen 2012; Beard and Johnson 2000; Bianchi et al. 2017; Cucina et al. 2004; Cucina et al. 2007; Eshel et al. 2020; Schroeder et al. 2013), and environmental exposure to pollutants (Alomary et al. 2006; Bocca et al. 2018; Eshel et al. 2020; Handler et al. 1986; Rasmussen et al. 2008; Reinhard and Ghazi 1992; Sandford 1993; Simpson et al. 2021). Teeth, in particular, have been widely used as bioindicators of ancient and contemporary human health both individually and at the population level (Alomary et al. 2006; Arruda-Neto et al. 2010; Asaduzzaman et al. 2017; Barton 2011; Brown et al. 2004; Dolphin et al. 2012; Goodman et al. 2003; Hedge et al. 2010; Malara et al. 2016). Beginning *in utero* and finishing in early adulthood, teeth develop incrementally forming layers of dental tissues, all the while accumulating trace elements, including heavy metals. After development, they do not remodel as bone does, thus providing a chronological record of trace element exposure (Humphrey 2016; Simpson et al. 2021). This record can reveal information about exposure to environmental pollutants, including those related to cultural activities (e.g. mining and smelting), which can negatively impact human health.

While trace element analysis of human dental tissues has been widely used to examine exposure to environmental pollution, the utility of this method has faced critiques due to methodological and sampling issues, including the reliance of unsuitable elements and

oversimplification of diagenetic effects on skeletal material (Simpson et al. 2021). Considering this, it is essential to not only account for potential diagenetic processes, but to also have a fundamental understanding of the chemical composition of skeletal tissues to successfully interpret results. Furthermore, having a foundational comprehension of the technique used for measuring trace element concentrations allows for a better understanding of how results were obtained. This section presents information on trace elements and heavy metals, the development and chemical composition of dental tissues, the use of laser ablation-inductively coupled plasma-mass spectrometry (LA-ICP-MS) in trace element analysis, and diagenesis to provide necessary context for this research.

2.1.1 | Trace Elements and the Body

Elements that exist in the human body can be broadly classified as major or trace elements based on their quantity and roles within the body. Major elements exist in larger quantities and serve as vital structural components. For instance, carbon (C), nitrogen (N), hydrogen (H), and oxygen (O) compose 96% of living tissue (Fraga 2005; Sandford 1993), of which they are essential components making up amino acids, nucleotides, sugars, and fatty acids. Other major elements include sodium (Na), magnesium (Mg), chlorine (Cl), sulfur (S), and potassium (K). Calcium (Ca) and phosphorous (P) are also considered major elements as they are the primary components of the mineral content in skeletal tissues (Sandford 1993).

Trace elements exist in limited quantities, making up about .01% of total body mass and can be divided into essential and non-essential (Sandford 1993). Essential trace elements are thus categorized because of their vitalness to the function of the human body (Fraga 2005). They play essential roles in enzymatic reactions (Sandford 1993) and act as crucial constituents of

biological structures (Fraga 2005). They include zinc (Zn), copper (Cu), iron (Fe), manganese (Mn), chromium (Cr), selenium (Se), fluorine (F), iodine (I), cobalt (Co), vanadium (V), and molybdenum (Mo) (Fraga 2005; Sandford 1993). Non-essential trace elements are not known to be vital to biological function but exist within the human body in limited quantities, such as strontium (Sr) and barium (Ba), both of which have been used to reconstruct past diets because they are accumulated from dietary intake (Sandford 1993). While excessive levels of almost all trace elements are toxic, other non-essential trace elements, including heavy metals such as lead (Pb), cadmium (Cd), and arsenic (As), are toxic in small doses (Fraga 2005; Sandford 1993).

2.1.1.1 | Heavy Metals and the Body

For the purposes of this thesis, heavy metals are those metals or metalloids that have a density greater than 4.5 g/cm^3, are stable, and have toxic effects on human health (United Nations 2014). Heavy metals fall under the category of trace elements because they occur in trace concentrations in a variety of environmental matrices (Tchounwou et al. 2012). While they naturally exist in the atmosphere and the earth's crust, environmental contamination and human exposure to heavy metals stem from anthropogenic activities, such as mining, smelting, and refinement of metallic ores (Engwa et al. 2019; Tchounwou et al. 2012). Such activities release heavy metals into the air, water bodies, and soil. Subsequently, erosion and run-off transport and deposit them throughout an ecosystem (Engwa et al. 2019).

Humans bioaccumulate heavy metals via a variety of processes including ingestion (food and water), inhalation, and dermal contact. Many trace element studies evaluating environmental exposure to heavy metals have focused on exposure to lead (Pb) (Giffen et al. 2017; Lopez-Costas et al. 2020; Montgomery et al. 2010). However, this research expands its focus to include

Cd and As in addition to Pb. These heavy metals are known to cause multiple organ damage even at low dosage levels and have been shown to release into the environment via ancient and contemporary copper production activities (Bech et al. 1997; Chen et al. 2022; Christou et al. 2017; Filimon et al. 2021; Fraga 2005; Ghaderian and Ravandi 2012; Kerfoot et al. 2016; Knabb 2019; Knabb et al. 2016; Nassiri et al. 2023; Sandford 1993; Tchounwou et al. 2012; Wilson and Pyatt 2007).

Pb, Cd, and As are among the heavy metals that pose a significant risk to public health due to their high degree of toxicity and role in carcinogenicity (Tchounwou et al. 2012). All four are considered non-essential trace elements in that they serve no necessary biological function (Balali-Mood et al. 2021; Jaishankar et al. 2014; Tchounwou et al. 2012). Upon entering the body, they are transported and distributed into cells and tissues, binding to proteins and nucleic acids, disrupting cellular function, and causing deleterious health effects (Engwa et al. 2019; Jaishankar et al. 2014). These heavy metals accumulate throughout the body by way of mimicking and competing with essential trace elements that have similar functions and behaviors (Ufelle and Barchowsky 2019). Essential trace elements possess distinct physical and chemical characteristics that are crucial for regulating and operating metabolic pathways. The mimicry of essential trace elements by heavy metals is the primary mechanism leading to toxicity as they bind to the physiological sites typically reserved for essential trace elements, disrupting their function and associated processes (Ufelle and Barchowsky 2019). Exposure can lead to inhibition of metabolic pathways, metabolic abnormalities, loss of enzymatic activities, damage to blood constituents, immune system dysfunction, alteration in hormones, and congenital disorders (Balali-Mood et al. 2021; Engwa et al. 2019; Ufelle and Barchowsky 2019). These heavy metals can also produce free radicals, primarily reactive oxygen species (ROS), which can

cause oxidative stress ultimately leading to cellular damage. This coupled with their disruption of DNA synthesis and repair and cellular apoptosis contribute to their carcinogenicity (Balali-Mood et al. 2021). For further description of each heavy metal and their associated health effects refer to Appendix A. Due to their toxicity in small doses, interpretation of concentrations of these toxic elements should be clearer than attempting to interpret concentrations of essential trace elements found in skeletal material.

2.1.2 | Human Dentition

Teeth are divided into two sections: the crown and the root. The crown is the section that is visible, projecting into the mouth whereas the root section extends into the jaw (Figure 2). Teeth are composed of three hard tissues: enamel, dentine, and cementum (Hillson 2024). Enamel forms the crown of the tooth, dentine forms the core of both the crown and root sections, and a thin layer of cementum covers the root. Enamel and dentine protect the interior of the tooth that houses the pulp chamber, which contains soft tissues like nerves and blood vessels that provide nutrients to the tooth. Cementum attaches the root of the tooth to the periodontal ligament of the alveolar bone (Hillson 2024).

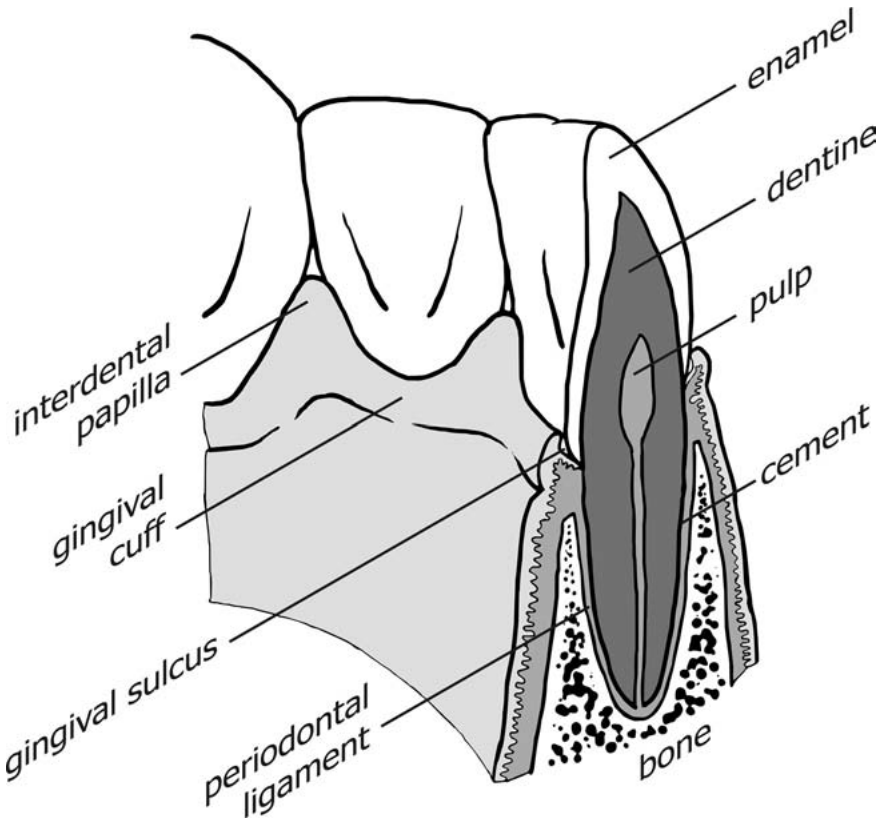


Figure 2 | General structure of teeth (Hillson 2012: 9).

2.1.2.1 | Tooth Growth and Development

Initiation of tooth growth begins approximately 14 weeks *in utero* and then continues almost uninterrupted throughout adolescence into young adulthood (Goodman et al. 2003; Hillson 2024; Humphrey 2016). All deciduous teeth begin forming during the gestational period. Intrauterine tooth formation begins with the first deciduous incisor at about 14 to 16 weeks and ends with the formation of the 1st permanent molar at about 30 weeks (Hillson 2024). Table 1 outlines the timing sequence for the initiation of intrauterine tooth formation. The postnatal development sequence begins with the permanent incisors at about 3-5 months after birth and ends with the 3rd molars, which are highly variable and may not occur until 8 years of age (Hillson 2024). The sequence of tooth crown and root formation are both more variable than the

initiation of tooth growth, but the general sequence is represented in Table 2 along with the timing of crown growth initiation.

Tooth	Formation Initiation
1st Deciduous Incisor	14 to 16 weeks
2nd Deciduous Incisor	16 to 18 weeks
Deciduous Canines	17 to 19 weeks
3rd Deciduous Premolars	15 weeks
4th Deciduous Premolars	18 to 19 weeks
1st Permanent Molar	~ 30 weeks

Table 1 | Intrauterine tooth formation timing sequence (Hillson 2024: 160-162).

Tooth	Crown Initiation	Crown Completion	Root Completion
1st Molar	~ 30 weeks *in utero*	About 3 years	Between 9-10 years
Incisors	3-5 months	Between 4-5 years	Between 9-10 years
Canines	9-10 months	Between 5-6 years	Between 12-15 years
3rd Premolars	1.8 years	Between 5-6 years	Between 12-15 years
4th Premolars	2.8 years	Between 5-6 years	Between 12-15 years
2nd Molar	3 years	About 6 years	Between 12-15 years
3rd Molar	~ 8 years (highly variable)	About 11 years	Early 20s

Table 2 | Postnatal tooth development timing sequence (Hillson 2024: 162-164).

Enamel matrix is secreted in layers by ameloblasts, beginning at the cusps and continuing out and down toward the root at an approximate rate of 4 to 6 μm a day (Goodman et al. 2003; Hillson 2024; Webb et al. 2005). The daily, developmental rhythm of enamel is represented by

regular incremental layering known as cross-striations and a longer eight to nine-day rhythm is represented by incremental markings known as striae of Retzius (Hillson 2024; Humphrey 2016). In this way, the pattern of sequential enamel deposition is preserved in each tooth. The initial enamel secretion consists of a jelly-like protein-mineral matrix with a composition of 30% protein, 30% mineral, and 30% water and provides a structural scaffold for the mineralization process (Hillson 2024). Throughout the initial matrix are tiny, ribbon or filament-like crystallites that are left after the removal of the protein portion of the matrix during transition to the maturation phase of development (Hillson 2024; Humphrey 2016). This results in a porous, mineral matrix with fluid filled spaces interspersed throughout. Subsequently, the crystallites grow in diameter, increasing the mineral content, until they touch one another forming solid, mature enamel. Much of this maturation phase takes place prior to eruption into the oral cavity; however, enamel continues to mineralize after eruption. The resulting mature enamel contains no living cells and is mostly composed of hydroxyapatite crystals, which bundle together to form the basic unit of enamel structure called prisms (Hillson 2024).

2.1.2.2 | Chemical Composition of Dental Tissues

The primary mineral component of skeletal tissue is hydroxyapatite, the structure of which requires two calcium phosphate molecules: $Ca_{10}(PO_4)_6(OH)_2$. Based on the stoichiometry of hydroxyapatite, it ideally should contain approximately 38% Ca and 18% P (Burton 2008). Enamel is a composite material consisting of an inorganic or mineral component and an organic component. It is highly mineralized (96% inorganic and 1% organic) and is primarily composed of hydroxyapatite crystallites that are about 3-7 μm in diameter (Humphrey 2016; Webb et al. 2005).

During tooth development, the hydroxyapatite component of enamel experiences elemental substitutions. Na, Mg, Sr, Ba, and Pb often replace calcium ions, while fluorine (F) and chlorine (Cl) replace hydroxyl ions (Humphrey 2016). Close to 50 different elements have been found in enamel; however, they vary in concentrations as they reflect an individual's dietary intake and environmental exposure (Dolphin et al. 2012). Within enamel, the concentrations of various elements follow patterns with the accumulation of some, e.g. Fe, Zn, Pb, and Ba, higher at the surface while decreasing toward the dentine. Others show a higher concentration toward the dentine and decrease moving toward the crown surface, e.g. Mg and Na, or are relatively evenly distributed throughout, e.g. Sr and Cu (Dolphin et al. 2012; Hillson 2024).

The maturation phase of tooth development is highly variable throughout enamel (Coffin et al. 2022; Gregoricka et al. 2014; Müller et al. 2019). While enamel matrix secretion results in daily cross-striations and striae of Retzius, mineralization occurs in multi-directional fronts that do not follow discrete units of growth (Gregoricka et al. 2014). Thus, determination of mineralization rates and exact timing in the uptake of heavy metals during this process is not possible (Coffin et al. 2022; Gregoricka et al. 2014; Müller et al. 2019). Rather, elemental signatures measured in enamel reflect average values that span the interval between the matrix secretion and mineralization phases (Coffin et al. 2022; Gregoricka et al. 2014; Humphrey 2016).

After mineralization is completed, enamel becomes inert and, mostly, does not remodel, providing a permanent, chronological record of individual elemental exposure (Asaduzzaman et al. 2017; Goodman et al. 2003). Taking a life course approach, this thesis sampled from enamel across the incremental growth markings, which should be indicative of elemental exposure throughout an individual's early life.

2.1.3 | LA-ICP-MS Methodology

One of the most used techniques for trace element analysis of dental tissues is laser ablation-inductively coupled plasma-mass spectrometry (LA-ICP-MS). The technique has proved to have a wide range of applications and has been used in material sciences, marine studies, ornithology, gemology, earth sciences, and archaeology (Durrant and Ward 2005; Fricker and Gunther 2016) and has been successfully used on human skeletal tissues (Cucina et al. 2004; Cucina et al. 2011; Dolphin et al. 2009; Dudgeon et al. 2016; Farell et al. 2013; Goodman et al. 2003; Kang et al. 2004; Lee et al. 1999; Punshon et al. 2024; Uryu et al. 2003).

Samples and calibration materials are placed into an airtight glass chamber known as the ablation cell (Fricker and Gunther 2016). A high-energy pulsed laser beam is directed onto the sample at a pre-determined site. Interaction between the sample and laser beam results in a vaporized aerosol that is transported to the plasma region by a carrier gas, usually argon or helium. Within the plasma region, the ablated micro-sample is exposed to very high temperatures, is converted to atoms, and then ionized. These ions are then extracted into the mass spectrometer where they go through different types of analyzers that separate ions based on differences in mass-to-charge ratios. Finally, the separated ions are gathered on a detector and counted to determine the amount of each that occurred in the original sample (Goodman et al. 2003; Fricker and Gunther 2016; Linge and Jarvis 2009). See Figure 2 for a basic diagram of a LA-ICP-MS instrument.

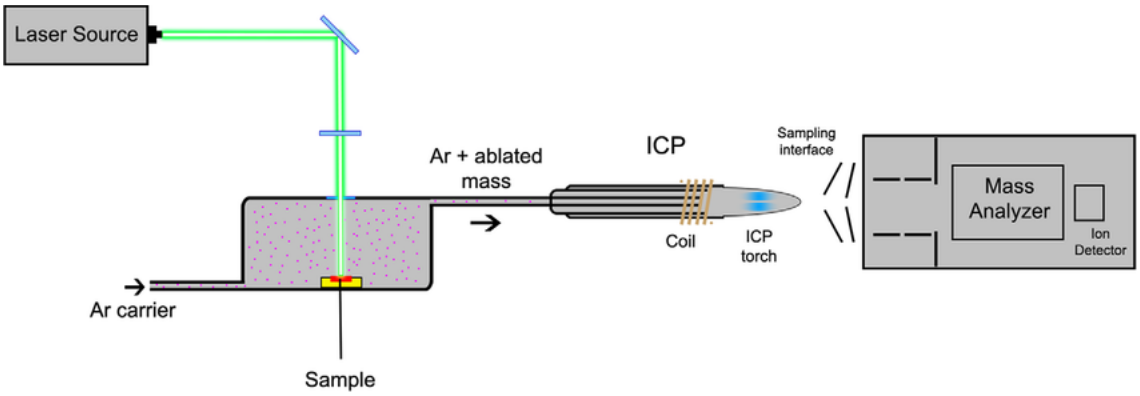


Figure 3 | Diagram of a LA-ICP-MS instrument (Barbosa and Sussulini 2019: 48).

2.1.3.1 | Benefits

LA-ICP-MS combines the fine spatial resolution of laser ablation with the multi-element, semi-quantitative abilities of ICP-MS (Goodman et al. 2003). The laser component acts as a method of sample introduction for ICP-MS and allows for the direct ablation of the sample surface (Durrant and Ward 2005). The fine spatial resolution of laser ablation allows for minimal sample destruction while maximizing elemental measurements (Dolphin et al. 2016; Goodman et al. 2003). Bulk sampling strategies used for trace element analysis usually entail the dissolution of a whole tooth or large portions of a tooth (Alomary et al. 2006; Dolphin 2012; Webb 2005). This not only causes homogenization of elemental variation within an individual tooth, but also destroys most if not all the sample (Dolphin 2012). In contrast to bulk sampling methods, dissolution of whole or part of a sample is not required for laser ablation (Dolphin et al. 2012; Lee et al. 1999). Additionally, sample preparation is minimal, and the chance of contamination is low (Goodman et al. 2003). The fundamental purpose of ICP-MS is to differentiate between elements using atomic mass (Linge and Jarvis 2009). It is a highly sensitive analytical technique with low detection limits and high sample throughput that allows for the simultaneous detection

of multiple elements (Goodman et al. 2003). Thus, the use of LA-ICP-MS in this thesis not only aligns with the preservation ethic discussed in Chapter 1, but also offers the opportunity to obtain data on multiple elements throughout the tooth without homogenizing the results.

2.1.3.2 | Limitations

The most significant limitation of LA-ICP-MS is that it is not always fully quantitative, which requires satisfactory calibration using suitable reference materials (Dolphin et al. 2012; Hare et al. 2012). Without quantification, it can be difficult to interpret variation in chemical composition as significant, typical heterogeneity of biological systems, or caused by variability of instrumentation. It also makes it difficult to conduct comparisons across studies (Dolphin et al. 2012; Hare et al. 2012; Punshon et al. 2024).

Inherent characteristics of laser ablation and plasma spectrochemistry present obstacles in achieving accurate quantification, including elemental fractionation and matrix effects (Hare et al. 2012). Elemental fractionation is a phenomenon that can be affected by each process in LA-ICP-MS, which causes the resulting abundances to be non-representative of the actual composition of the sample. This process is further influenced by a variety of factors including sample chemical composition, laser parameters, and incomplete ionization of large particles in the plasma region (Hare et al. 2012; Zhang et al. 2016). Matrix effects refer to the impacts of the chemical properties of the sample on accurate measurement. The ablation process can result in aerosol particles of various size and geometry or changes in mass, which can affect transportation, atomization, and ionization efficiencies (Limbeck et al. 2015). In addition, interferences can be caused by different ions that have the same mass-to-charge ratio being measured together and changes that occur during transportation to the plasma region, ionization,

and extraction to the mass spectrometer, which affect the number of ions that make it to the detector for measurement (Linge and Jarvis 2009).

To improve quantification, LA-ICP-MS studies use elements as internal standards and matrix-matched or certified reference materials (CRM) as external standards for calibration. The element used as an internal standard should exist at known concentrations in the sample and display similar ablation, transportation, and ionization behaviors (Hare et al. 2012; Limbeck et al. 2015). In the case of teeth, calcium is employed as an internal standard or reference element, on the assumption that calcium distribution in teeth is relatively uniform (Hare et al. 2012; Punshon et al. 2024). This has also led to the utilization of calcium ratios to interpret the results of trace element analysis on skeletal tissues as an expression of elemental abundances (Punshon et al. 2024). The composition of an external standard or reference material should be as close to the sample's as possible, exhibiting similar ablation, transportation, and ionization behaviors (Limbeck et al. 2015). Calibration using an appropriate reference material that matches the matrix of the sample can correct elemental fractionation and compensate for matrix effects. This is often achieved by using a CRM or preparation of matrix-matched reference materials when there is a lack of available appropriate CRMs (Hare et al. 2012; Limbeck et al. 2015). The benefit of using CRMs for calibration purposes is that they have been fully characterized and often improve accuracy and precision (Hare et al. 2012).

2.1.4 | Diagenesis

Diagenesis refers to a set of complex processes occurring in the burial environment that result in the post-mortem chemical and physical alteration of skeletal remains (Burton 2008; Simpson 2021). Particles found in the groundwater or soil can contaminate skeletal tissue through ionic substitution or exchanges while biogenic elements can leak from skeletal tissue

into the burial environment. Additionally, microbial activity from soil fungi and bacteria can physically degrade or chemically alter remains. Conditions within the burial environment such as pH, high temperatures, humidity, and hydrological movements can exacerbate diagenetic effects on skeletal remains (Simpson 2021). If diagenesis is not evaluated or controlled for, interpretation of trace element analysis results can be misleading. Several factors should be taken into consideration when designing a trace element study to limit the impact of diagenesis on results, including sampling choices and determining which elements to measure. Bone is characteristically highly porous and highly chemically reactive, both of which increase its susceptibility to diagenesis (Burton 2008). In contrast to bone, the densely packed crystallite structure of enamel as well as its chemical stability make it less susceptible to diagenesis (Burton 2008). Even if enamel is less susceptible to diagenesis, accurate interpretation of trace element analysis results requires testing for post-mortem alterations. This thesis prioritized controlling for diagenesis during sample selection and evaluated multiple indicators of diagenesis using LA-ICP-MS, as detailed in Chapter 3.

2.2 | Social and Archaeological Context

Located in southern Jordan, Wadi Faynan is an isolated area situated between the Mountains of Edom to the east, the Wadi ‘Arabah to the west and south, and the Jordan Tablelands to the north and east (Figure 4) (Adams 2002; Hunt et al. 2007; Palmer et al. 2007). Wadi ‘Arabah runs from the Dead Sea to the Red Sea and represents a geographical bridge connecting the different regions of the southern Levant: Palestine, modern-day Israel, Jordan, Hijaz, and Sinai. In addition, it is thought to have been a part of a route connecting the southern Levant to Lebanon, Syria, and Anatolia (Hauptmann 2007). The environment is characterized today as a stony desert with a hot and arid climate and limited vegetation (Palmer et al. 2007;

Pyatt et al. 2000). The region is populated by Bedouin pastoralists who mostly live in settled households (Palmer et al. 2007) but also inhabit scattered traditional encampments that have been repeatedly occupied over hundreds of years (Grattan et al. 2005; Pyatt et al. 2005). Investigations into metallurgical and social development across Faynan have been ongoing for the past 30 years, making it one of Jordan's most studied areas.

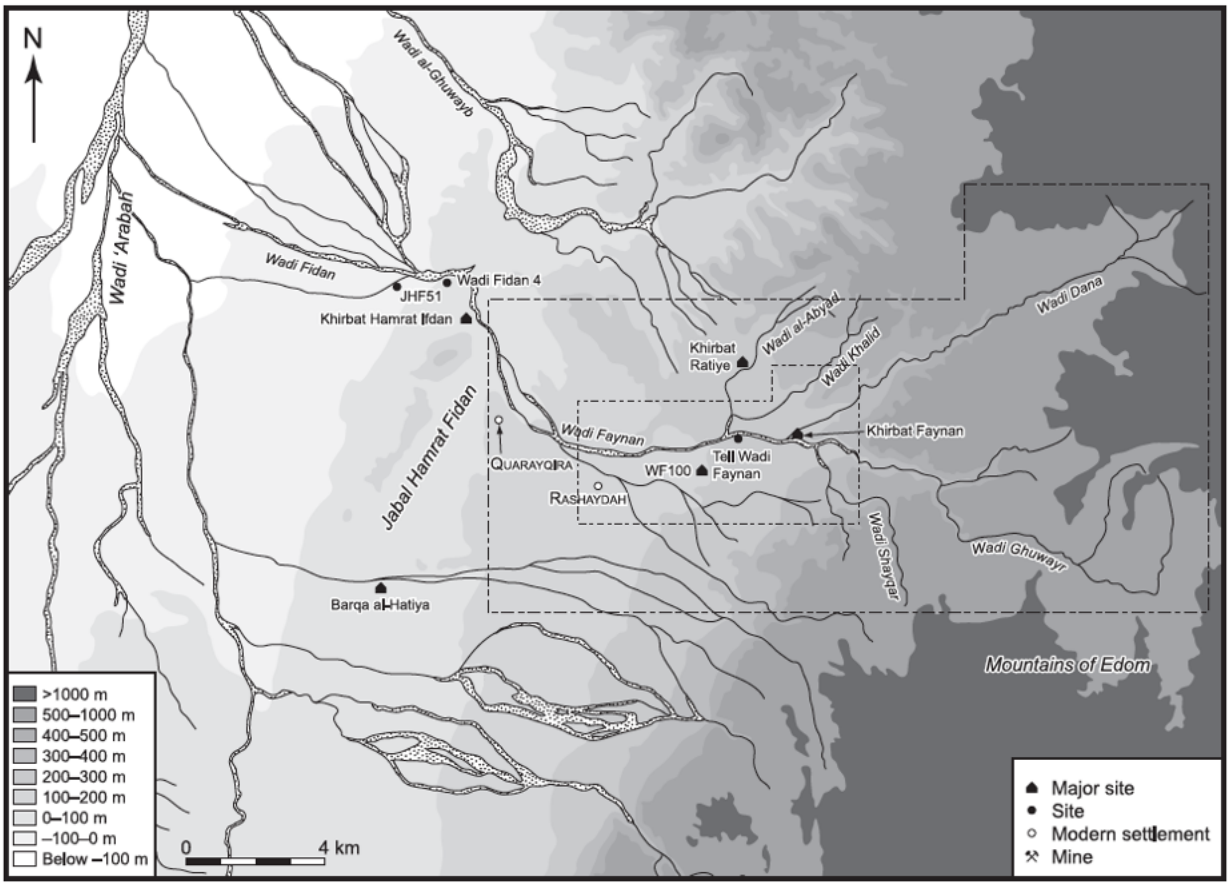


Figure 4 | Location of Wadi Faynan between Wadi 'Arabah and the Mountains of Edom and in relation to other significant archaeological sites in the Faynan region (Barker et al. 2007: 229).

2.2.2 | Early Bronze Age Society and Copper Production

The Early Bronze Age (EBA) in Jordan was a ~1500 yearlong period marked by significant social and economic change (Adams 2002), specifically, a transition towards

urbanization, construction of fortified communities, and increased population density (Chesson and Goodale 2014; Kennedy 2015); advancements in subsistence practices including use of irrigation, wide use of pack animals, cultivation via ox-drawn ploughs, and wider availability of metal tools (Philip 2008); and transformation from small-scale, community-level, low intensity copper production to large-scale, highly developed, intensive copper production (Adams 2002; Adams et al. 2017). EBI (3600-3000 BCE) marked the beginning of local copper production in Faynan, representing a transition from long-distance transport of copper ores to smelting centers in the Negev (Ben-Yosef et al. 2016; Levy et al. 2002). Importantly, Faynan copper was still widely traded throughout the EBA (Adams et al. 2017; Barker et al. 2007; Hauptmann 2007; Wright et al. 1997) and Adams (2006) asserts that despite being located away from 'mainstream' cultural developments, Faynan's "central role of copper production and trade…played a significant role in technological and social developments in the broader region during this period" (137).

EBAI mining was restricted to easily accessible or already exposed ore bodies (Adams 2002). Following veins of ore, irregular, rounded open gallery mines were constructed in Umm Ishrin Sandstone (also known as Massive Brown Sandstone [MBS]) using rudimentary stone hammers or were gathered from erosion debris originating in the Burj Dolomite Shale Formation (also known as Dolomite Limestone Shales [DLS]) (Adams 2002; Hauptmann 2007). The beginning of metallurgy in Faynan during the EBAI relied on the use of ceramic crucibles for smelting copper ores, which were transported from the mining locations to the settlement for smelting. These were placed on a bed of charcoal and likely covered by more charcoal and subsequently heated by human breath through blowpipes from above like the Egyptian depiction in Figure 5 (Adams 2002; Adams and Genz 1995; Hauptmann 2007). While there is evidence for

the possible use of furnaces in the Negev during the Chalcolithic, there is no indication that furnaces were used for smelting in Faynan prior to EBAII (3000-2750 BCE) (Hauptmann 2007).

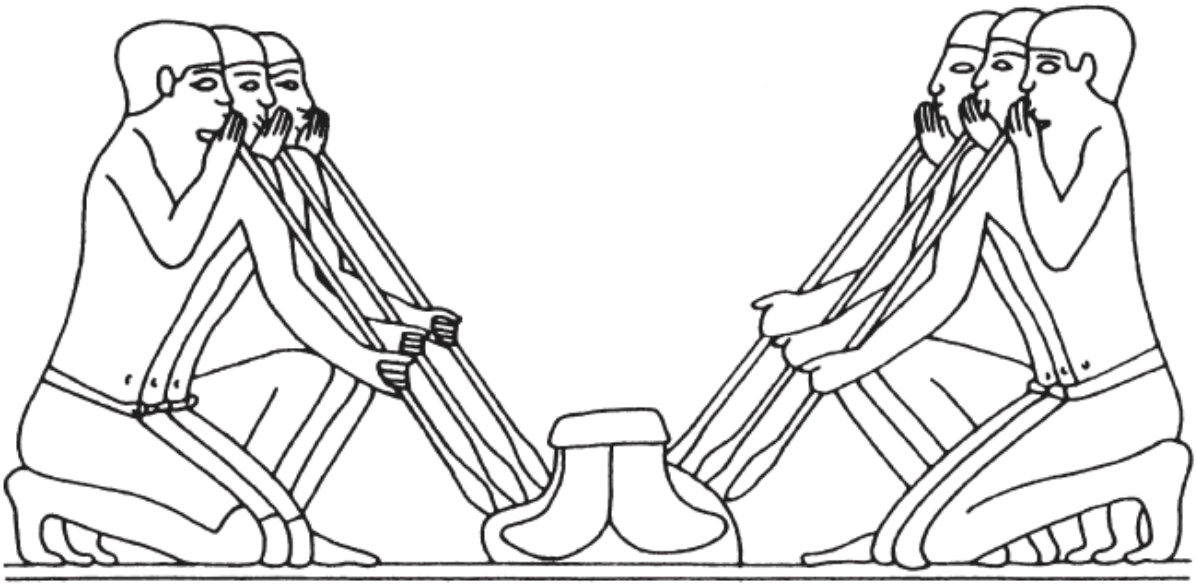


Figure 5 | Egyptian depiction of smelting using a crucible and blowpipes from above. Saqqara, tomb of Mereruka, 6th dynasty, 2450-2350 BCE (Hauptmann 2007: 220).

2.2.1 | Legacies of Pollution

Human activities in Faynan were polluting soils with heavy metals caused by introducing copper ores into fires as early as ~7,000 years ago, resulting in the world's first polluted river (Grattan 2016). This legacy of heavy metal pollution is visible throughout the Faynan landscape in the form of massive spoil and slag heaps, containing high concentrations of heavy metals such as Cu, Pb, and manganese (Mn), and over 250 mines scattered across the valleys and tributaries of the region (Knabb 2019; Pyatt et al. 2000; Pyatt et al. 1999). Faynan's annual rainfall averages ~63 mm creating an extremely arid environment (Grattan et al. 2005), which prevents pollutants emitted over the millennia from ancient metallurgy from dissipating (Pyatt and Grattan 2001).

Additionally, heavy metals are continually released from eroding spoil and slag heaps and ancient smelting sites (Grattan et al. 2003).

While there have been several studies that use bone and/or teeth to investigate exposure to heavy metals in the past, many of these studies either do not sufficiently account for diagenesis or overstate their findings. Researchers found enhanced Cu and Pb concentrations in Byzantine (Grattan et al. 2002; Grattan et al. 2005; Grattan et al. 2003b; Pyatt et al. 2005) and Bronze Age human skeletal remains as well as ancient goat and sheep teeth and bones (Pyatt et al. 2005), indicating that ancient populations living during periods of active copper mining and smelting bioaccumulated Cu and Pb in their skeletons. However, these studies did not include sufficient testing for diagenesis. This is especially problematic because each study used human bone, which is highly porous and chemically reactive making it highly susceptible to diagenesis (Burton 2008).

In contrast, Beherec et al. (2016) measured Pb and Cu levels in the enamel and dentine of 36 individuals dating to the Iron Age (ca. 1200-500 BCE) population from Wadi Fidan 40. Using Pb/Ca molar ratios from the enamel, they found elevated concentrations not attributed to diagenesis in three individuals. In addition, they found elevated Pb concentrations in the dentine in two other individuals. Based on their results, they concluded that most of the population at Wadi Fidan 40 was not exposed to heavy metal pollution *in vivo*. Similarly, Eshel et al. (2020) evaluated Pb concentrations in 41 samples from 31 Iron Age (n=28) and Persian Period (n=3) teeth excavated from seven sites across northern and central modern-day Israel. Also looking at Pb/Ca molar ratios measured from enamel, they found that only five individuals appeared to have been exposed to Pb. Additionally, they found that four individuals were “possibly polluted” (Eshel et al. 2020). Knabb (2019) uses the results from Beherec et al. (2016) and a geochemical

analysis of 39 soil samples collected from agricultural terraces across Wadi Faynan to investigate the pervasiveness of environmental contamination in the area. Of the 39 soil samples, 19 were considered contaminated with anthropogenic Pb and spatial analysis of the distribution of contaminated sites indicated that Pb enrichment within the agricultural terraces is predominately found near channels containing ancient mines. The results from their geochemical analysis and Beherec et al.'s (2016) analysis lead Knabb (2019) to conclude that the food systems in Wadi Faynan were not extensively contaminated with Pb because of a lack of elevated Pb levels throughout Beherec et al.'s sample. He further concludes that previous researchers have largely inflated the ubiquity of environmental contamination from ancient mining throughout Wadi Faynan.

While the studies using bone to examine heavy metals could be considered inconclusive due to insufficient evaluation of diagenesis (Knabb 2019), Knabb's assertion seems overstated. Beherec et al. (2016) only examined 36 individuals out of the 200 that were excavated at the Wadi Fidan 40 cemetery. With evidence suggesting that copper production has been ongoing for ~7,000 years, using evidence from 36 individuals from one period hardly seems adequate to formulate Knabb's conclusion. Furthermore, both Beherec et al. (2016) and Eshel et al. (2020) use dental tissues in their investigations limiting the timeframe of their results to concentrations bioaccumulated during childhood. This thesis also exclusively uses dental tissues in its analysis; however, it is crucial to acknowledge that any results are limited to early life chemical signatures. Trace element analysis on teeth will not be indicative of heavy metals accumulated later in life when individuals might be more likely to actively participate in copper production activities.

Studies conducted on contemporary soils, vegetation, and materials found in domestic contexts are indicative of the pollution legacy left by ancient populations. Heavy metals have been measured at excessive concentrations in herbivorous and carnivorous invertebrates (Pyatt et al. 2002b), vegetation (Pyatt et al. 1999; Pyatt et al. 2000), sediment (Grattan et al. 2013; Grattan et al. 2003b; Hunt and el-Rishi 2010; Pyatt et al. 2000); animal feces and tissues (Grattan et al. 2003b; Pyatt et al. 2000); floor sediment collected from local Bedouin tents and around their hearths (Grattan et al. 2003b; Grattan et al. 2002), and foods prepared by local Bedouin (Pyatt et al. 2002a). Despite a period of ~1500 years since copper production in Faynan ceased, the resulting pollution remains a public health hazard for contemporary human populations (Grattan et al. 2005).

2.2.3 | Wadi Faynan 100 Site Description

Originally discovered in 1994 (Barnes et al. 1995) and dating to EBA Ib (3300-3000 BCE), Wadi Faynan 100 (WF100) is roughly trapezoidal in shape, covering approximately 11 hectares. It lies on an east/west linear terrace that slopes downward toward the west and runs parallel to the main Faynan channel. It is surrounded on the north, south, and east by substantial outer walls that mark the boundary of dense surface material distribution (Barker et al. 2007; Wright et al. 1997). While Wright et al. (1997) conducted preliminary excavations, the site did not undergo further investigation until the Barqa Landscape Project's (BLP) most recent field seasons in 2019 and 2023 (Adams et al. 2019; Adams et al. 2023).

Occupational evidence at WF100 includes remnants of an enclosure wall, house-and-courtyard compounds, paddocks, fire installations, pits, and other dense surface material as well as evidence of food production. Additionally, there is clear evidence of metallurgical activities,

including copper ores, slag, hammer-stones, and molds (Barker et al. 2007; Wright et al. 1997). It is thought that extracted copper ores were transported to WF100 where it was broken up and smelted prior to being used to craft objects via molds and hammer-stones (Barker et al. 2007).

BLP's goals at WF100 included sampling heavy metal pollution in the area contributing to the larger effort to map pollution throughout Faynan, surveying WF100 to better understand the relationship between the landscape and architectural structures, and recovery of human remains to investigate the effects of heavy metal pollution on the population (Adams et al. 2019; Adams et al. 2023). The 2019 field season at WF100 saw the first excavations since the late 1990s (Wright et al. 1997) with a total of five graves excavated (Adams et al. 2019). All burials excavated had been looted at some point in time and contained highly commingled and fragmentary remains (Adams et al 2019; Dolphin and Adams 2023). One of the most significant finds of the 2019 season was the discovery of charnel houses, a type of burial not previously reported in Faynan. These charnel houses are rectilinear structures excavated into the bedrock likely topped with mudbrick. Another notable find was a piece of pottery identified as a non-local variety. Other funerary objects found in the burials included three complete pots, bone and stone beads, a complete copper awl, and an incomplete copper mold (Dolphin and Adams 2023). This season resulted in a large sample of teeth that could be used to investigate how pollution affected WF100 individuals (Adams et al. 2019).

Efforts to map the heavy metal pollution across Faynan by p-XRF analysis and to survey the WF100 landscape continued during the most recent 2023 BLP field season; however, the primary focus was excavation of WF100 burials (Figure 6) (Adams et al. 2023). The excavation team recovered human remains from eight charnel houses and three circular structures that were deemed possible burials. While sharing some features such as orthostats flanking a small

doorway facing the north, rectilinear shape, and construction into the bedrock, the charnel houses varied in terms of size, corner shape, subterranean depth, and size or existence of stones lining the burial chamber (Adams et al. 2023). The team collected commingled remains representing as many as 100 individuals with 28 boxes of whole and fragmentary bones and 165 bags of hundreds of human teeth. Funerary objects included beads, pottery, and modified faunal bone. Again, all burials showed evidence that they experienced looting at some point in time (Adams et al. 2023).

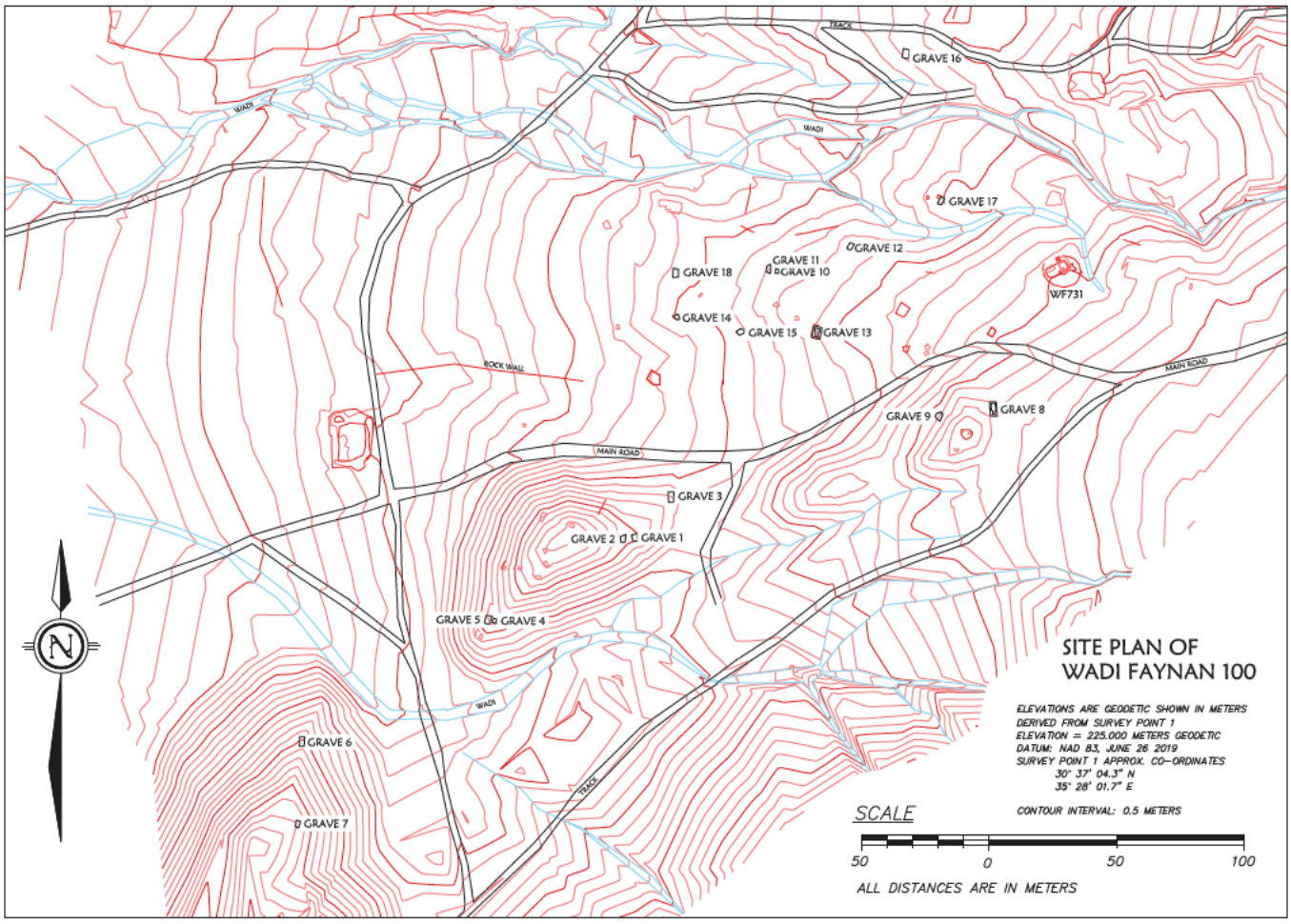


Figure 6 | Site plan of Wadi Faynan 100 (Adams et al. 2023: 2).

Chapter 3: Materials and Methods

3.1 | Sample Selection and Preparation

Teeth were selected from multiple graves excavated in 2019 and 2023. The 2023 inventory was examined and complete teeth or tooth fragments that were easily put back together were identified. All teeth chosen were permanent and lacked significant wear while having at least one cusp intact. Teeth absent of dental caries, enamel hypoplasia, and cracks were prioritized. To maximize sample size, three different tooth types were chosen, all representative of different developmental periods: first molars, premolars, and third molars. To ensure that each tooth selected represented a unique individual, position and tooth type were carefully considered. For instance, in Grave 6, only lower left first molars were chosen. Within each tooth type grouping, single teeth represent one individual; however, across these groupings, teeth from the same grave could belong to the same individual. Using Grave 6 again as an example, while only lower left first molars were selected, upper left third molars and lower left third premolars were also selected. The final chosen sample is represented in Table 3.

After the selected samples were finalized, non-metric traits and pathology for each tooth were recorded (refer to Appendix C), all teeth were thoroughly photographed, and target cusps were determined based on level of wear and presence or absence of cracks. Following documentation, each tooth was placed into a plastic mold (Peel-a-Way) with target cusps facing up, and embedded in resin (Struers EpoFix). Once teeth were embedded in resin, the plastic mold was placed into a Buehler Cast N' Vac 1000 Castable Vacuum System to remove air bubbles from the resin and air from inside the pulp cavity. Then, the embedded teeth were left to cure for 48 hours. After the resin hardened, each tooth was cut in half longitudinally and then into

sections approximately 5-7 mm thick using a Buehler Isomet 1000 low-speed diamond precision saw. Finally, the sections were mounted to glass slides using Crystalbond adhesive.

Grave	Tooth Sample	Target Cusp	ID	Slide ID
6	Lower Left 1st Molar	Hypoconid	M101	01
6	Lower Left 1st Molar	Entoconid	M102	02
8	Upper Left 1st Molar	Protocone	M103	03
8	Upper Left 1st Molar	Hypocone	M104	04
11	Lower Left 1st Molar	Hypoconid	M105	05
17	Upper Right 1st Molar	Hypocone	M106	06
1	Lower Right 1st Molar	Hypoconid	M107	07
1	Lower Right 1st Molar	Hypoconulid	M108	08
3	Lower Left 1st Molar	Metaconid	M109	09
3	Lower Left 1st Molar	Hypoconid	M110	10
9	Upper Right 1st Molar	Protocone	M111	11
8	Upper Left 3rd Molar	Paracone	M301	12
6	Upper Left 3rd Molar	Paracone	M302	13
6	Upper Left 3rd Molar	Hypocone	M303	14
6	Upper Left 3rd Molar	Protocone	M304	15
8	Upper Left 3rd Molar	Protocone	M305	16
8	Upper Left 3rd Molar	Paracone	M306	17
11	Upper Left 3rd Molar	Paracone	M307	18
12	Lower Left 3rd Molar	Entoconid	M308	19
17	Upper Left 3rd Molar	Protocone	M309	20
3	Upper Right 3rd Molar	Metacone	M310	21
3	Upper Right 3rd Molar	Protocone	M311	22
5	Upper Left 3rd Molar	Protocone	M312	23
6	Lower Left 3rd Premolar	Buccal Cusp	PM01	24
6	Lower Left 3rd Premolar	Lingual Cusp	PM02	25
8	Lower Left 4th Premolar	Lingual Cusp	PM03	26
1	Lower Left 4th Premolar	Lingual Cusp	PM04	27
3	Upper Right 3rd Premolar	Lingual Cusp	PM05	28
5	Upper Left 3rd Premolar	Buccal Cusp	PM06	29

Table 3 | Sample inventory.

3.2 | LA-ICP-MS Instrumentation

Laser ablation-inductively coupled plasma-mass spectrometry analysis was conducted in the Metal Isotope Geochemistry Laboratory run by Dr. Chris Yakymchuk in the Department of Earth and Environmental Science at the University of Waterloo. Following the process outlined in Chapter 2, the prepared samples were placed in an enclosed chamber where a high-energy pulsed laser beam was directed onto each sectioned tooth following a predetermined path through the enamel and dentine. Each predetermined path in the enamel and dentine was pre-ablated at 60 μm prior to actual sampling to remove any impurities on the surface. The laser beam was directed to run longitudinally along the enamel, ablating 40 μm wide sample lines across the growth layers, followed by similar lines running longitudinally through the dentine beginning near the dentine-enamel junction (DEJ) and down to the end of the root. The interaction of a solid sample and the laser beam resulted in a vaporized micro-sample that was transported in argon gas to the plasma region. High temperatures produced singly, positively charged ions which were subsequently extracted and measured by the mass spectrometer. Calibration occurred after each tooth was sampled using a primary Certified Reference Material (CRM), NIST-612 (standard glasses), and two secondary CRM's, NIST-1486 (bone meal) and FEBS-1 (powdered red snapper otolith). The operating parameters are summarized in Table 4.

Instrument Parameters	
Photon Machines 193 nm ArF Excimer Laser	
Cell	Two volume Helex cell
Sample Transport tubing	1.5 m length (to Agilent), PTFE 2 mm x 4 mm
MFC 1	0.8 L min^{-1} (He)
MFC 2	0.4 L min^{-1} (He)
MFC 3	0.7 min^{-1} (Ar)
Washout Time	<1 s
Wavelength	193 nm ArF
Fluence	4 J cm^{-2}
Spot Size	40 μm diameter circle
Scan Speed	15 μm s^{-1}
Repetition Rate	20 Hz
Agilent Technologies 8800 ICP-MS Triple Quadrupole	
RF Power	1550 W
RF Matching	1.77 V
Sample Cone	Nickel (x-lens)
Skimmer Cone	Nickel (x-lens)
Sample Depth	6.5 mm
Dilution Gas	0.25 L min^{-1} (Ar)
Reflected Power	18 W
Integration Time	10 ms
Masses Measured	P_{31}, Ti_{47}, V_{51}, Cr_{52}, Mn_{55}, Fe_{57}, Co_{59}, Ni_{60}, Cu_{63}, Zn_{66}, As_{75}, Se_{78}, Sr_{88}, Mo_{95}, Ag_{107}, Sn_{118}, Cd_{111}, Sb_{121}, Ba_{137}, La_{139}, Au_{197}, Hg_{201}, Tl_{205}, Pb_{208}, Bi_{209}, U_{238}
Scan Type	Single Quadrupole mode

Table 4 | LA-ICP-MS operating parameters provided by Dr. Chris Yakymchuk, Department of Earth and Environmental Science, University of Waterloo.

3.3 | Data Reduction and Analysis

The mass spectrometer measures elemental signals, and the results must be converted into concentrations (ppm). This was done by Dr. Yakymchuk using Iolite (Version 3.6) software. Resulting concentrations were smoothed using an average of 5 seconds to minimize noise and plotted against the corresponding distance (μm) of the transect along the dental tissue based on the laser scan speed of 15 μm/s. While exact timing in the uptake of heavy metals during mineralization is not possible and elemental signatures measured in enamel reflect average

values spanning the interval between matrix secretion and mineralization (See Chapter 2.1.2), the incorporation of heavy metals into enamel still occurs sequentially. Estimates in the number of days based on an assumed enamel growth rate of 4 μm /day have been successfully used to illustrate broad temporal changes throughout development (Coffin et al. 2022; Goodman et al. 2003; Hillson 2024; Meijer et al. 2019; Rey et al. 2022; Webb et al. 2005). Thus, the resulting concentrations were analyzed temporally based on an assumed enamel growth rate of 4 μm /day. All representations of time in data visualizations are estimates and not indicative of actual dates.

3.4 | Analysis of Diagenesis

While sample selection focused on controlling for diagenesis by choosing teeth largely absent of dental caries, cracks, enamel hypoplasia, and limited wear, evaluation of post-mortem chemical alterations was still necessary to ensure that the resulting concentrations were not caused by the burial environment. To further monitor for diagenesis, variations in the concentrations of uranium (U) and the rare earth element (REE), lanthanum (La), were evaluated along each ablation transect. Concentrations of U and REE are not biogenically accumulated in the body and are considered "phosphorous-seeking" elements; thus, they have been used as indicators of diagenesis (Burton 2008; Grimstead et al. 2018; Guede et al. 2017; Kamenov et al. 2018; Simpson 2021). Additionally, simultaneous fluctuations of copper (Cu), manganese (Mn), and lead (Pb) with U and La were used to assess for potential diagenetic alteration. Based on Kamenov et al. (2018), the maximum threshold concentration (MTC) for U and La were 0.05 ppm and 0.1 ppm, respectively, and values above the MTCs are considered elevated. Fluctuations of U and La below 0.05 ppm and 0.1 ppm were not considered to be indicative of diagenesis (Guede et al. 2017; Kamenov et al. 2018; Kohn et al. 2013); however, elevated

concentrations, particularly when multiple metals also show correlated increases, were interpreted as representative of diagenetic alteration. Lastly, by examining the teeth under a microscope after LA-ICP-MS analysis, sections of some samples showing chemical alteration were also found to exhibit physical damage, changes in color, or interference from the Crystalbond adhesive or epoxy resin. For instance, Figure 7 shows M101 after LA-ICP-MS analysis. The area within the rectangle indicates possible interference from the Crystalbond adhesive and/or epoxy resin that corresponds to the simultaneous fluctuation of Pb, U, La, Cu, and Mn that occurs at ~1050 days in Figure 8. Areas considered to be chemically altered are shaded gray and labelled in all data visualizations and were excluded from the main analysis and interpretations.

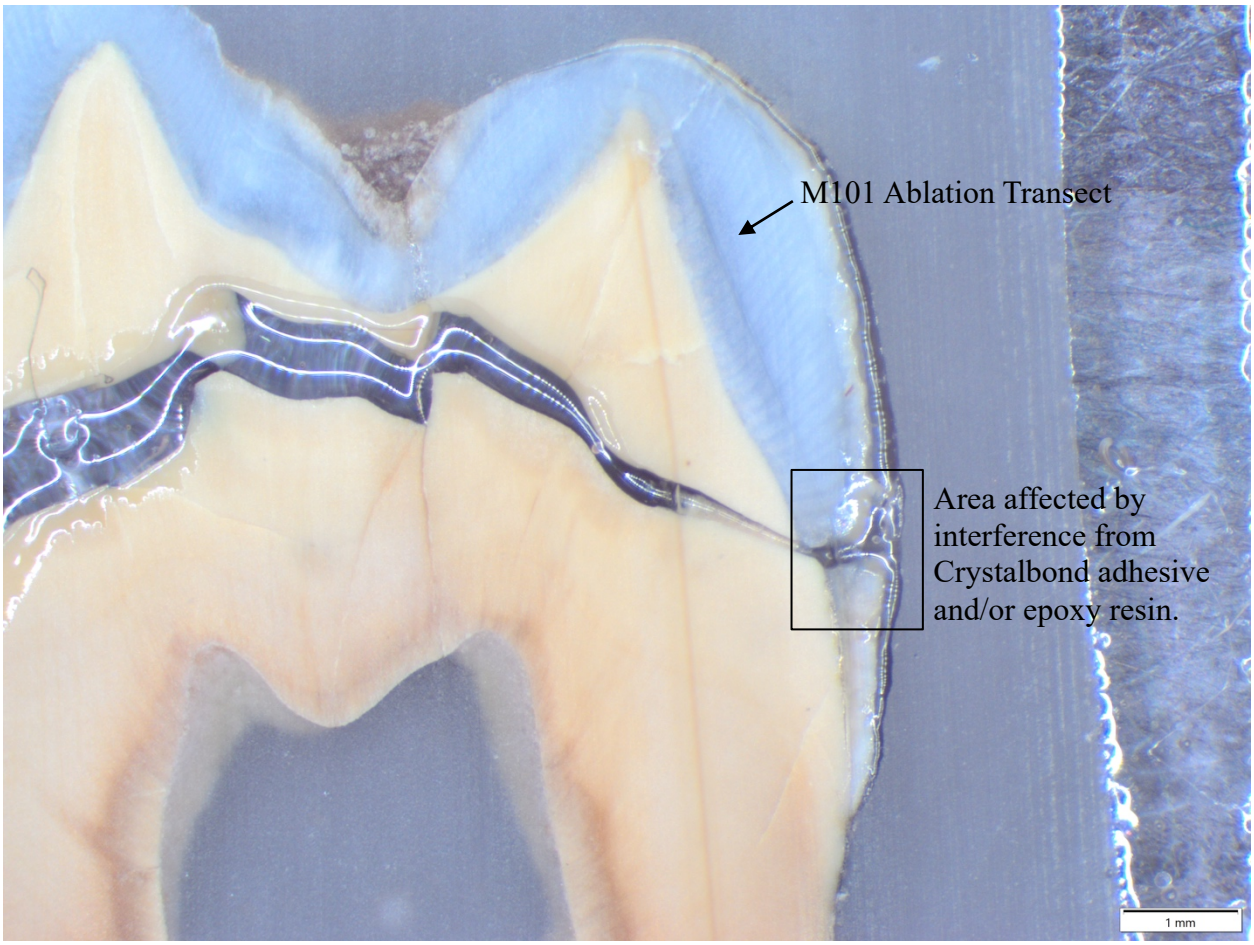


Figure 7 | M101 after LA-ICP-MS. Rectangle indicates an area identified as affected by interference from the Crystalbond adhesive and/or epoxy resin that corresponds to the simultaneous fluctuation of Pb, U, La, Cu, and Mn that occurs at ~1050 days in Figure 8.

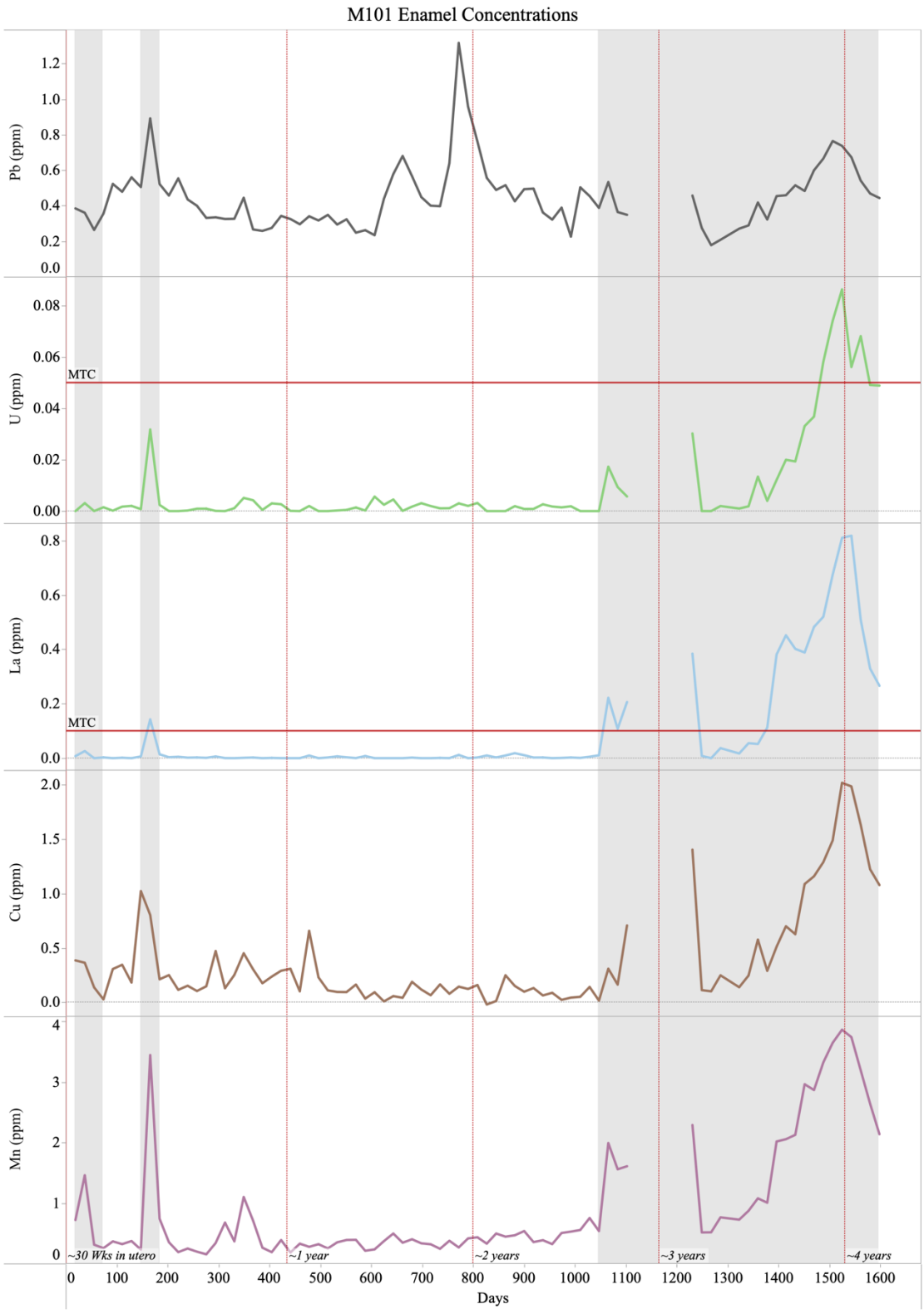


Figure 8 | Concentrations of Pb, U, La, Cu, and Mn along ablation transect of M101. Areas highlighted in light gray represent potential postmortem alteration. MTC for U = 0.05 ppm; MTC for La = 0.01 ppm.

Chapter 4: Results

4.1 | Analysis of Diagenesis

The sampled dentine of each tooth had elevated concentrations of U and La surpassing their respective MTCs, indicating that, like bone, dentine is more susceptible to postmortem alteration. As such, all dentine samples were excluded from the main analysis and interpretations. See Table 5 for maximum and minimum concentrations found in the dentine samples.

For enamel, 7 samples of the 29 total (M105, M107, M110, PM04, M305, M307, and M309), representing at least 3 individuals, were excluded from the main analysis and interpretations based on the criteria outlined in Chapter 3. For instance, U concentrations for M309 surpassed the MTC of 0.05 ppm along most of the enamel for ~600 days. Additionally, Pb, La, Cu, and Mn demonstrated corresponding peaks as seen in Figure 7. Minimum and maximum concentrations for U and La can be found in Table 5.

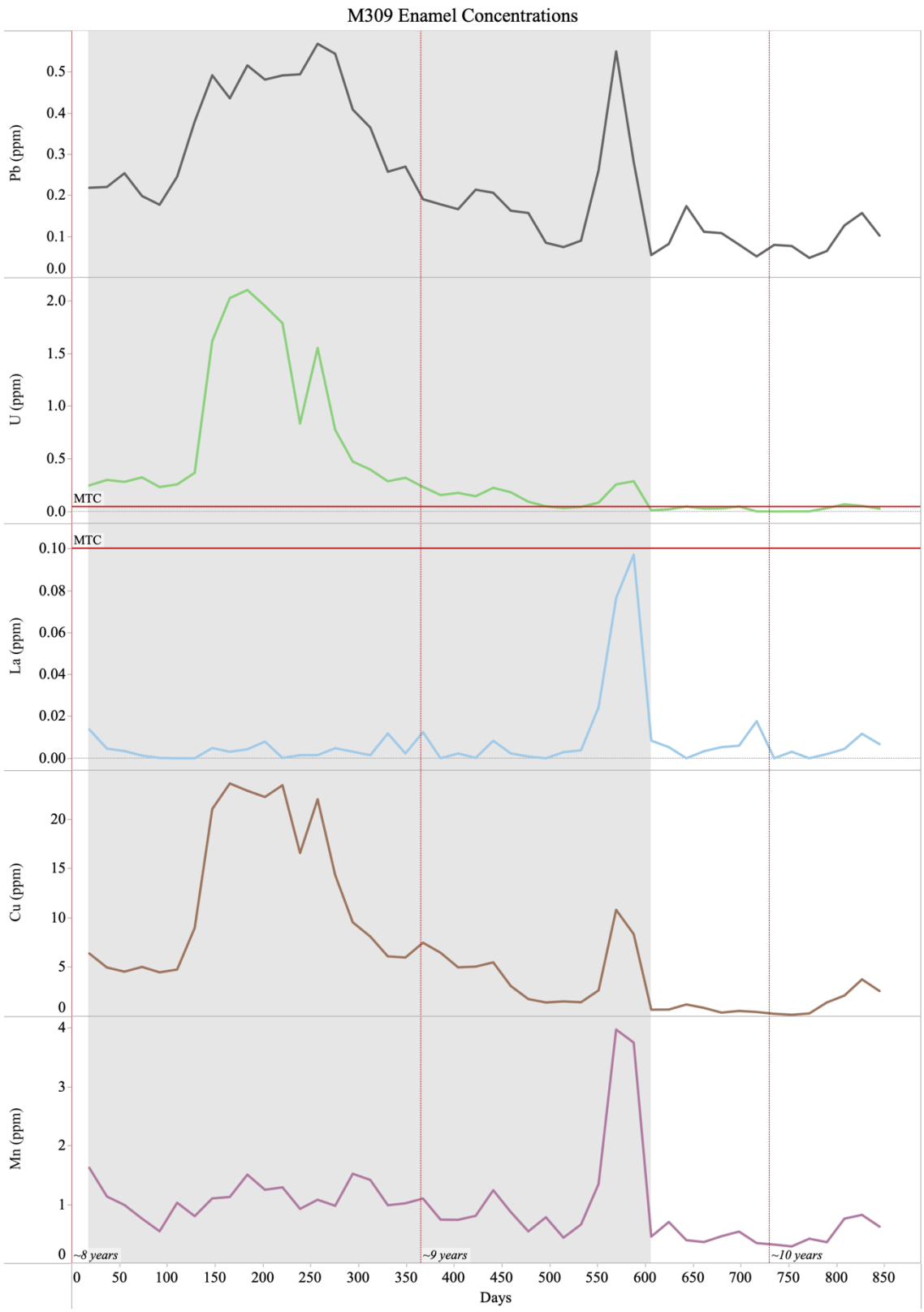


Figure 9 | Concentrations of Pb, U, La, Cu, and Mn along ablation transect of M309. Areas highlighted in light gray represent potential postmortem alteration. MTC for U = 0.05 ppm; MTC for La = 0.01 ppm.

Tooth ID	U Min - Max (ppm)	La Min - Max (ppm)
M101	0-0.006	0-0.026
M102	0-0.032	0-0.042
M103	0-0.022	0-0.011
M104	0-0.007	0-0.021
M105*	N/A	N/A
M106	0-0.045	0-0.016
M107*	N/A	N/A
M108	0-0.035	0-0.015
M109	0-0.018	0-0.015
M110*	N/A	N/A
M111	0-0.006	0-0.007
M301	0-0.020	0-0.046
M302	0-0.014	0-0.008
M303	0-0.030	0-0.007
M304	0-0.006	0-0.008
M305*	N/A	N/A
M306	0-0.023	0-0.060
M307*	N/A	N/A
M308	0-0.010	0-0.007
M309*	N/A	N/A
M310	0-0.007	0-0.006
M311	0-0.027	0-0.008
M312	0-0.040	0-0.007
PM01	0-0.018	0-0.020
PM02	0-0.012	0-0.026
PM03	0-0.025	0-0.024
PM04*	N/A	N/A
PM05	0-0.013	0-0.011
PM06	0-0.046	0-0.066

Table 5 | Minimum and maximum concentrations of U and La found in enamel not identified as diagenetically altered. (*) = excluded from main analysis for potential postmortem alteration based on criteria outlined in Chapter 3.

4.2 | Temporal Variation of Lead Exposure During Early Life

Results for Pb are presented by tooth group and within each tooth group, each tooth represents one individual. Broadly, the variation of Pb concentrations found in the enamel of teeth from WF100 can be classified into four different trends: (1) stable over time, (2) variable exposure over time with concentrations rising and falling at least two times, (3) increasing exposure over time, and (4) decreasing exposure over time. Teeth classified in (1) have

concentrations of a heavy metal that are stable over time without notable fluctuations throughout the enamel. Teeth classified in (2) have concentrations with no clear trends but rather periodic exposure episodes that vary along the enamel. Teeth classified in (3) have concentrations that largely increase over time. Finally, teeth classified in (4) largely decrease over time. Results classified in (3) or (4) may also include periodic exposure episodes but largely either increase or decrease over time. The above groupings are used to identify overall trends in Pb uptake along each tooth revealing intra- and interindividual variation over time. Minimum and maximum concentrations and patterns of exposure for Pb in each tooth are presented in Table 6.

Tooth ID	Pb Min - Max (ppm)	Pattern of Exposure
M101	0.228-1.318	Variable
M102	0.074-0.839	Variable
M103	0.051-0.271	Variable
M104	0.061-0.470	Decreasing
M105*	N/A	N/A
M106	0.170-0.572	Decreasing
M107*	N/A	N/A
M108	0.171-0.372	Decreasing
M109	0.066-0.223	Decreasing
M110*	N/A	N/A
M111	0.013-0.074	Stable
M301	0.031-0.219	Stable
M302	0.033-0.184	Decreasing
M303	0.037-0.143	Stable
M304	0.047-0.144	Variable
M305*	N/A	N/A
M306	0.025-0.093	Stable
M307*	N/A	N/A
M308	0.047-0.190	Variable
M309*	N/A	N/A
M310	0.115-0.987	Variable
M311	0.016-0.082	Stable
M312	0.027-0.288	Decreasing
PM01	0.007-0.125	Variable
PM02	0.023-0.114	Decreasing
PM03	0.022-0.416	Increasing
PM04*	N/A	N/A

PM05	0.237-1.074	Decreasing
PM06	0.112-0.244	Decreasing

Table 6 | Minimum and maximum concentrations and patterns of exposure for Pb in each tooth not identified as diagenetically altered. (*) = excluded from main analysis for potential postmortem alteration based on criteria outlined in Chapter 3.

4.2.1 | First Molars

4.2.1.1 | Temporal Variation of Lead (~30 weeks in utero - ~3 years old)

Of the eight first molars included in the main analysis, one (M111) can be classified as (1) stable over time (Figure 10), three (M101, M102, and M103) can be classified as (2) variable exposure over time (Figures 11, 12, and 13), and four (M104, M106, M108, and M109) can be classified as (4) decreasing over time (Figures 14, 15, 16, and 17). One sample (M101) has a maximum Pb concentration above 1 ppm that occurs at ~770 days or an estimated age of about 2 years old. Two samples (M102 and M106) have maximum Pb concentrations greater than 0.5 ppm but less than 1 ppm, five samples (M103, M104, M108, M109, and M110) have concentrations greater than 0.1 ppm but less than 0.5 ppm, and one sample (M111) has a maximum Pb concentration below 0.1 ppm.

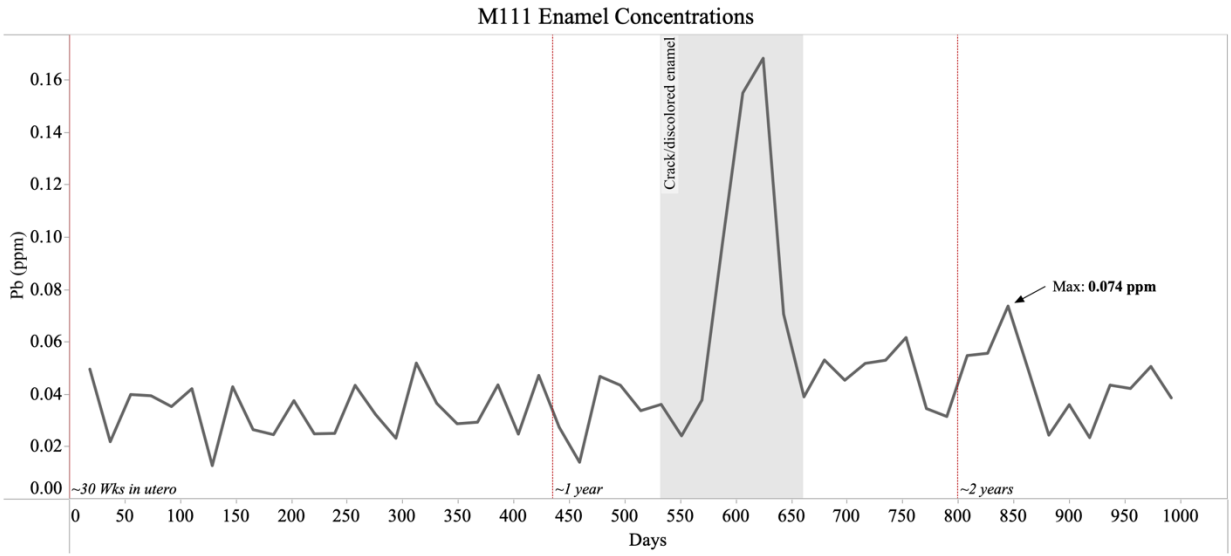


Figure 10 | Concentration of Pb along ablation transect of M111 enamel. Maximum concentration indicated. Classified as (1) stable over time. Areas highlighted in light gray represent potential postmortem alteration and are excluded from analysis.

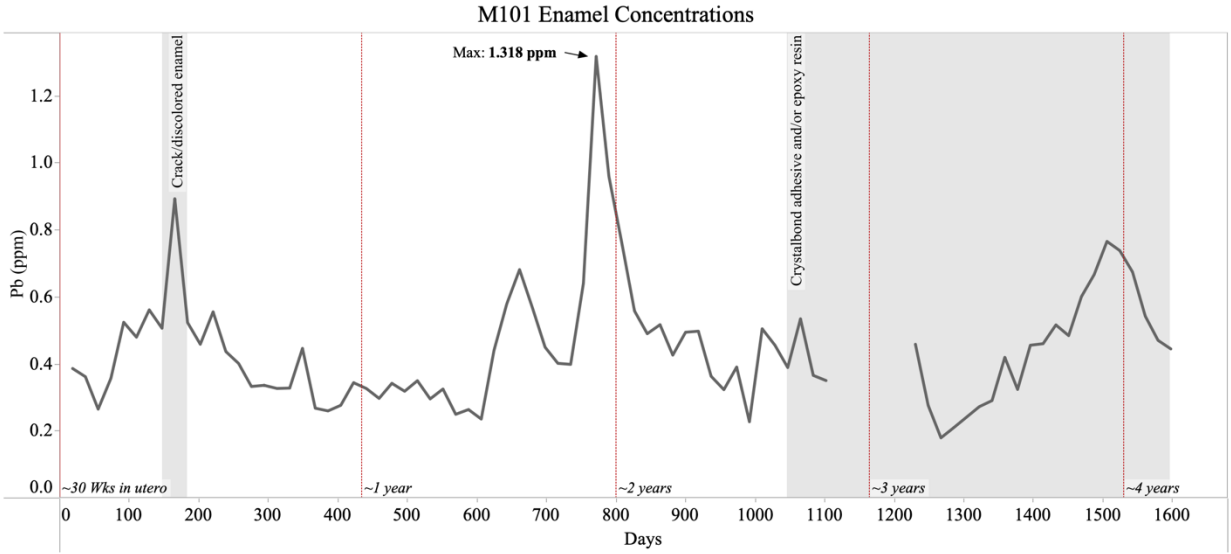


Figure 11 | Concentration of Pb along ablation transect of M101 enamel. Maximum concentration indicated. Classified as (2) variable over time. Areas highlighted in light gray represent potential postmortem alteration and are excluded from analysis.

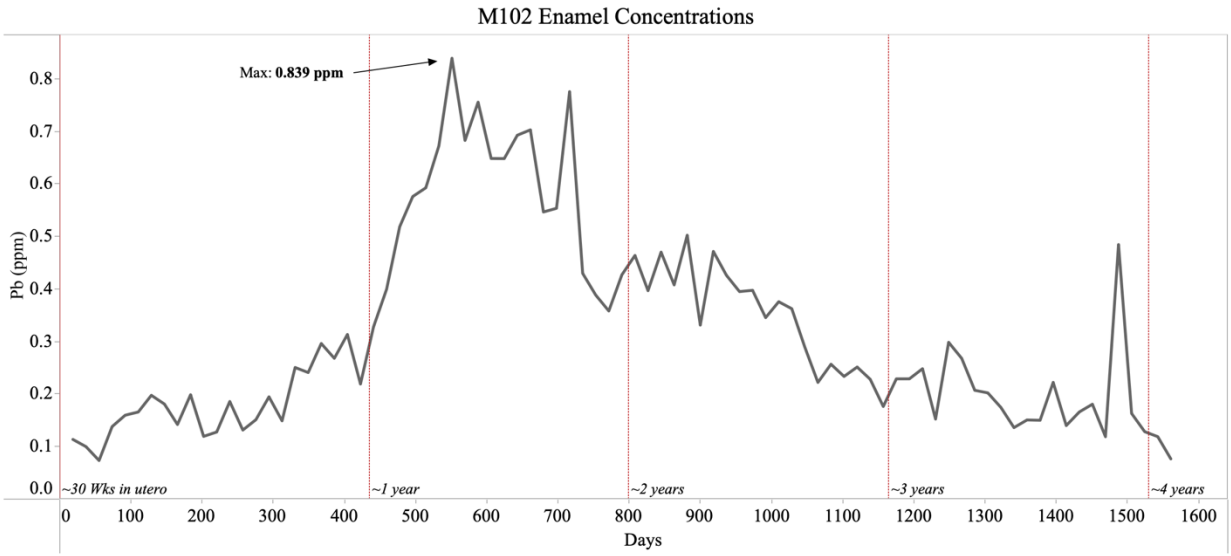


Figure 12 | Concentration of Pb along ablation transect of M102 enamel. Maximum concentration indicated. Classified as (2) variable over time. Areas highlighted in light gray represent potential postmortem alteration and are excluded from analysis.

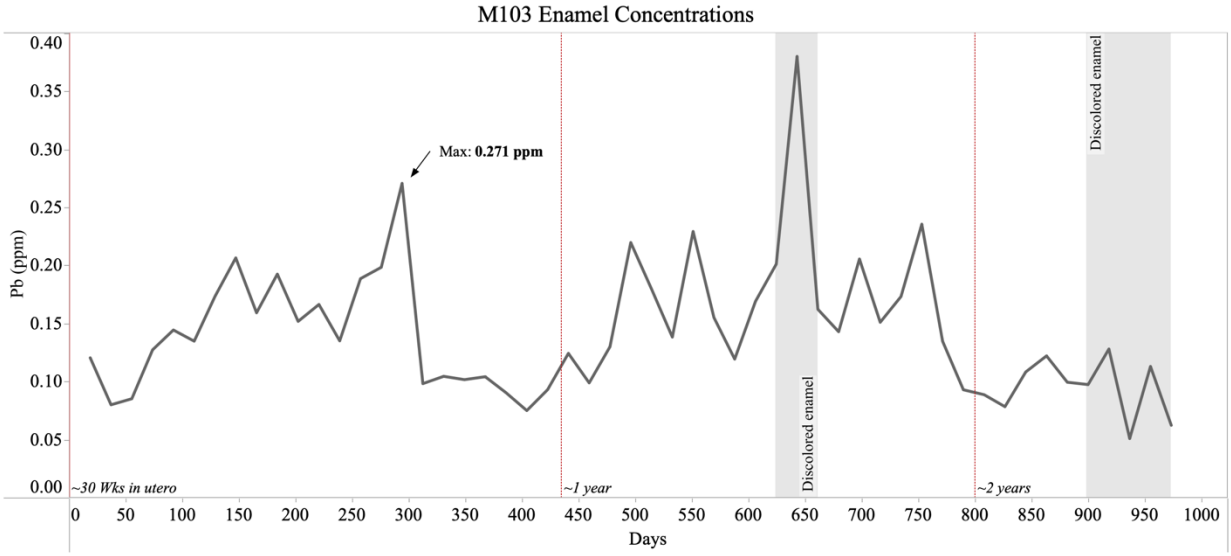


Figure 13 | Concentration of Pb along ablation transect of M103 enamel. Maximum concentration indicated. Classified as (2) variable over time. Areas highlighted in light gray represent potential postmortem alteration and are excluded from analysis.

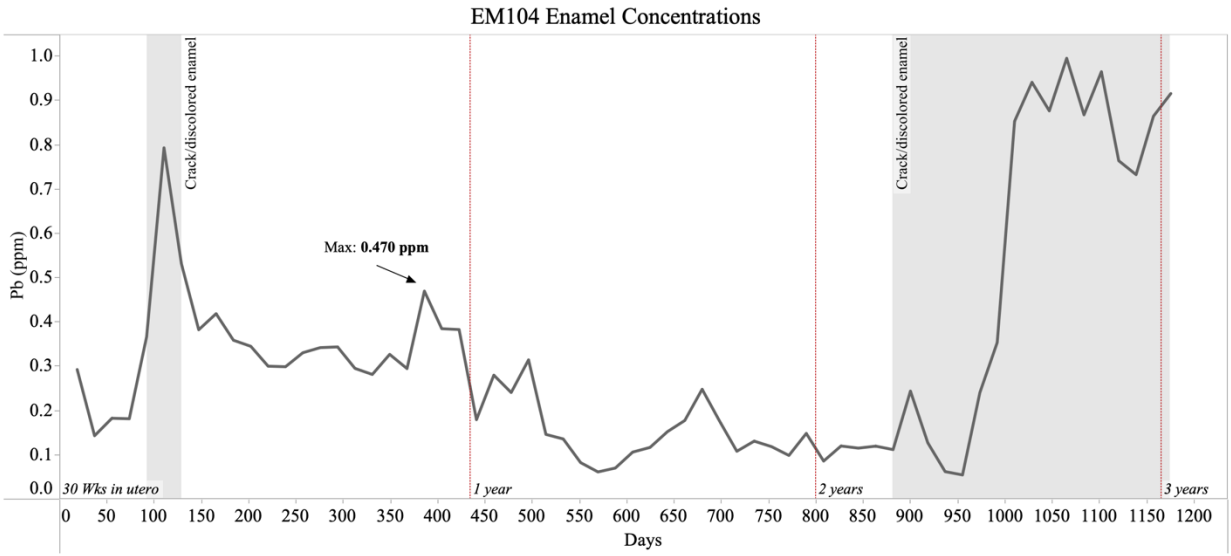


Figure 14 | Concentration of Pb along ablation transect of M104 enamel. Maximum concentration indicated. Classified as (4) decreasing over time. Areas highlighted in light gray represent potential postmortem alteration and are excluded from analysis.

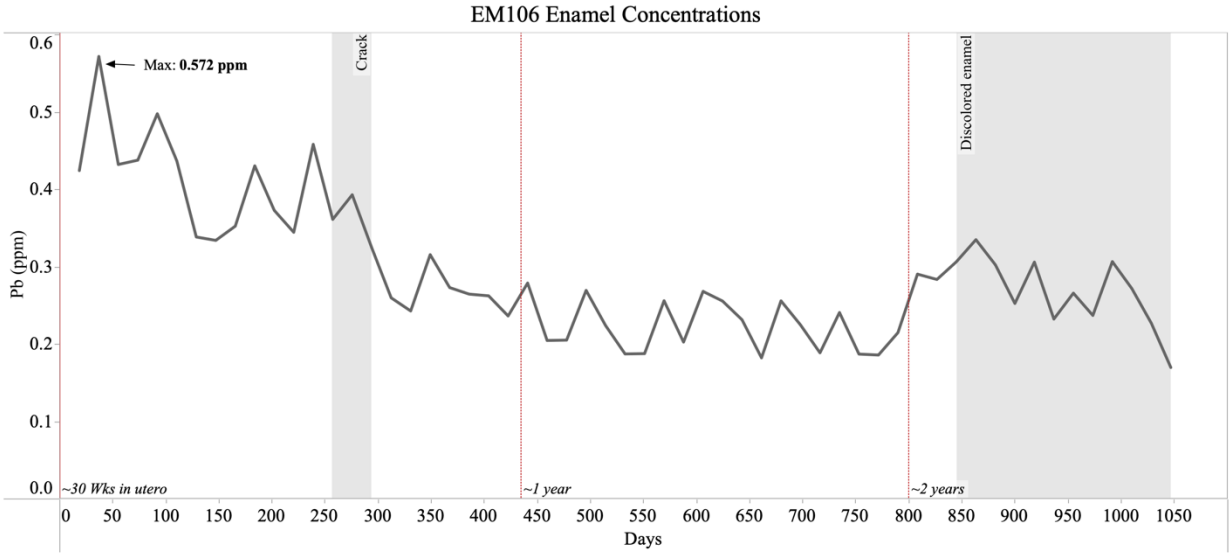


Figure 15 | Concentration of Pb along ablation transect of M106 enamel. Maximum concentration indicated. Classified as (4) decreasing over time. Areas highlighted in light gray represent potential postmortem alteration and are excluded from analysis.

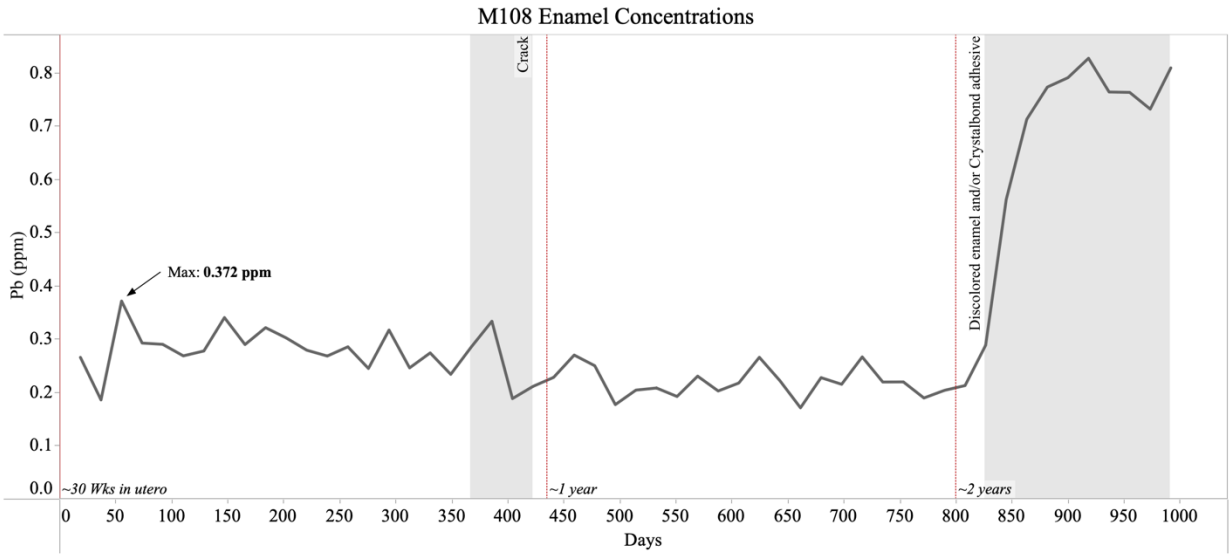


Figure 16 | Concentration of Pb along ablation transect of M108 enamel. Maximum concentration indicated. Classified as (4) decreasing over time. Areas highlighted in light gray represent potential postmortem alteration and are excluded from analysis.

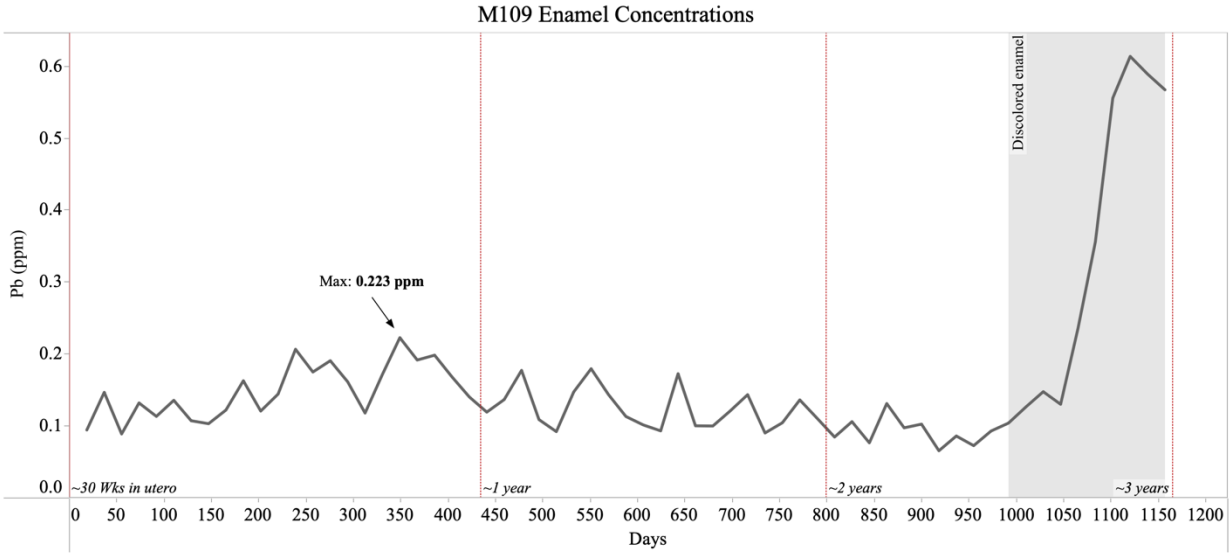


Figure 17 | Concentration of Pb along ablation transect of M109 enamel. Maximum concentration indicated. Classified as (4) decreasing over time. Areas highlighted in light gray represent potential postmortem alteration and are excluded from analysis.

4.2.2 | Premolars

4.2.2.1 | Temporal Variation of Lead (~1.8-2.8 to ~5-6 years old)

When examining variation in Pb concentrations found in premolars, one sample (PM01) can be classified as (2) variable over time (Figure 18), one sample (PM03) can be classified as (3) increasing over time (Figure 19), and three samples (PM02, PM05, and PM06) can be classified as (4) decreasing over time (Figures 20-22). One premolar (PM05) had a concentration greater than 1.0 ppm (1.074 ppm), four premolars (PM01, PM02, PM03, and PM06) had concentrations greater than 0.1 ppm but less than 0.5 ppm, and one premolar (PM04) had a maximum concentration below 0.1 ppm.

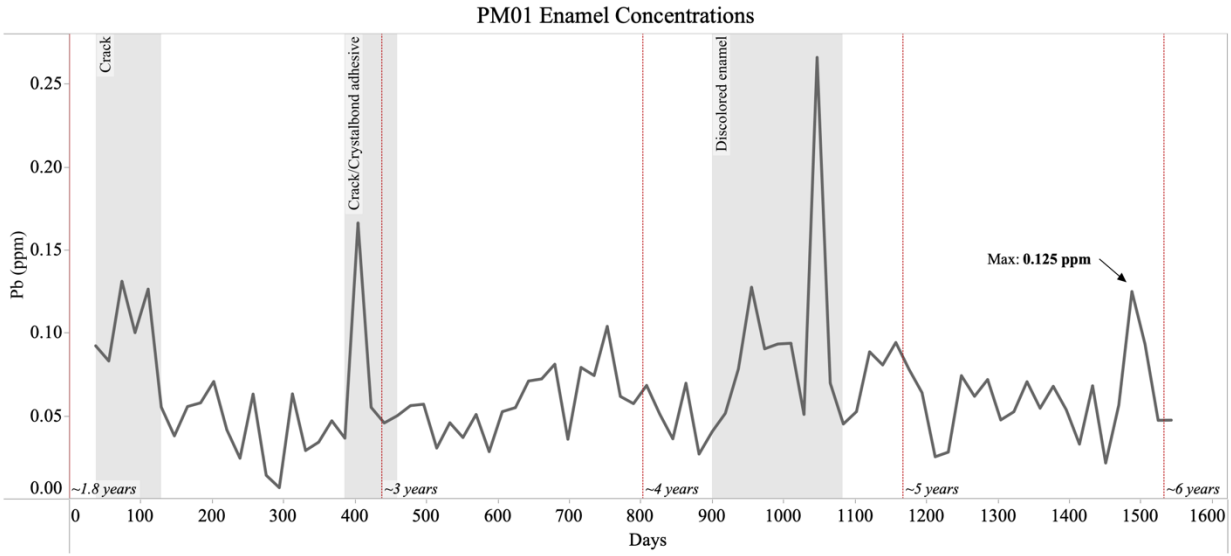


Figure 18 | Concentration of Pb along ablation transect of PM01 enamel. Maximum concentration indicated. Classified as (2) variable over time. Areas highlighted in light gray represent potential postmortem alteration and are excluded from analysis.

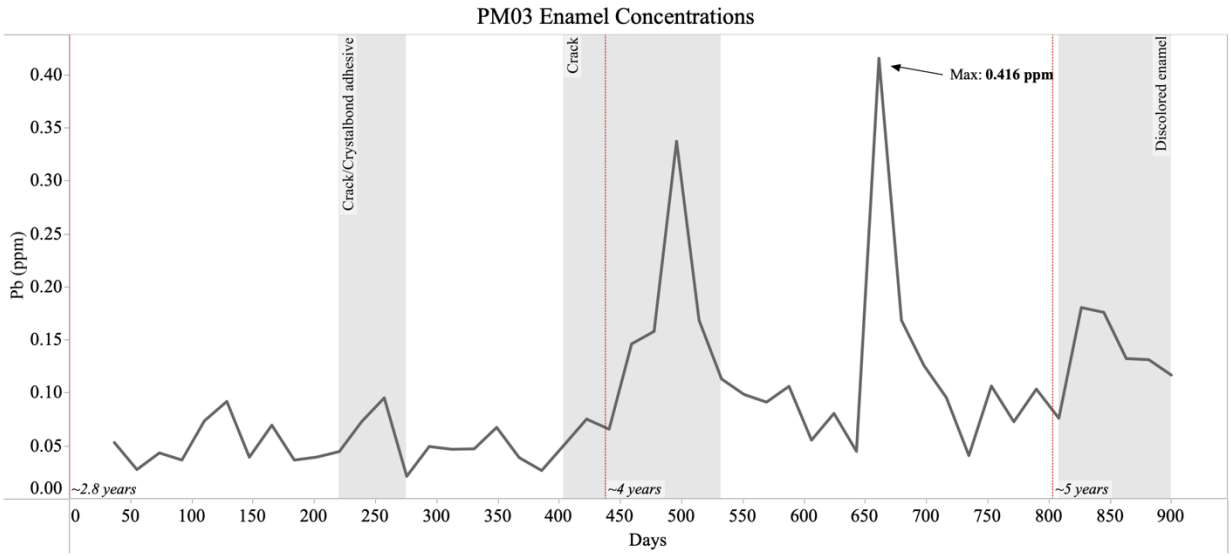


Figure 19 | Concentration of Pb along ablation transect of PM03 enamel. Maximum concentration indicated. Classified as (3) increasing over time. Areas highlighted in light gray represent potential postmortem alteration and are excluded from analysis.

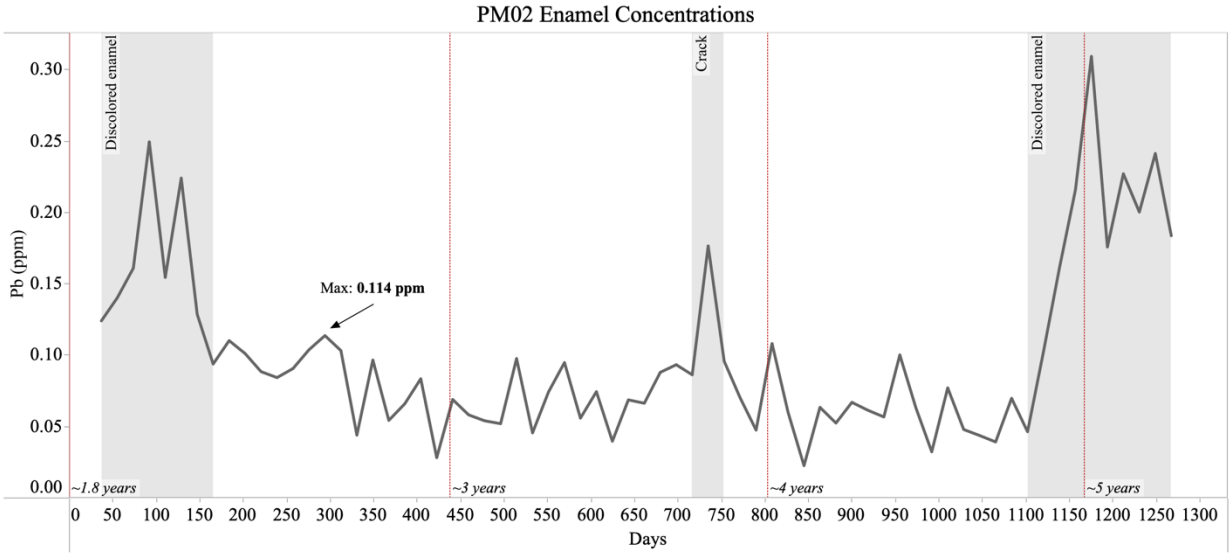


Figure 20 | Concentration of Pb along ablation transect of PM02 enamel. Maximum concentration indicated. Classified as (4) decreasing over time. Areas highlighted in light gray represent potential postmortem alteration and are excluded from analysis.

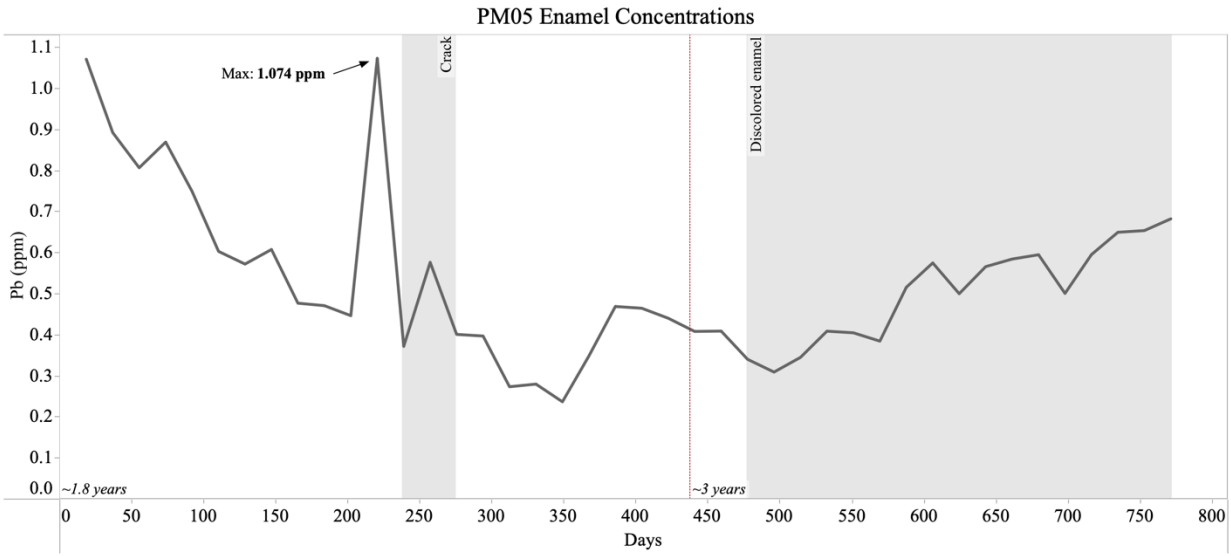


Figure 21 | Concentration of Pb along ablation transect of PM05 enamel. Maximum concentration indicated. Classified as (4) decreasing over time. Areas highlighted in light gray represent potential postmortem alteration and are excluded from analysis.

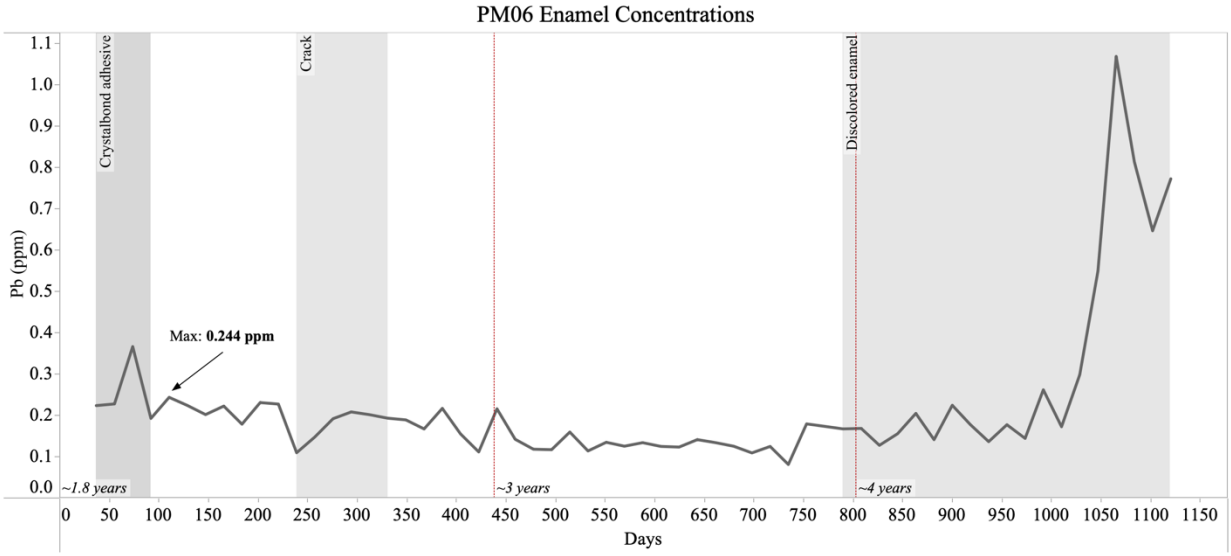


Figure 22 | Concentration of Pb along ablation transect of PM06 enamel. Maximum concentration indicated. Classified as (4) decreasing over time. Areas highlighted in light gray represent potential postmortem alteration and are excluded from analysis.

4.2.3 | Third Molars

4.2.3.1 | Temporal Variation of Lead (~8 years to ~11 years old)

When examining Pb concentrations in third molars, four of the nine samples included in the main analysis (M301, M303, M306, and M311) can be classified as (1) stable over time (Figures 23-26), three samples (M304, M308, and M310) can be classified as (2) variable exposure over time (Figures 27-29), and two samples (M302 and M312) can be classified as (3) decreasing over time (Figures 30 and 31). One third molar has a maximum Pb concentration greater than 0.5 ppm, six third molars (M301, M302, M303, M304, M308, and M312) have maximum Pb concentrations greater than 0.1 ppm but less than 0.5 ppm, and two samples (M306 and M311) have concentrations less than 0.1 ppm.

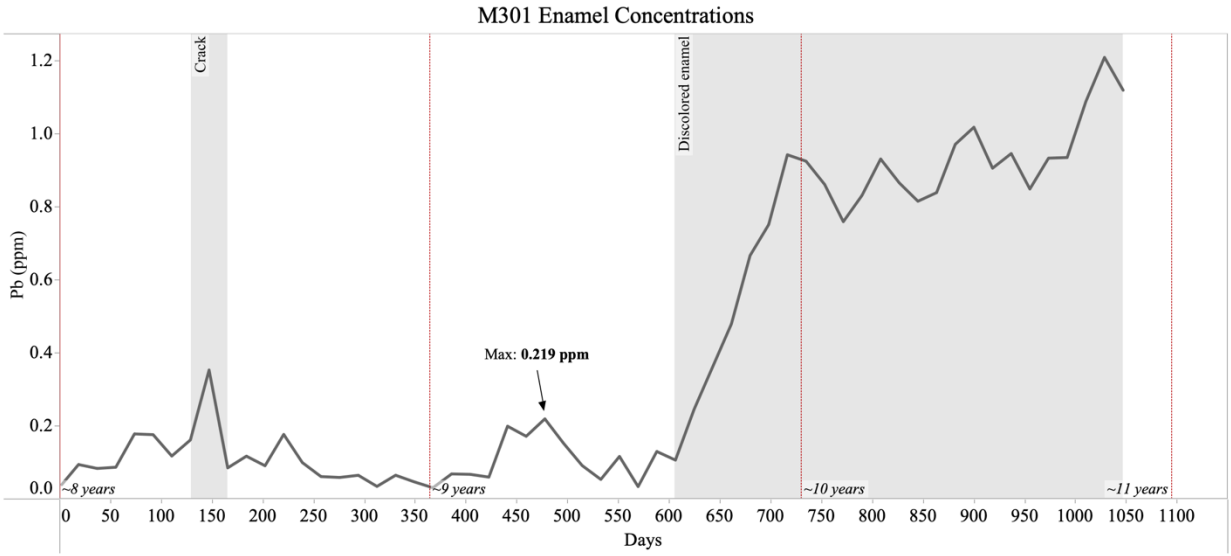


Figure 23 | Concentration of Pb along ablation transect of M301 enamel. Maximum concentration indicated. Classified as (1) stable over time. Areas highlighted in light gray represent potential postmortem alteration and are excluded from analysis.

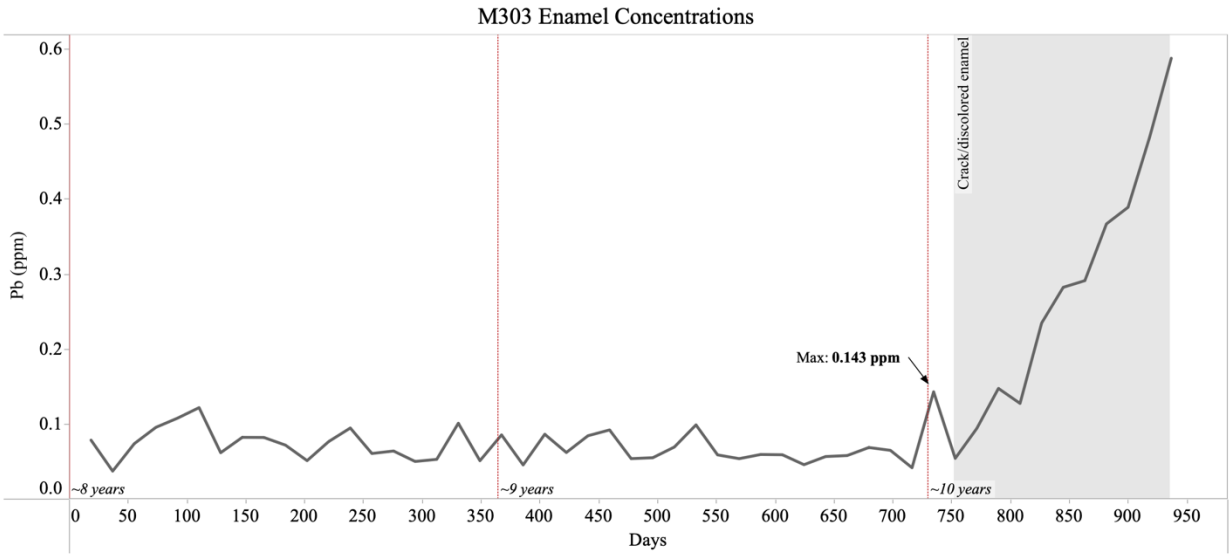


Figure 24 | Concentration of Pb along ablation transect of M303 enamel. Maximum concentration indicated. Classified as (1) stable over time. Areas highlighted in light gray represent potential postmortem alteration and are excluded from analysis.

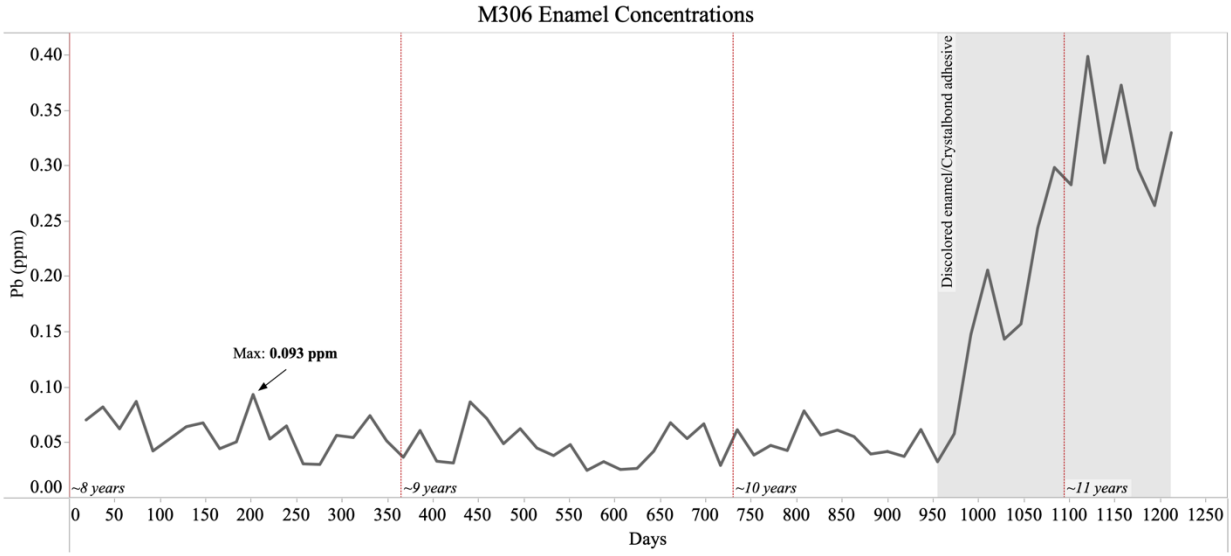


Figure 25 | Concentration of Pb along ablation transect of M306 enamel. Maximum concentration indicated. Classified as (1) stable over time. Areas highlighted in light gray represent potential postmortem alteration and are excluded from analysis.

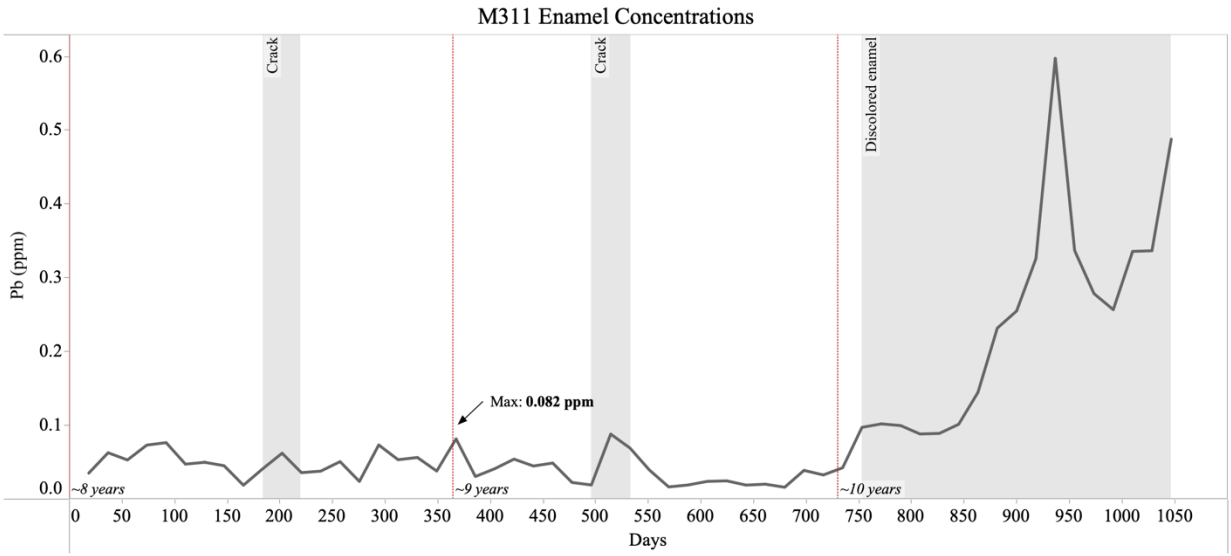


Figure 26 | Concentration of Pb along ablation transect of M311 enamel. Maximum concentration indicated. Classified as (1) stable over time. Areas highlighted in light gray represent potential postmortem alteration and are excluded from analysis.

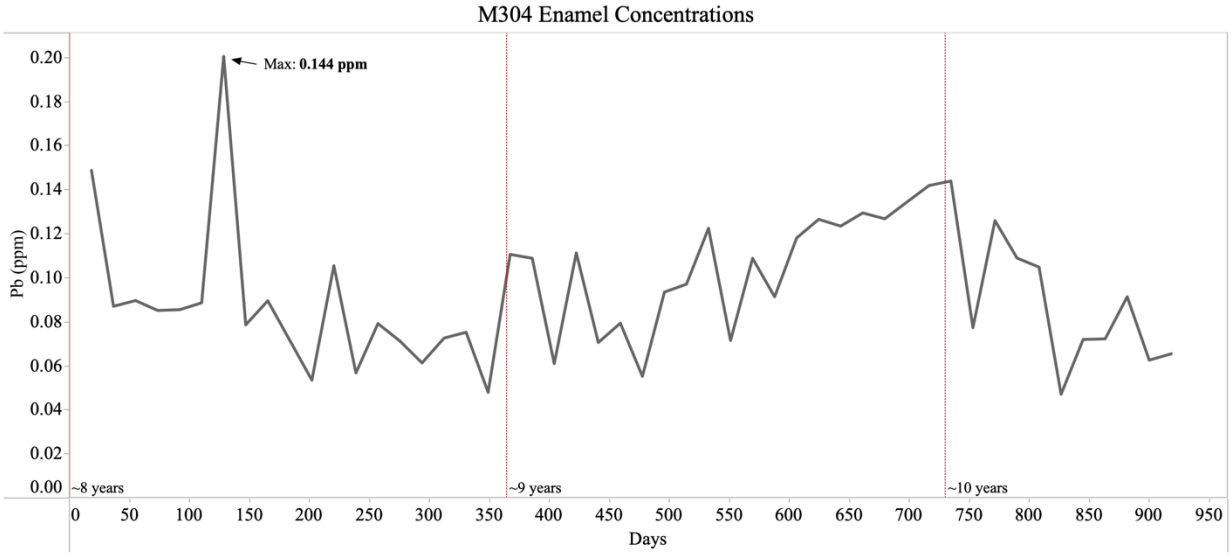


Figure 27 | Concentration of Pb along ablation transect of M304 enamel. Maximum concentration indicated. Classified as (2) variable over time. Areas highlighted in light gray represent potential postmortem alteration and are excluded from analysis.

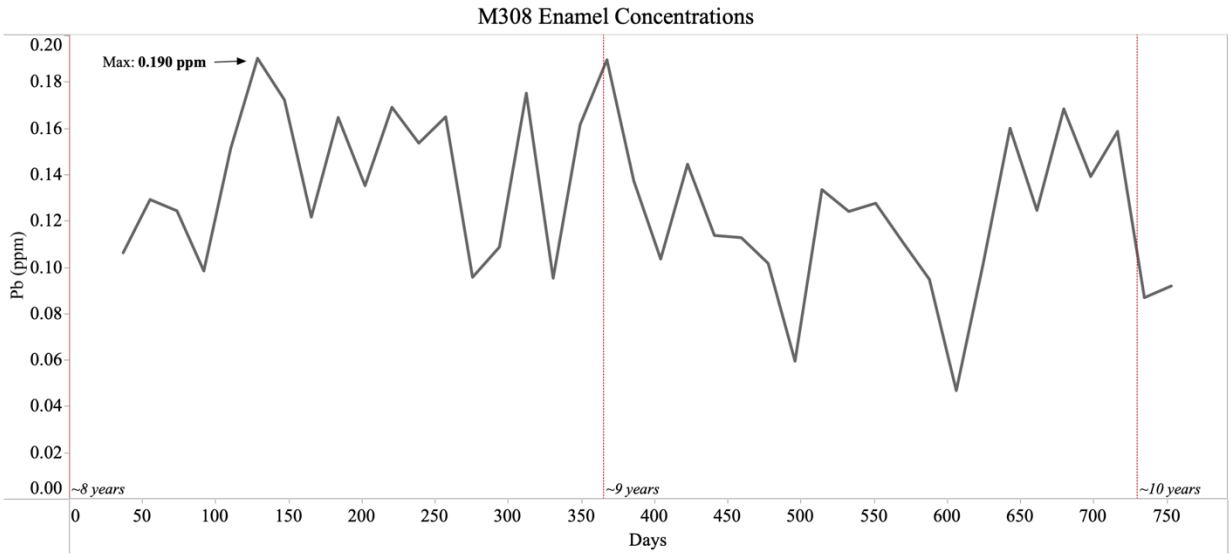


Figure 28 | Concentration of Pb along ablation transect of M308 enamel. Maximum concentration indicated. Classified as (2) variable over time. Areas highlighted in light gray represent potential postmortem alteration and are excluded from analysis.

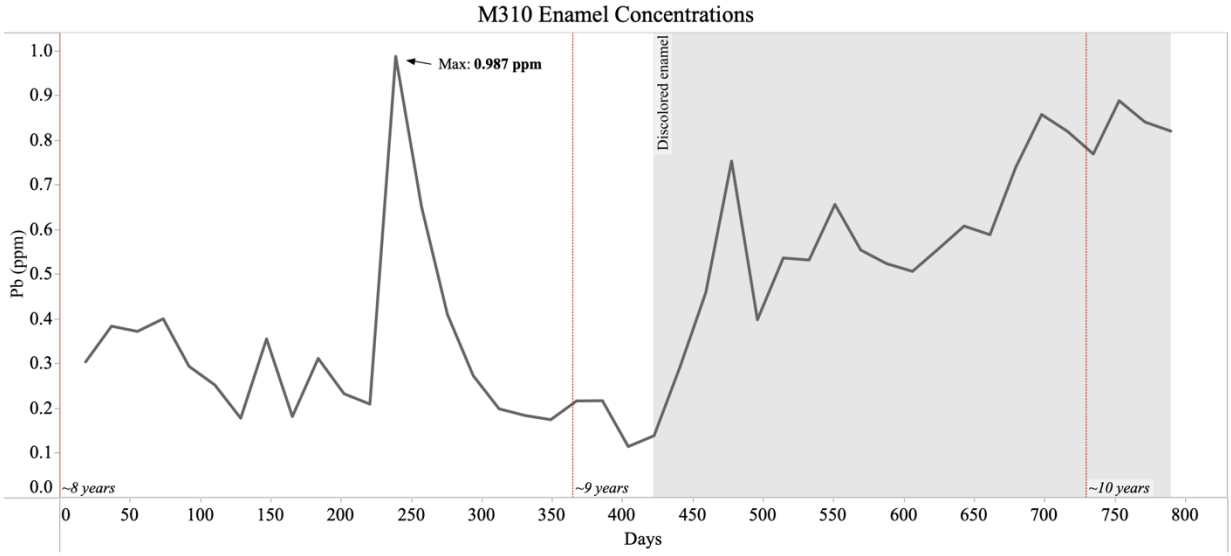


Figure 29 | Concentration of Pb along ablation transect of M310 enamel. Maximum concentration indicated. Classified as (2) variable over time. Areas highlighted in light gray represent potential postmortem alteration and are excluded from analysis.

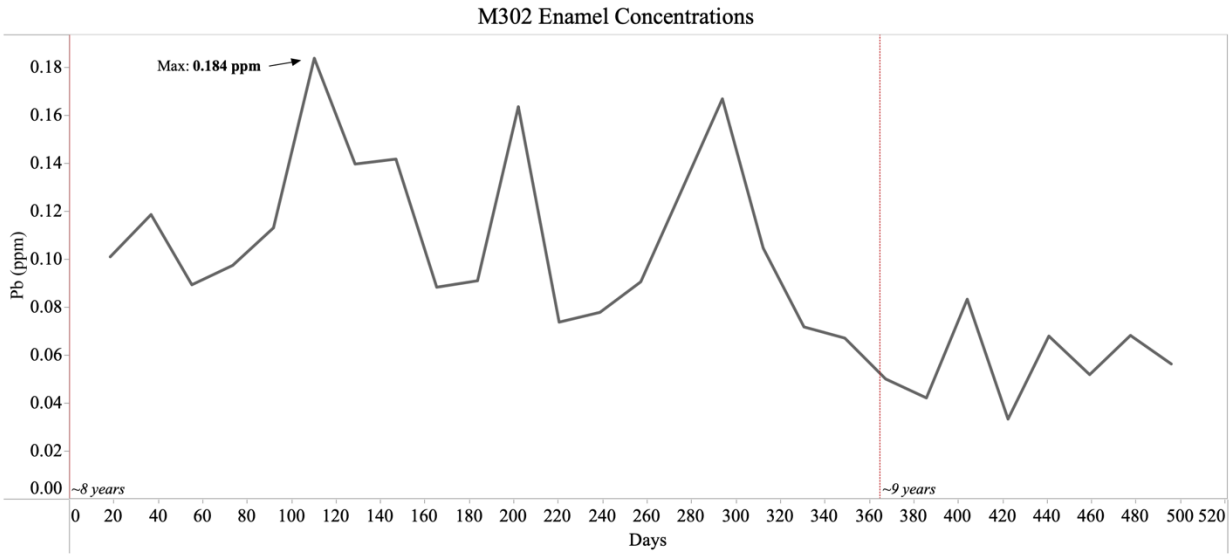


Figure 30 | Concentration of Pb along ablation transect of M302 enamel. Maximum concentration indicated. Classified as (4) decreasing over time. Areas highlighted in light gray represent potential postmortem alteration and are excluded from analysis.

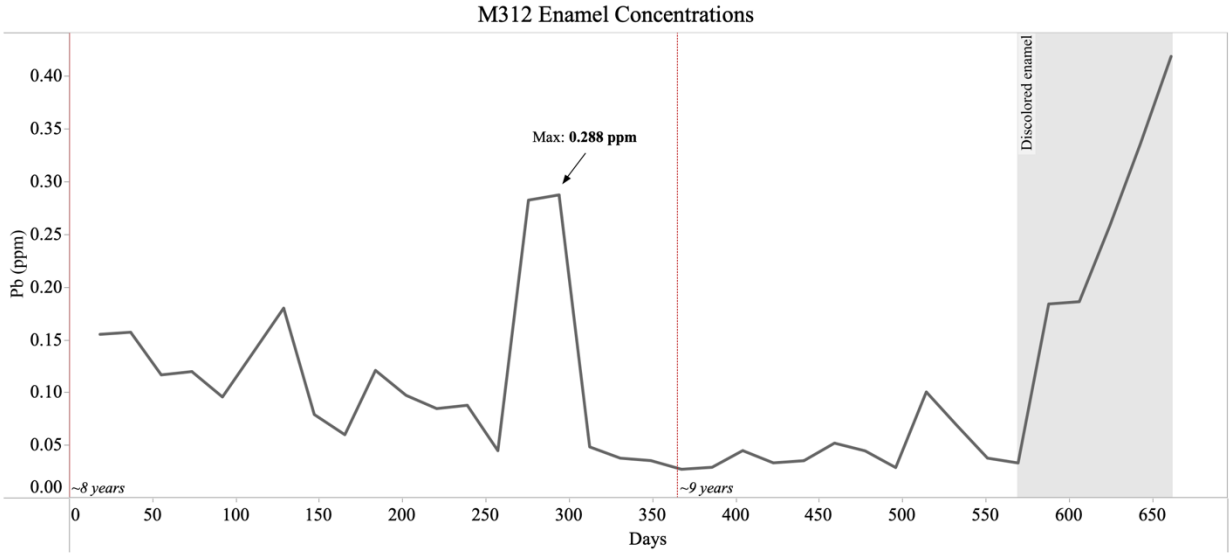


Figure 31 | Concentration of Pb along ablation transect of M312 enamel. Maximum concentration indicated. Classified as (4) decreasing over time. Areas highlighted in light gray represent potential postmortem alteration and are excluded from analysis.

4.3 | Temporal Variation of Cadmium and Arsenic Exposure During Early Life

The LA-ICP-MS instrument has higher backgrounds of Cd and As; thus, it is not as sensitive to them as is it to Pb (Dr. Chris Yakymchuk, email communication). This creates more noise in the resulting data and, therefore, it is more difficult to ascertain a pattern along the ablation transect. As such, results for Cd and As are presented as having concentrations above or below their average limit of detection (LOD) along the ablation transect. The average LOD's for Cd and As were 0.2 ppm and 0.5 ppm, respectively, and are marked by a blue line in data visualizations. Minimum and maximum concentrations and an indication of concentrations as above or below each heavy metal's LOD can be found in Table 7.

Tooth ID	Cd Min - Max (ppm)	Limit of Detection	As Min – Max (ppm)	Limit of Detection
M101	0.020-0.416	Above	0-0.648	Above
M102	0-0.271	Above	0-0.639	Above
M103	0-0.261	Above	0-0.465	Below
M104	0.002-0.317	Above	0-0.508	Above
M105*	N/A	N/A	N/A	N/A
M106	0-0.381	Above	0-0.591	Above
M107*	N/A	N/A	N/A	N/A
M108	0-0.199	Below	0-0.769	Above
M109	0-0.354	Below	0-0.849	Above
M110*	N/A	N/A	N/A	N/A
M111	0-0.172	Below	0-0.598	Above
M301	0-0.275	Above	0-0.638	Above
M302	0.026-0.351	Above	0-0.682	Above
M303	0.002-0.537	Above	0-0.472	Below
M304	0.007-0.311	Above	0-1.415	Above
M305*	N/A	N/A	N/A	N/A
M306	0-0.319	Above	0-0.359	Below
M307*	N/A	N/A	N/A	N/A
M308	0-0.354	Above	0-0.848	Above
M309*	N/A	N/A	N/A	N/A
M310	0-0.267	Above	0-0.659	Above
M311	0.008-0.504	Above	0-1.007	Above
M312	0-0.351	Above	0-0.754	Above
PM01	0-0.572	Above	0-0.778	Above
PM02	0-0.448	Above	0-0.674	Above
PM03	0-0.287	Above	0-0.615	Above
PM04*	N/A	N/A	N/A	N/A
PM05	0-0.498	Above	0-0.599	Above
PM06	0-0.299	Above	0-0.913	Above

Table 7 | Minimum and maximum concentrations for Cd and As found in each tooth and an indication of concentrations as above or below each heavy metal's LOD.

4.3.1 | Temporal Variation of Cadmium and Arsenic in First Molars (~30 weeks *in utero* to ~3 years old)

Of the eight first molars included in the main analysis, five (M101, M102, M103, M104, and M106) have peaks rising above the average LOD (0.2 ppm) for Cd (Figures 32-36). Concentrations in the other three first molars (M108, M109, and M111) remain below the average LOD along their ablation transects (Figures 37-39). For As, seven first molars (M101, M102, M104, M106, M108, M109, and M111) have peaks rising above the average LOD (0.5 ppm) (Figures 40-46) and one (M103) that remains below (Figure 47).

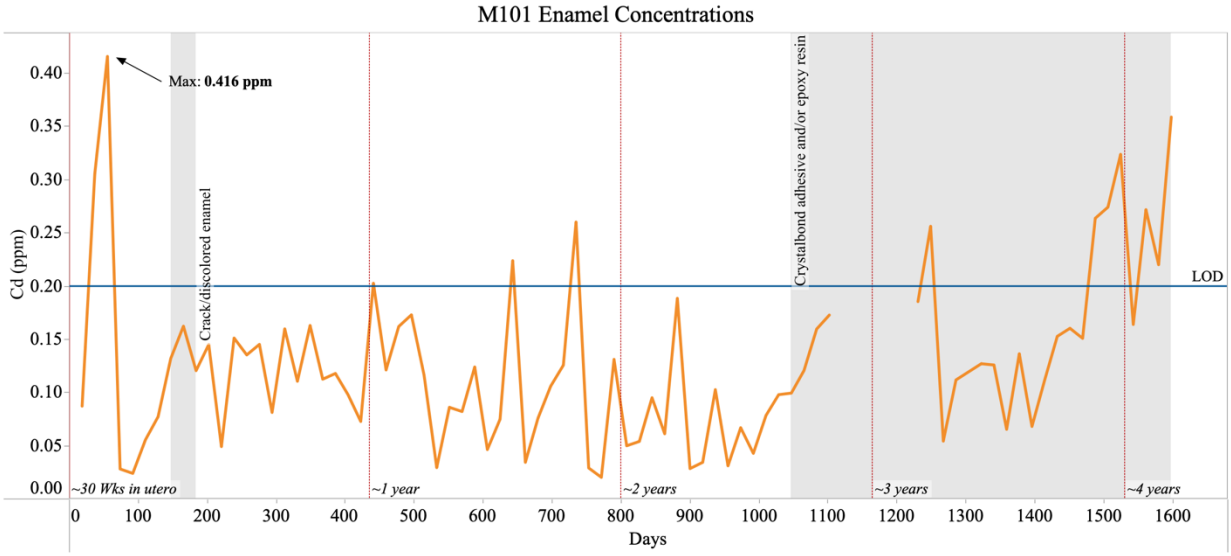


Figure 32 | Concentration of Cd along ablation transect of M101 enamel. LOD indicated by blue line. Areas highlighted in light gray represent potential postmortem alteration and are excluded from analysis.

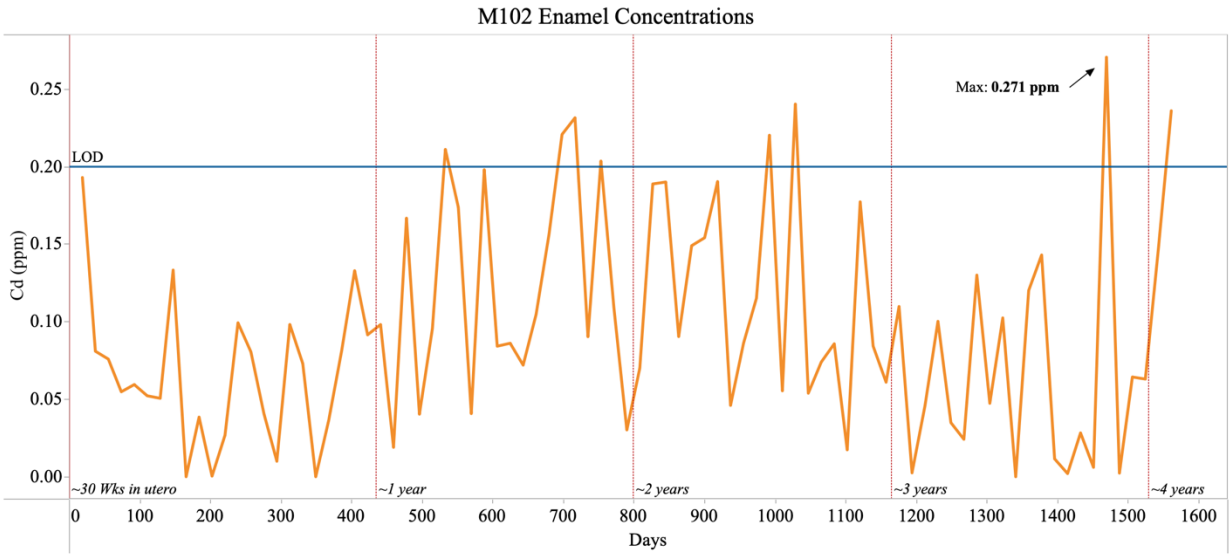


Figure 33 | Concentration of Cd along ablation transect of M102 enamel. LOD indicated by blue line. Areas highlighted in light gray represent potential postmortem alteration and are excluded from analysis.

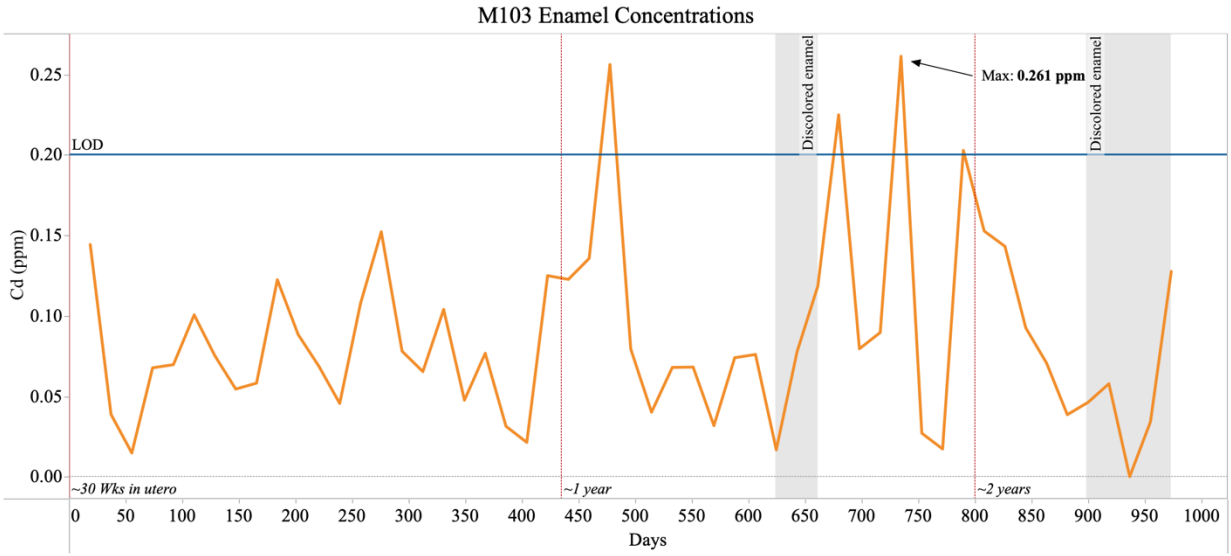


Figure 34 | Concentration of Cd along ablation transect of M103 enamel. LOD indicated by blue line. Areas highlighted in light gray represent potential postmortem alteration and are excluded from analysis.

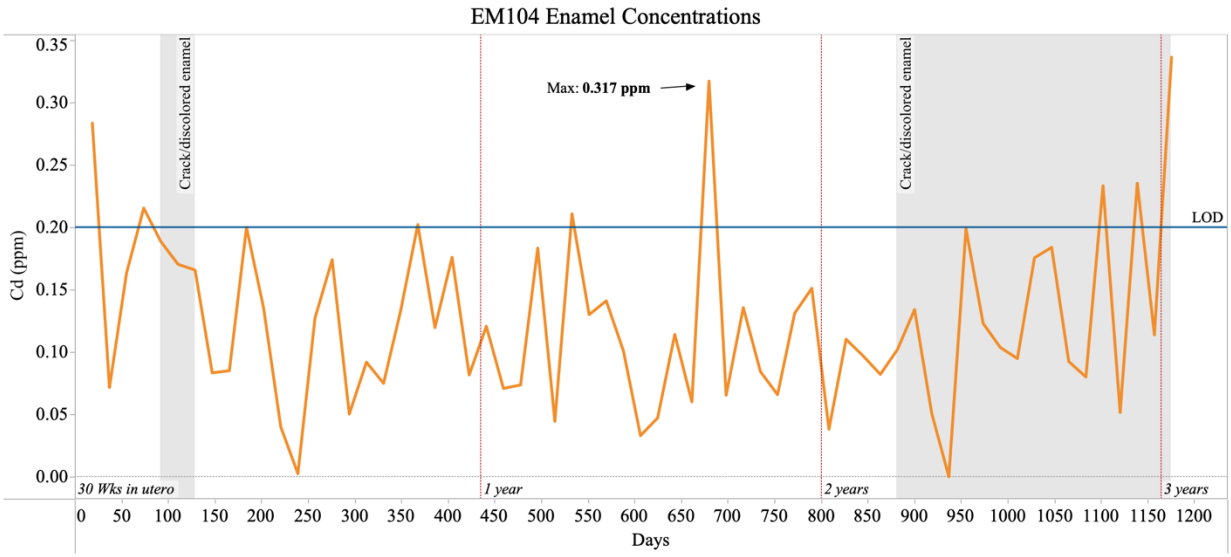


Figure 35 | Concentration of Cd along ablation transect of M104 enamel. LOD indicated by blue line. Areas highlighted in light gray represent potential postmortem alteration and are excluded from analysis.

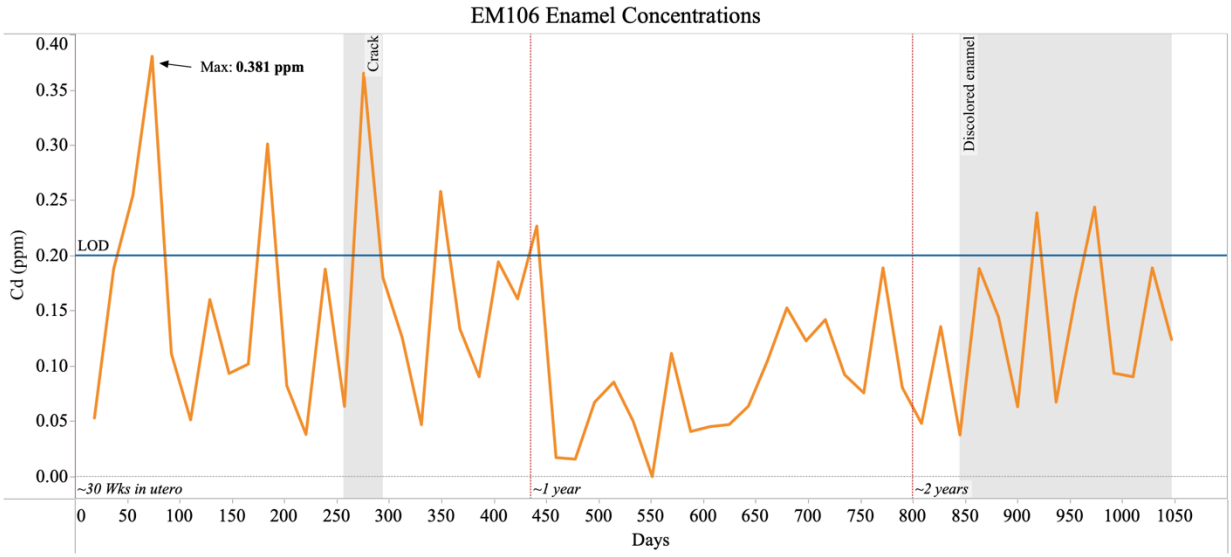


Figure 36 | Concentration of Cd along ablation transect of M106 enamel. LOD indicated by blue line. Areas highlighted in light gray represent potential postmortem alteration and are excluded from analysis.

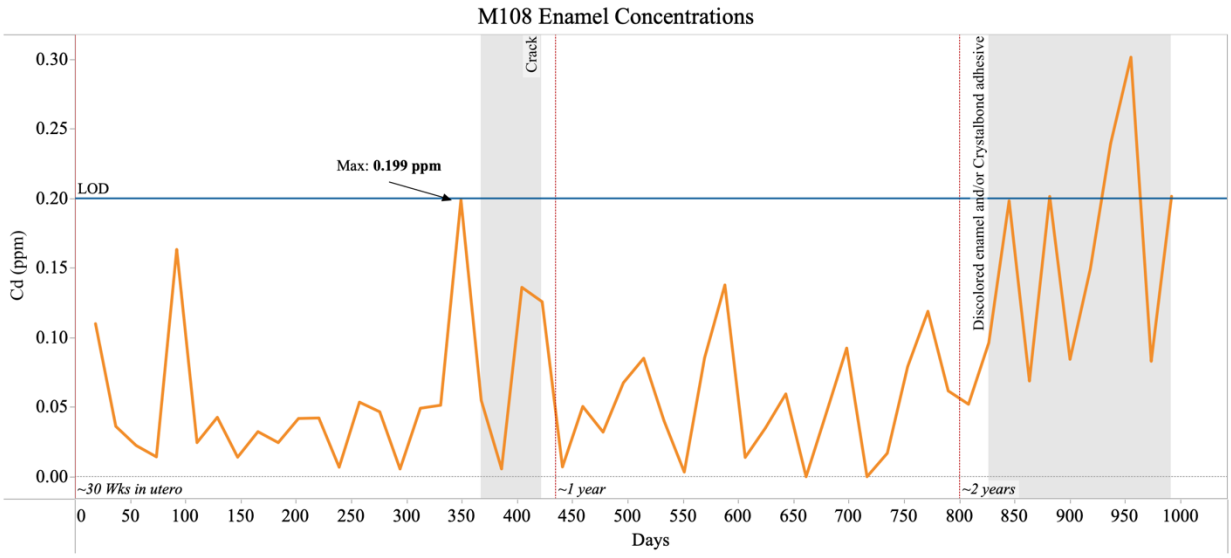


Figure 37 | Concentration of Cd along ablation transect of M108 enamel. LOD indicated by blue line. Areas highlighted in light gray represent potential postmortem alteration and are excluded from analysis.

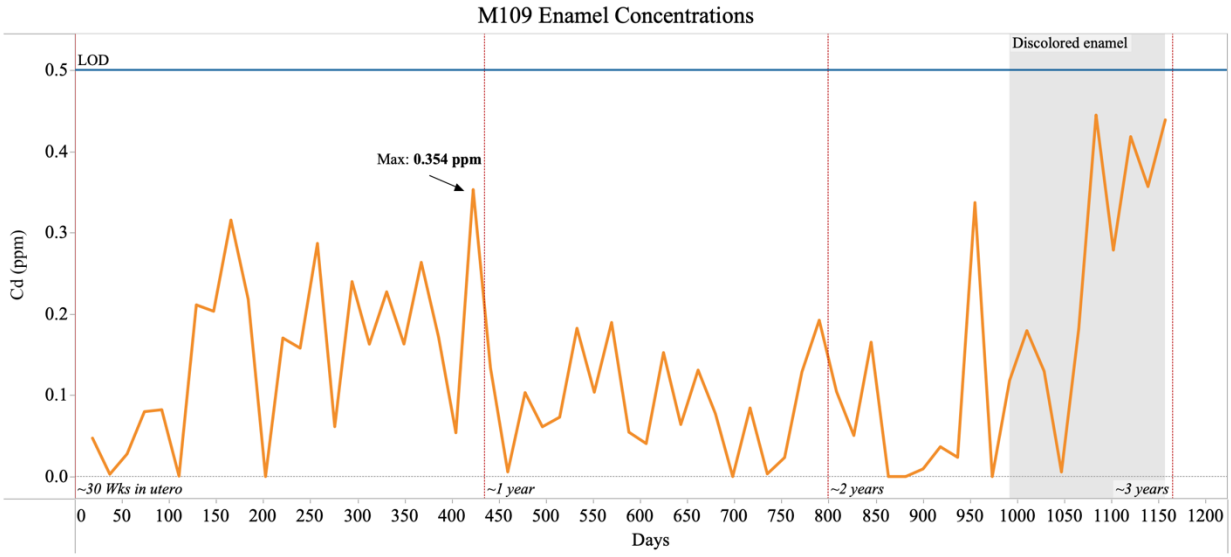


Figure 38 | Concentration of Cd along ablation transect of M109 enamel. LOD indicated by blue line. Areas highlighted in light gray represent potential postmortem alteration and are excluded from analysis.

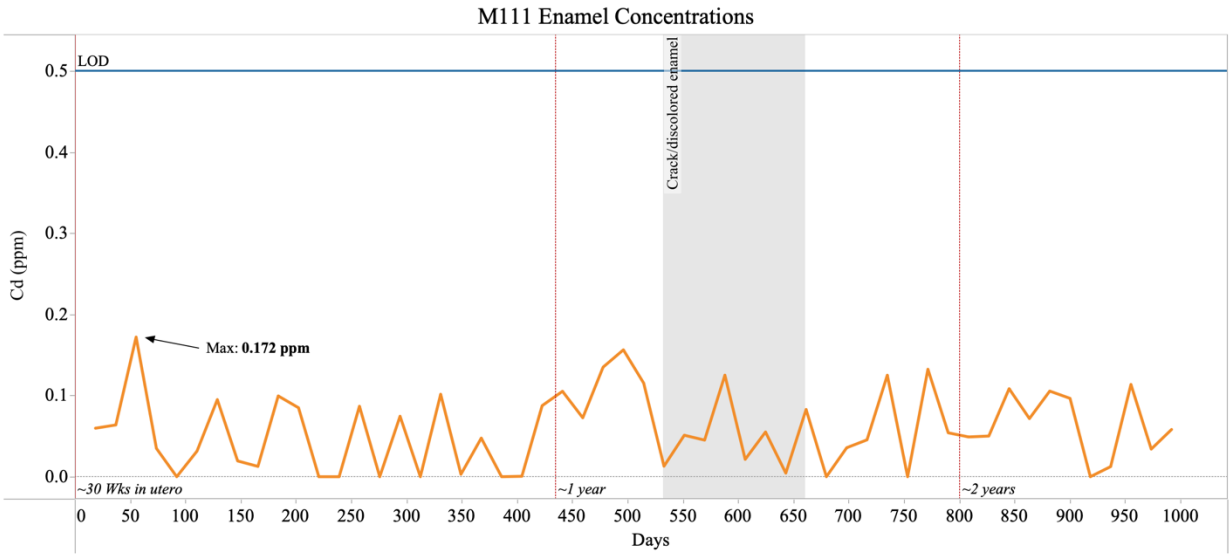


Figure 39 | Concentration of Cd along ablation transect of M111 enamel. LOD indicated by blue line. Areas highlighted in light gray represent potential postmortem alteration and are excluded from analysis.

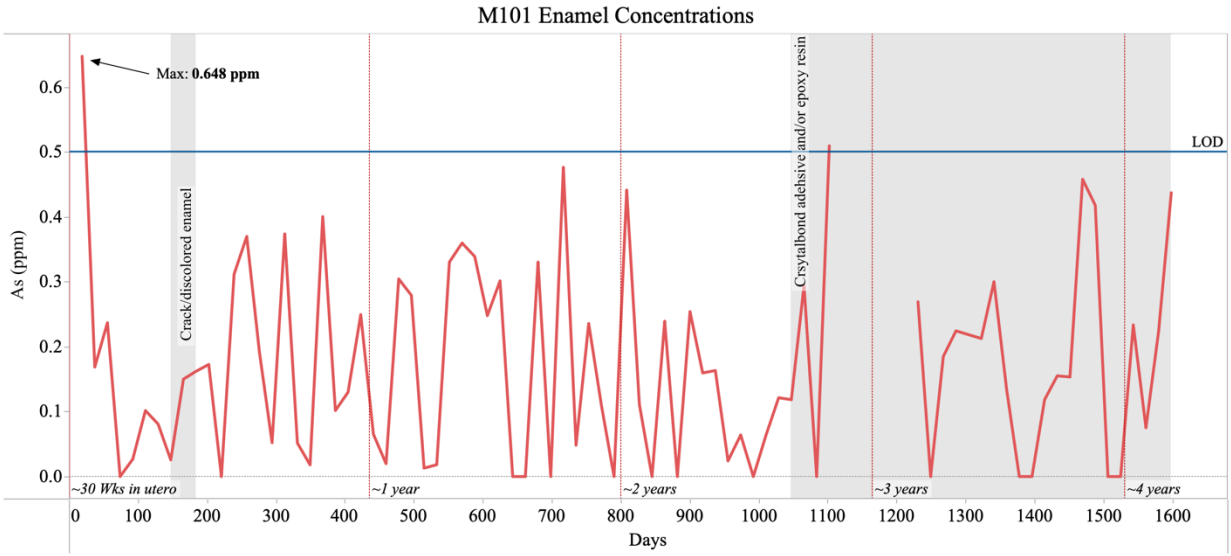


Figure 40 | Concentration of As along ablation transect of M101 enamel. LOD indicated by blue line. Areas highlighted in light gray represent potential postmortem alteration and are excluded from analysis.

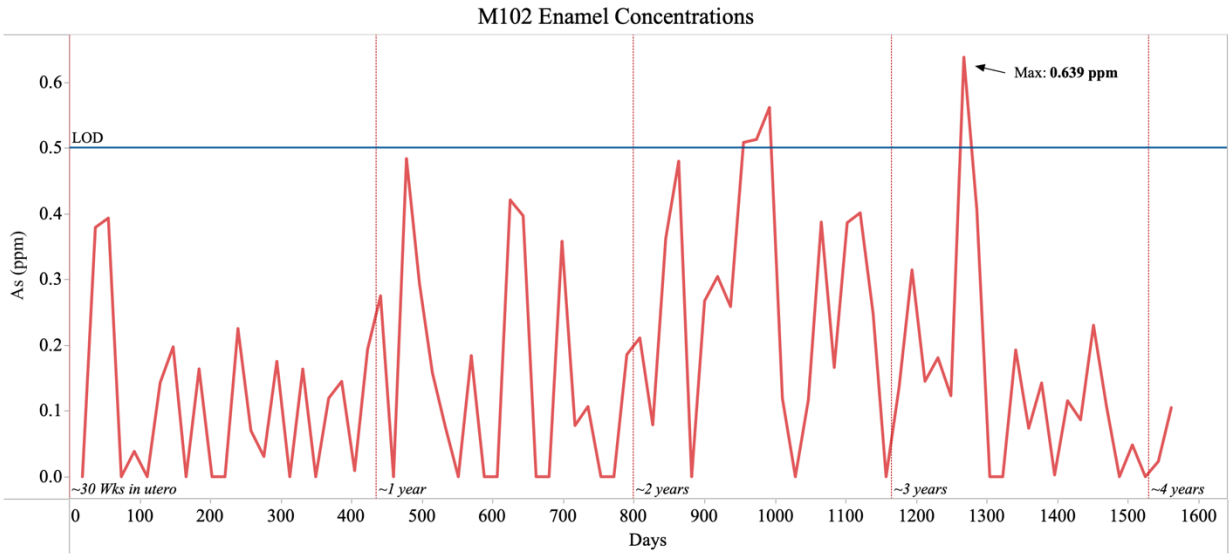


Figure 41 | Concentration of As along ablation transect of M102 enamel. LOD indicated by blue line. Areas highlighted in light gray represent potential postmortem alteration and are excluded from analysis.

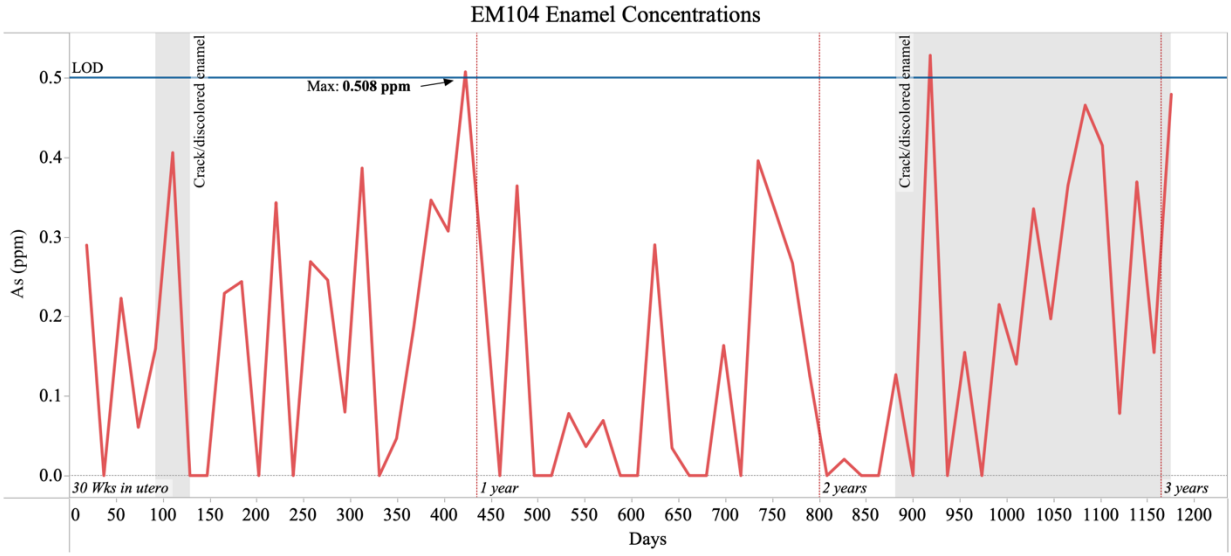


Figure 42 | Concentration of As along ablation transect of M104 enamel. LOD indicated by blue line. Areas highlighted in light gray represent potential postmortem alteration and are excluded from analysis.

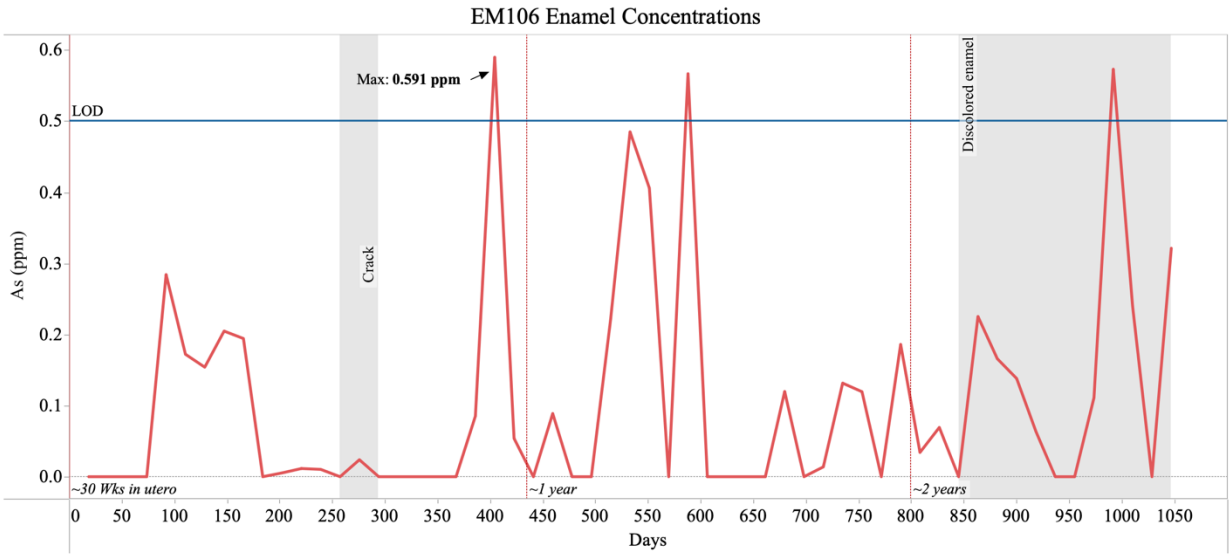


Figure 43 | Concentration of As along ablation transect of M106 enamel. LOD indicated by blue line. Areas highlighted in light gray represent potential postmortem alteration and are excluded from analysis.

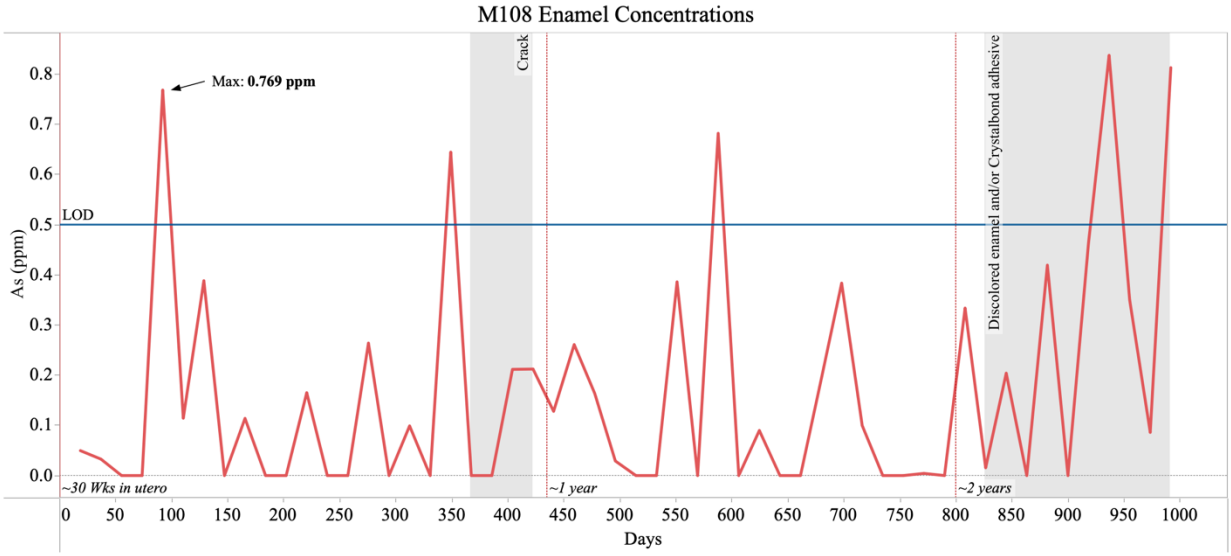


Figure 44 | Concentration of As along ablation transect of M108 enamel. LOD indicated by blue line. Areas highlighted in light gray represent potential postmortem alteration and are excluded from analysis.

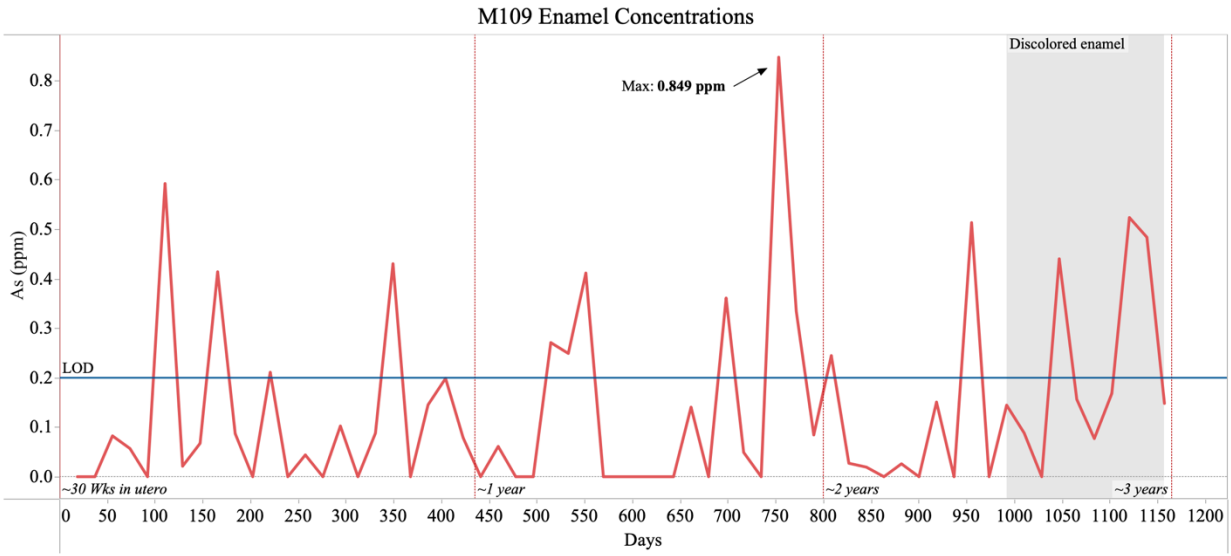


Figure 45 | Concentration of As along ablation transect of M109 enamel. LOD indicated by blue line. Areas highlighted in light gray represent potential postmortem alteration and are excluded from analysis.

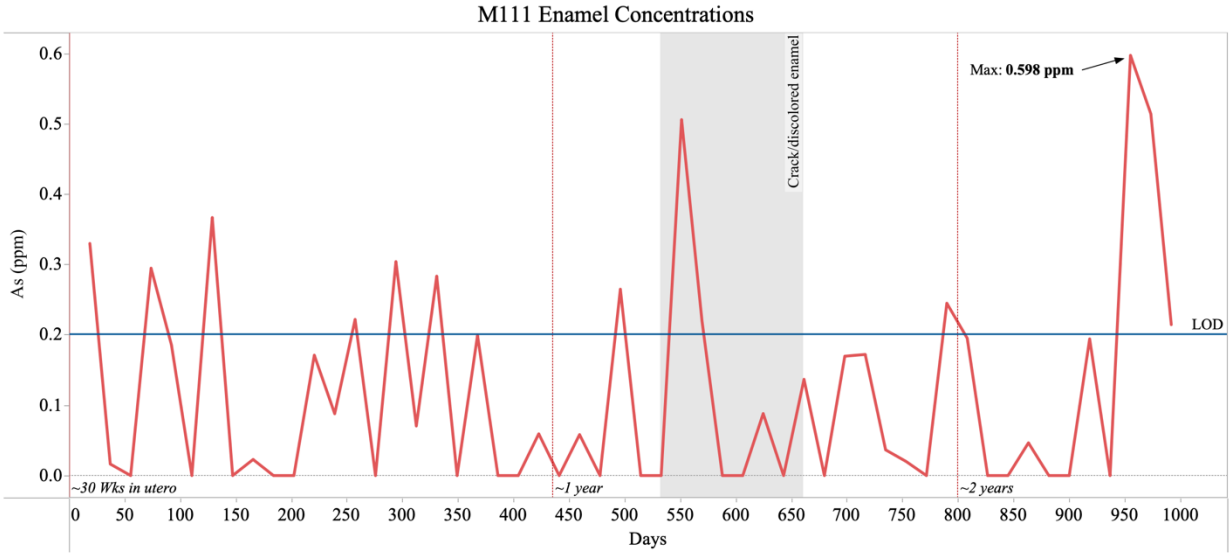


Figure 46 | Concentration of As along ablation transect of M111 enamel. LOD indicated by blue line. Areas highlighted in light gray represent potential postmortem alteration and are excluded from analysis.

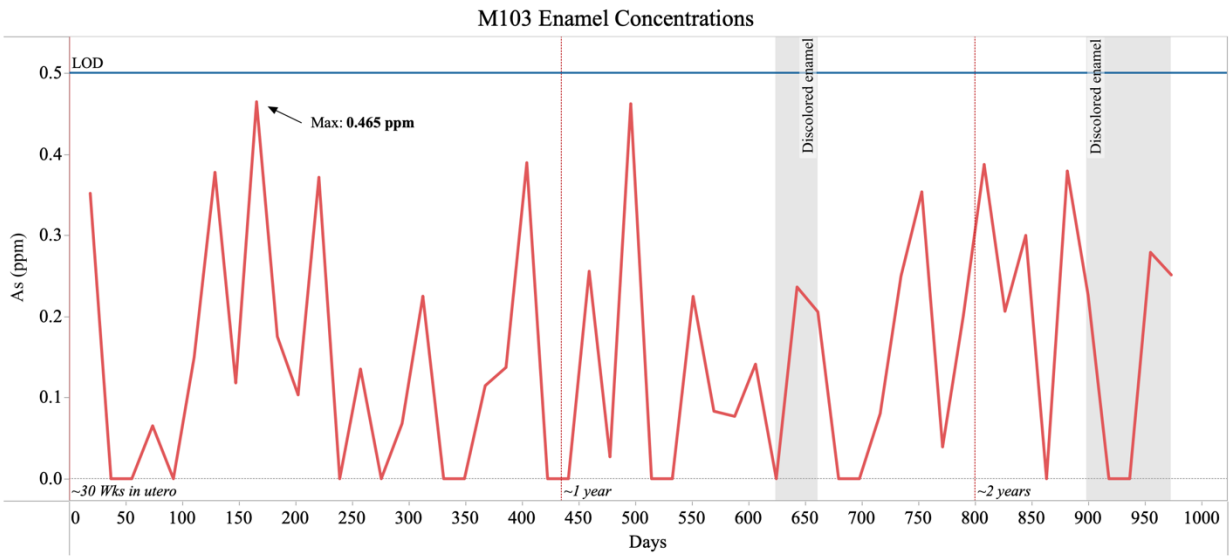


Figure 47 | Concentration of As along ablation transect of M103 enamel. LOD indicated by blue line. Areas highlighted in light gray represent potential postmortem alteration and are excluded from analysis.

4.3.2 | Temporal Variation of Cadmium and Arsenic in Premolars (~1.8-2.8 to ~5-6 years old)

All five premolars (PM01, PM02, PM03, PM05, and PM06) included in the main analysis have concentrations that rise above Cd's average LOD (0.2 ppm) (Figure 48-52). Similarly, all five premolars also have As concentrations that rise above the average LOD (0.5 ppm) (Figures 53-57).

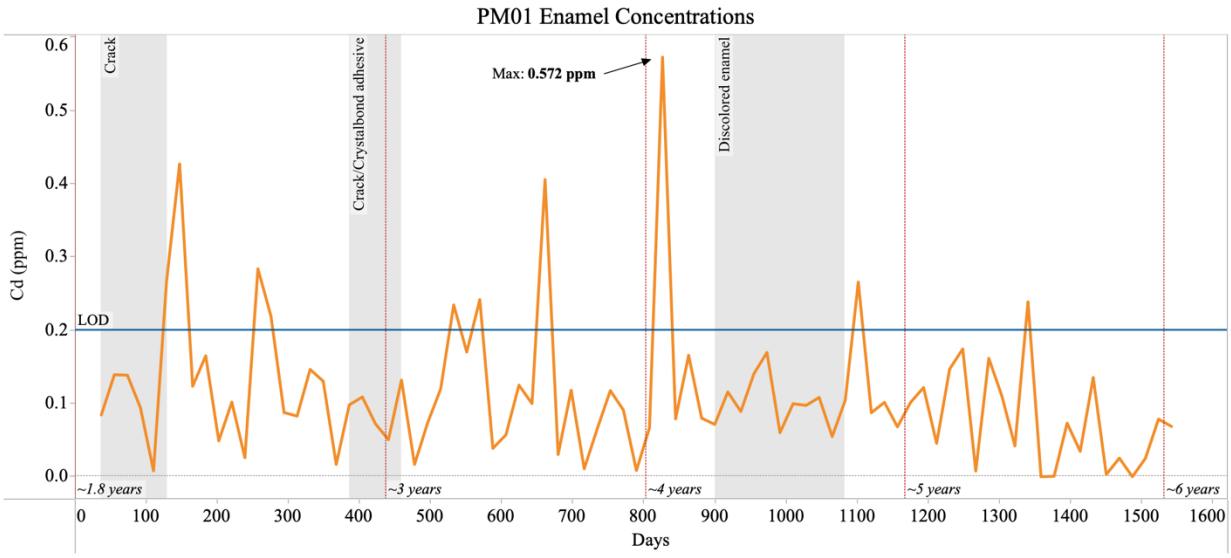


Figure 48 | Concentration of Cd along ablation transect of PM01 enamel. LOD indicated by blue line. Areas highlighted in light gray represent potential postmortem alteration and are excluded from analysis.

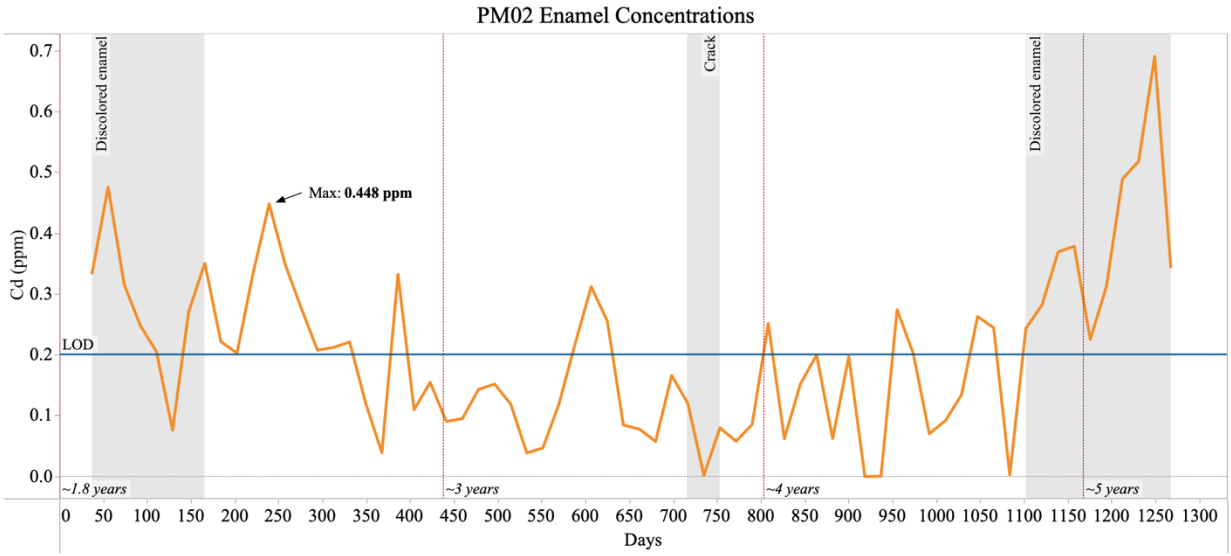


Figure 49 | Concentration of Cd along ablation transect of PM06 enamel. LOD indicated by blue line. Areas highlighted in light gray represent potential postmortem alteration and are excluded from analysis.

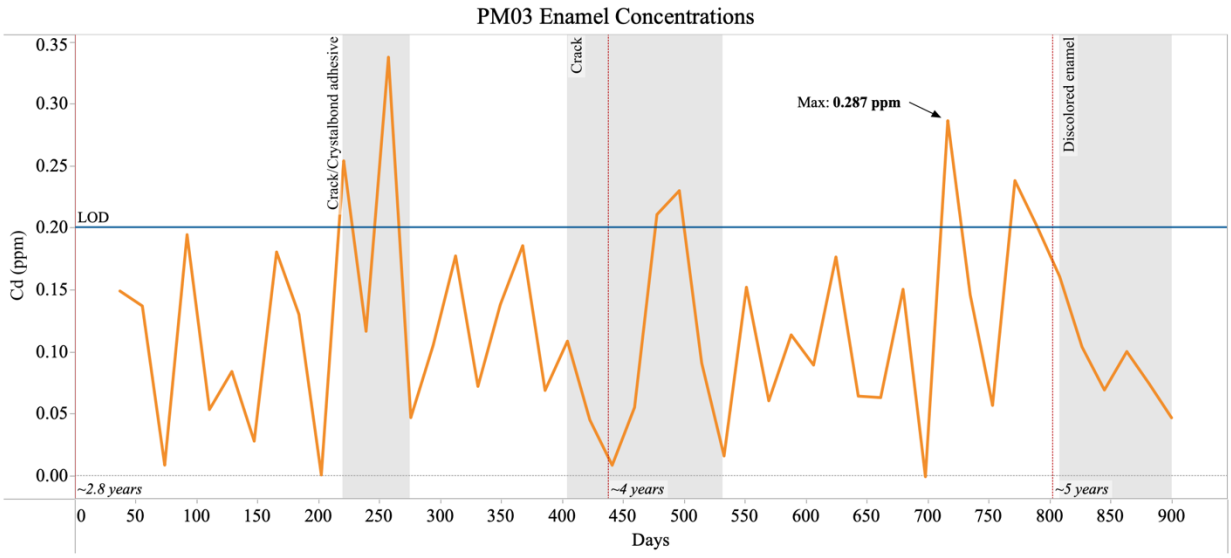


Figure 50 | Concentration of Cd along ablation transect of PM06 enamel. LOD indicated by blue line. Areas highlighted in light gray represent potential postmortem alteration and are excluded from analysis.

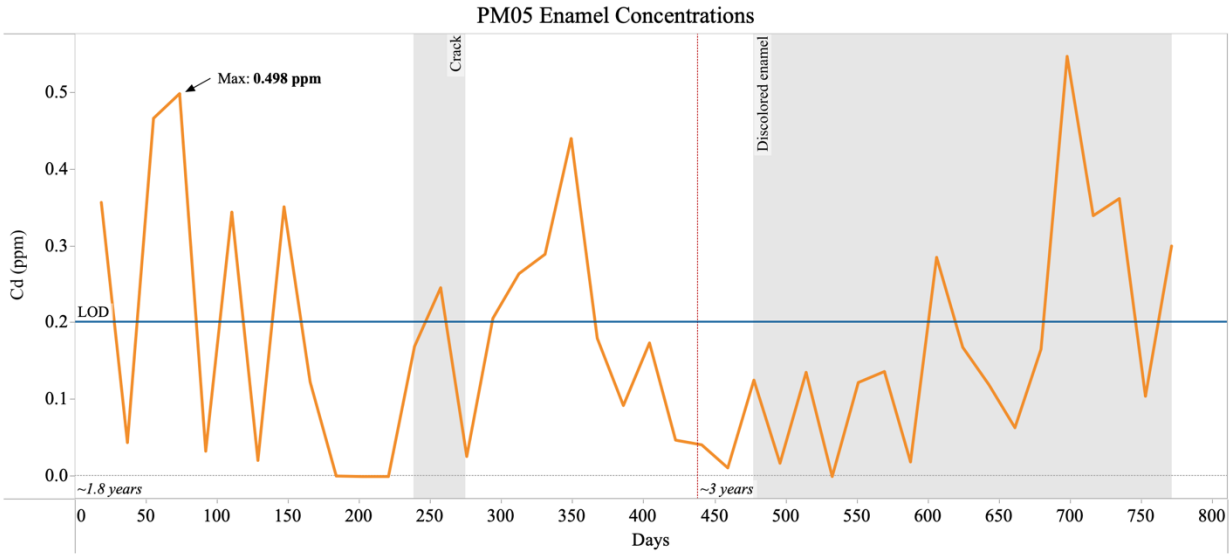


Figure 51 | Concentration of Cd along ablation transect of PM06 enamel. LOD indicated by blue line. Areas highlighted in light gray represent potential postmortem alteration and are excluded from analysis.

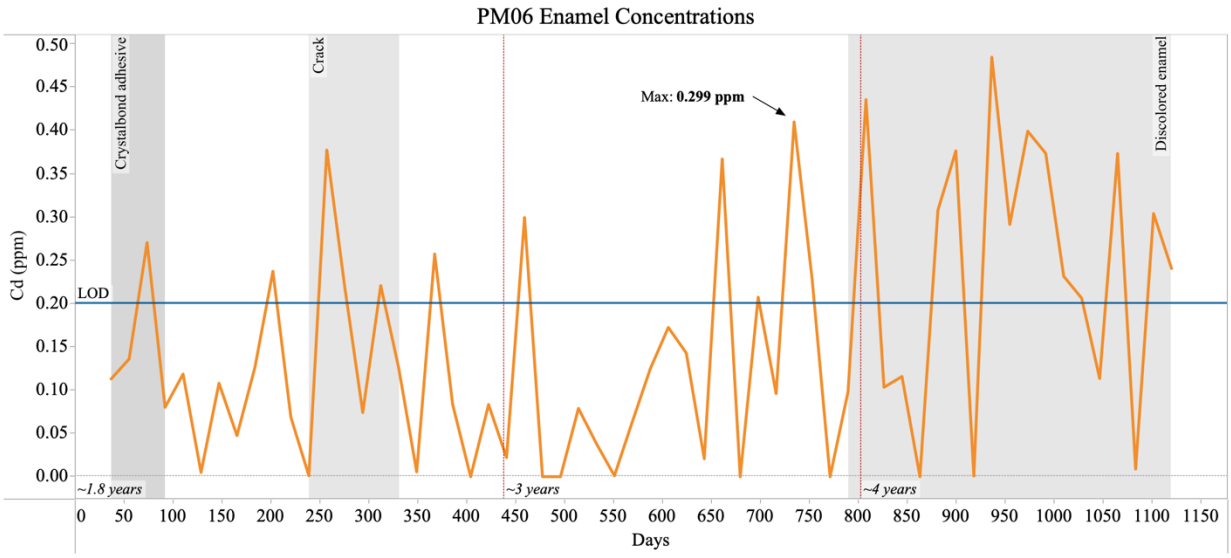


Figure 52 | Concentration of Cd along ablation transect of PM06 enamel. LOD indicated by blue line. Areas highlighted in light gray represent potential postmortem alteration and are excluded from analysis.

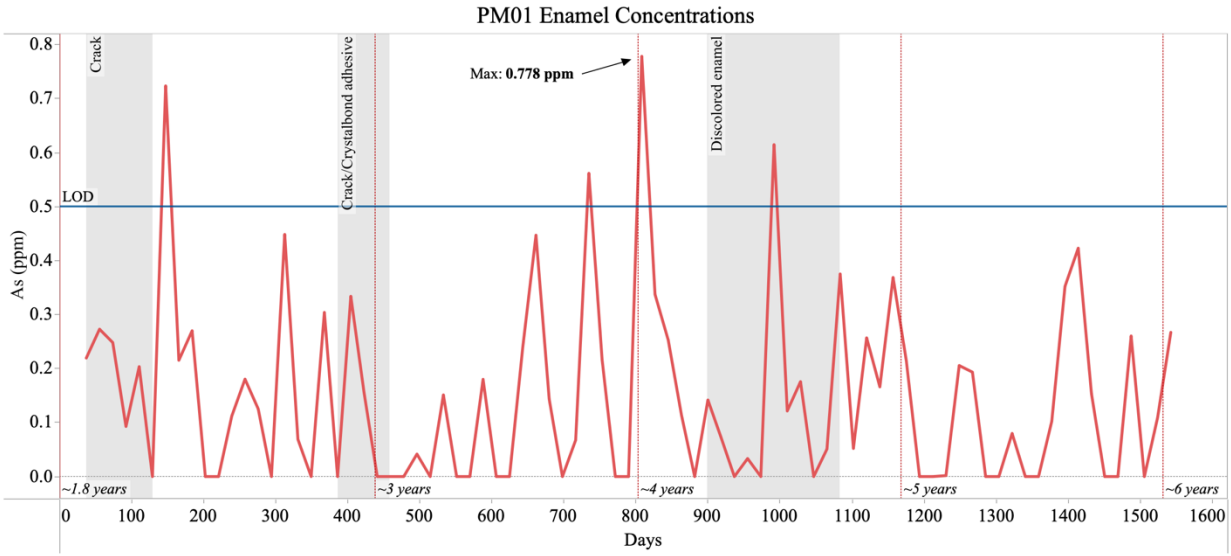


Figure 53 | Concentration of As along ablation transect of PM01 enamel. LOD indicated by blue line. Areas highlighted in light gray represent potential postmortem alteration and are excluded from analysis.

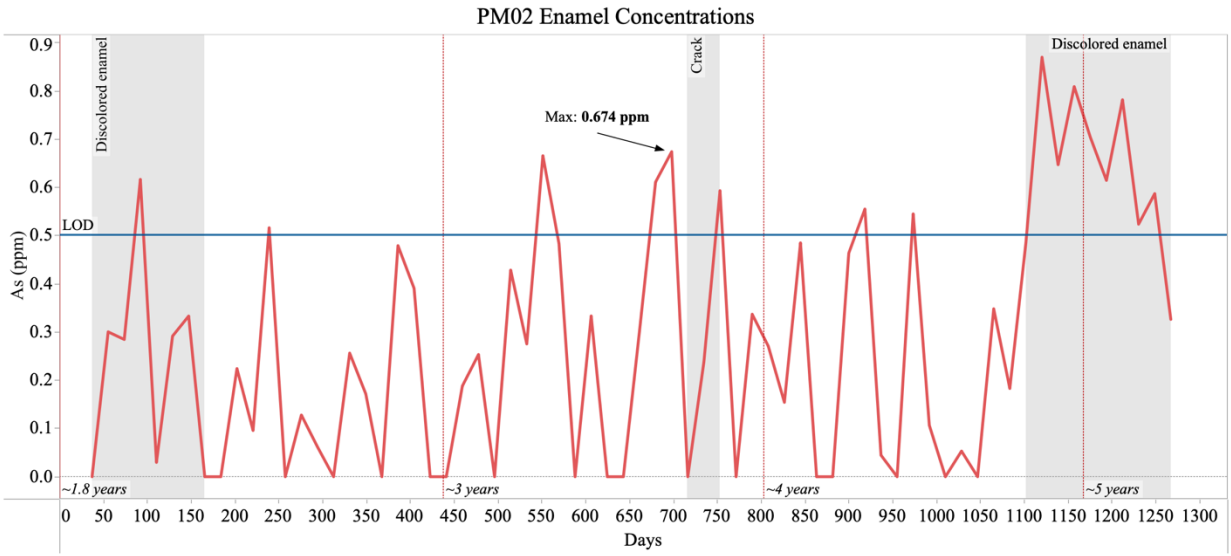


Figure 54 | Concentration of As along ablation transect of PM02 enamel. LOD indicated by blue line. Areas highlighted in light gray represent potential postmortem alteration and are excluded from analysis.

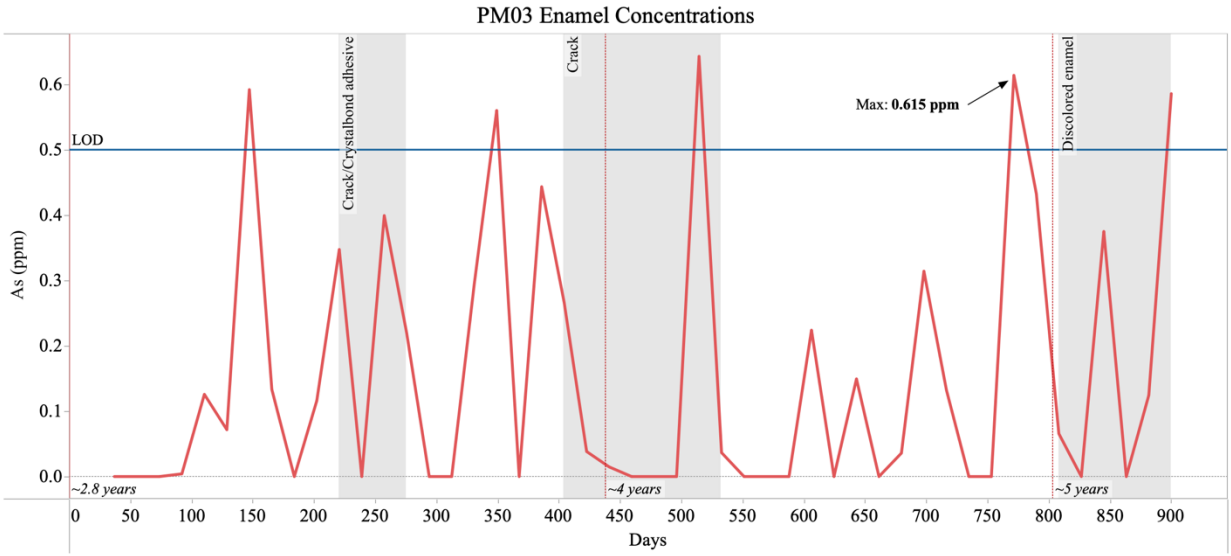


Figure 55 | Concentration of As along ablation transect of PM03 enamel. LOD indicated by blue line. Areas highlighted in light gray represent potential postmortem alteration and are excluded from analysis.

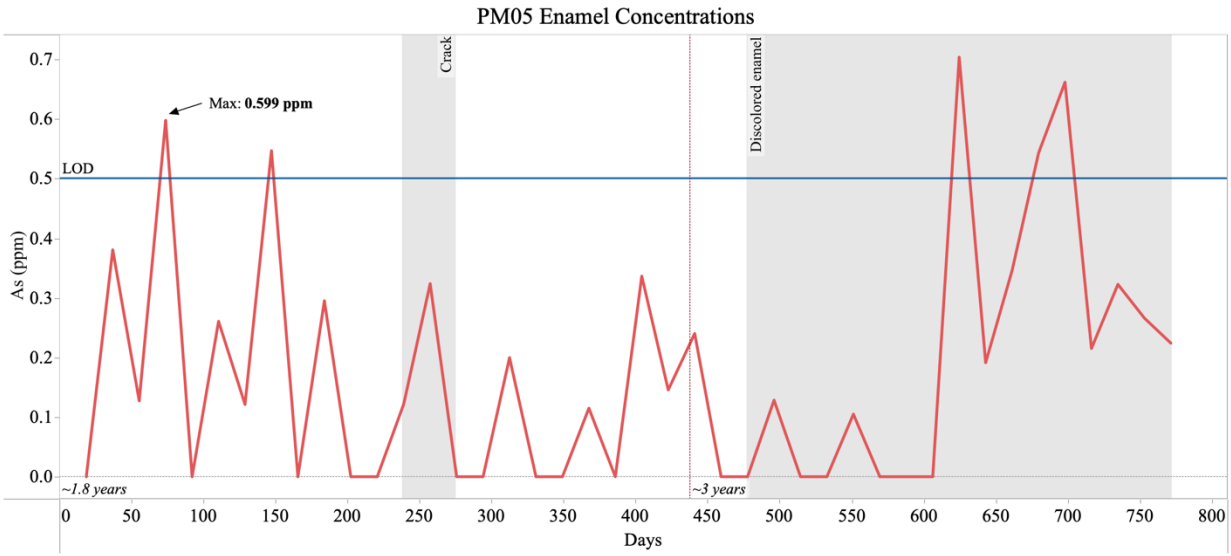


Figure 56 | Concentration of As along ablation transect of PM05 enamel. LOD indicated by blue line. Areas highlighted in light gray represent potential postmortem alteration and are excluded from analysis.

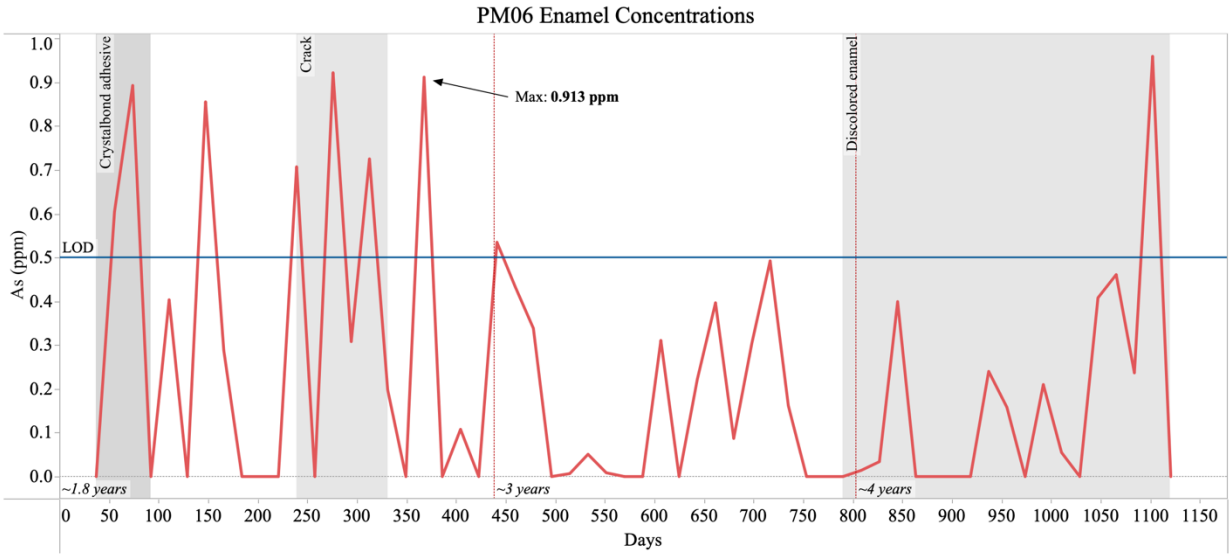


Figure 57 | Concentration of As along ablation transect of PM06 enamel. LOD indicated by blue line. Areas highlighted in light gray represent potential postmortem alteration and are excluded from analysis.

4.3.3 | Temporal Variation of Cadmium and Arsenic in Third Molars (~8 to ~11 years old)

All nine third molars (M301, M302, M303, M304, M306, M308, M310, M311, and M312) have Cd concentrations that rise above the average LOD (0.2 ppm) (Figures 58-66). For As, seven of the nine third molars (M301, M302, M304, M308, M310, M311, and M312) rise above the average LOD (0.5 ppm) (Figures 67-73) and two (M303 and M306) fall below the average LOD (Figures 74 and 75).

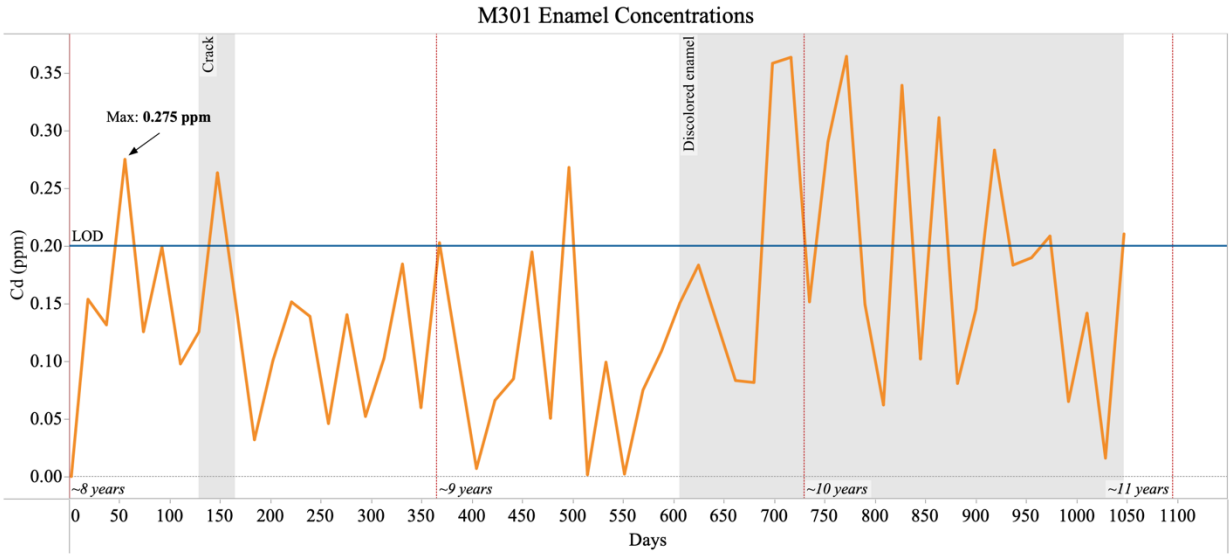


Figure 58 | Concentration of Cd along ablation transect of M301 enamel. LOD indicated by blue line. Areas highlighted in light gray represent potential postmortem alteration and are excluded from analysis.

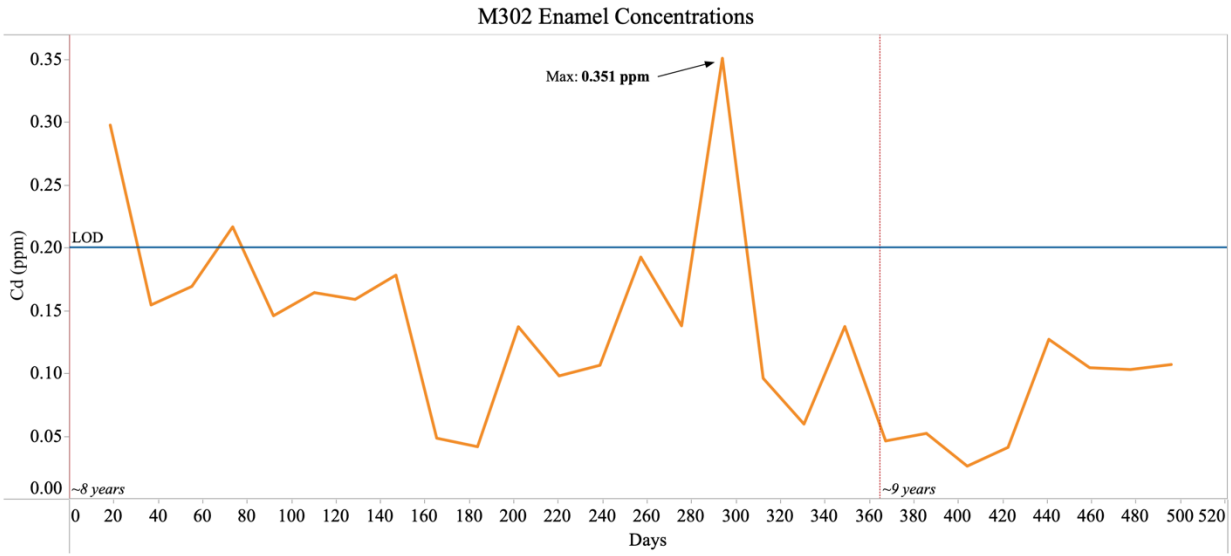


Figure 59 | Concentration of Cd along ablation transect of M302 enamel. LOD indicated by blue line. Areas highlighted in light gray represent potential postmortem alteration and are excluded from analysis.

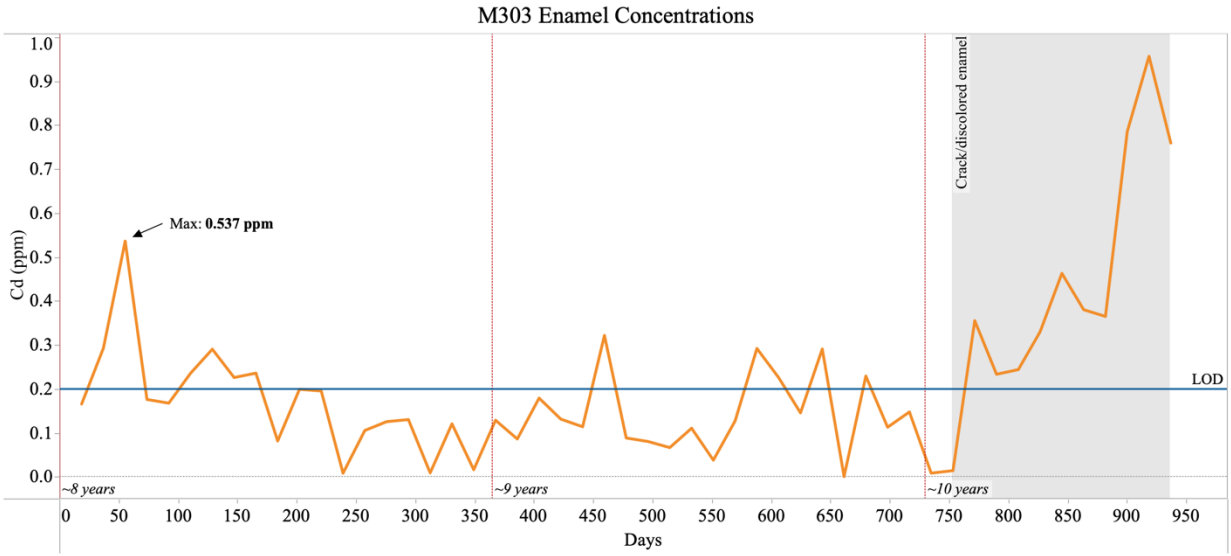


Figure 60 | Concentration of Cd along ablation transect of M303 enamel. LOD indicated by blue line. Areas highlighted in light gray represent potential postmortem alteration and are excluded from analysis.

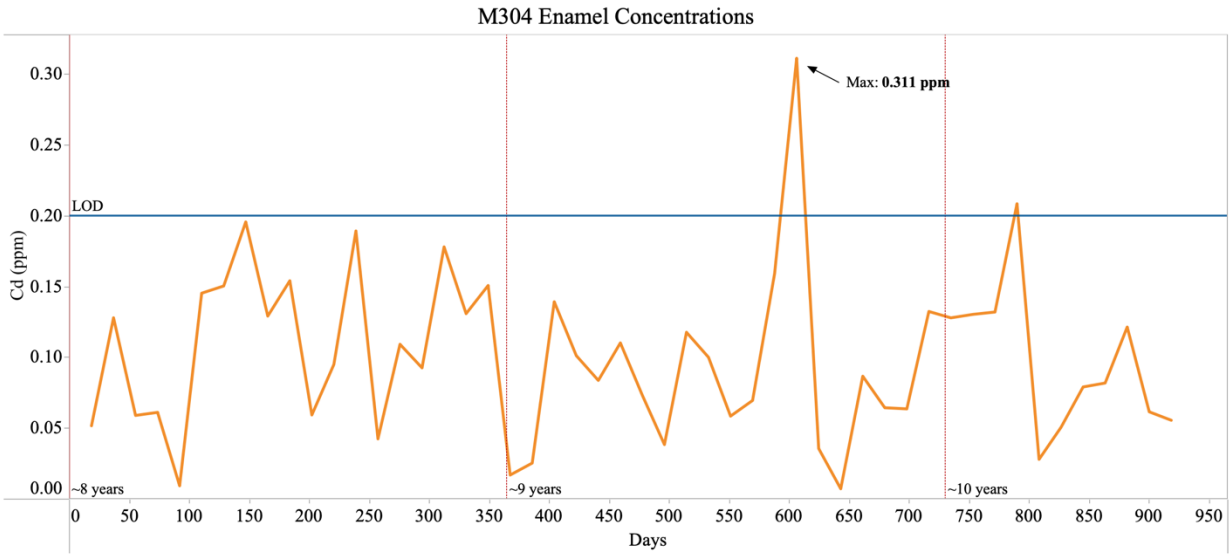


Figure 61 | Concentration of Cd along ablation transect of M304 enamel. LOD indicated by blue line. Areas highlighted in light gray represent potential postmortem alteration and are excluded from analysis.

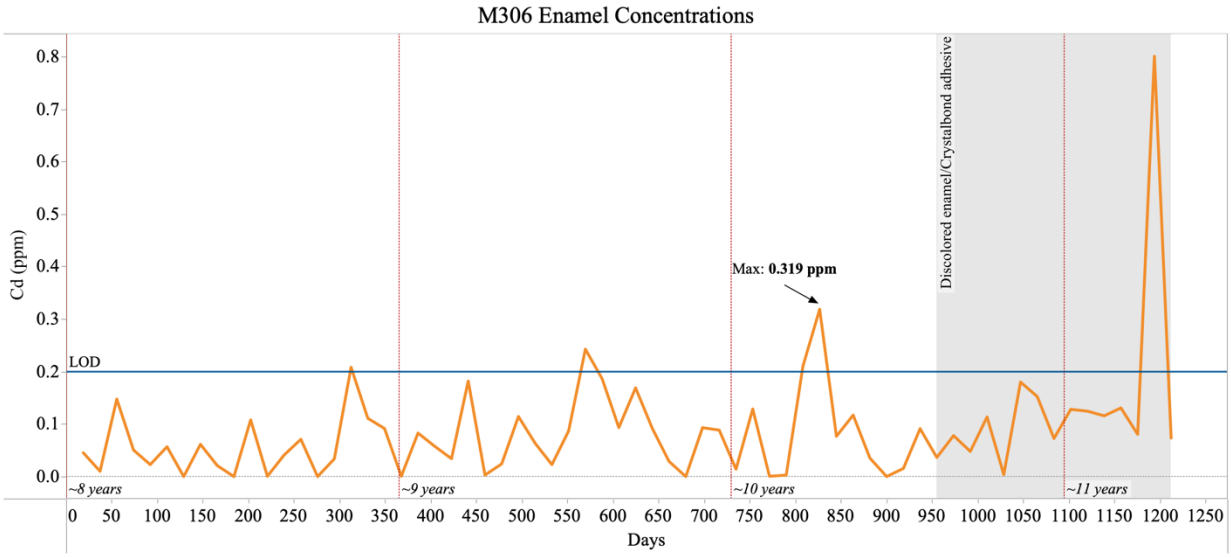


Figure 62 | Concentration of Cd along ablation transect of M306 enamel. LOD indicated by blue line. Areas highlighted in light gray represent potential postmortem alteration and are excluded from analysis.

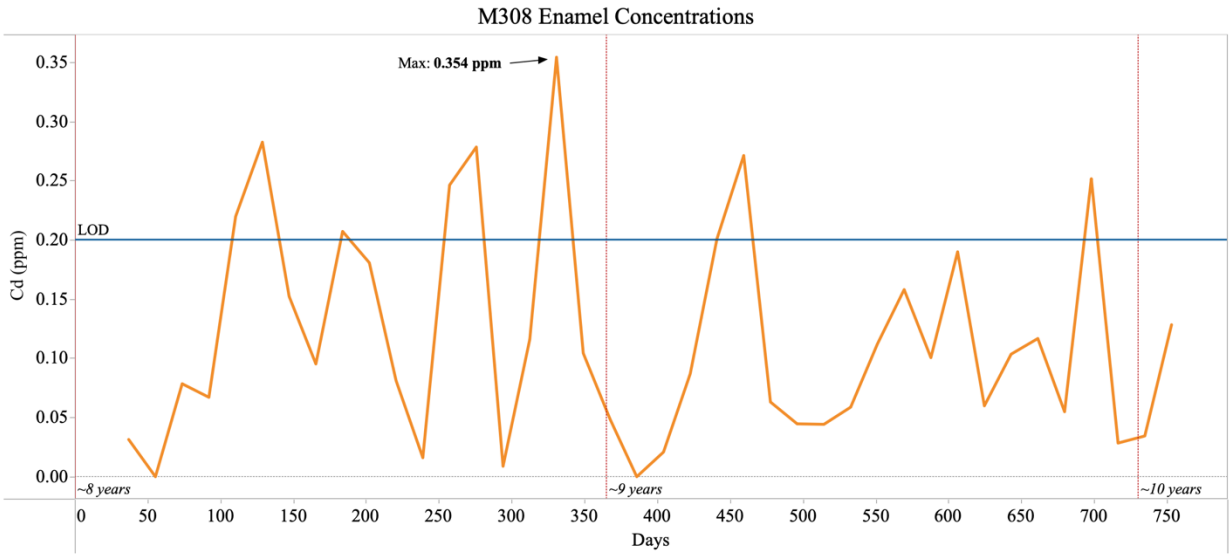


Figure 63 | Concentration of Cd along ablation transect of M308 enamel. LOD indicated by blue line. Areas highlighted in light gray represent potential postmortem alteration and are excluded from analysis.

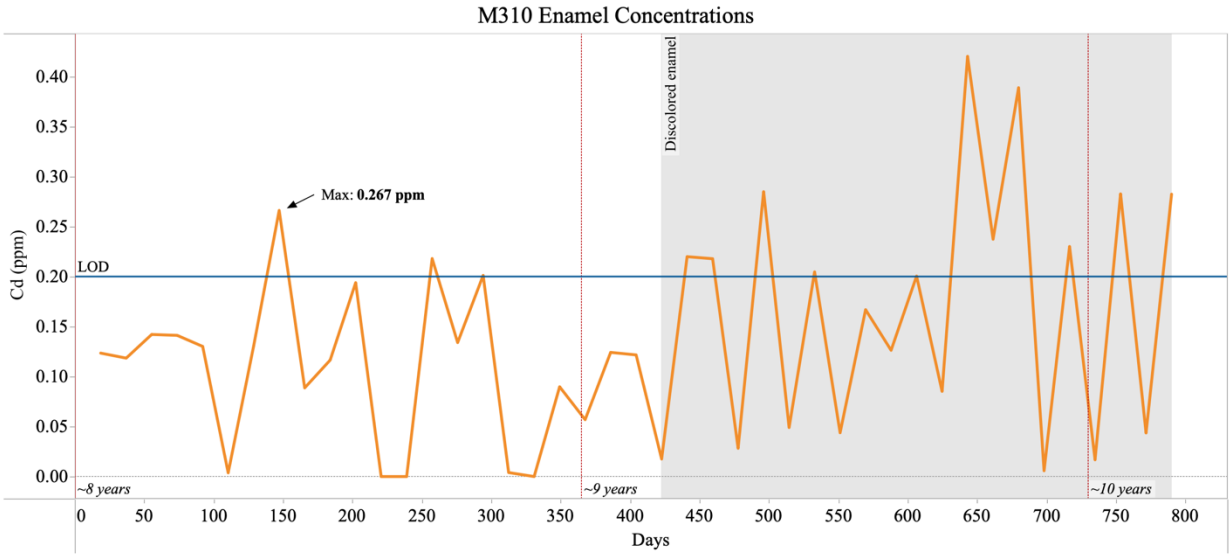


Figure 64 | Concentration of Cd along ablation transect of M310 enamel. LOD indicated by blue line. Areas highlighted in light gray represent potential postmortem alteration and are excluded from analysis.

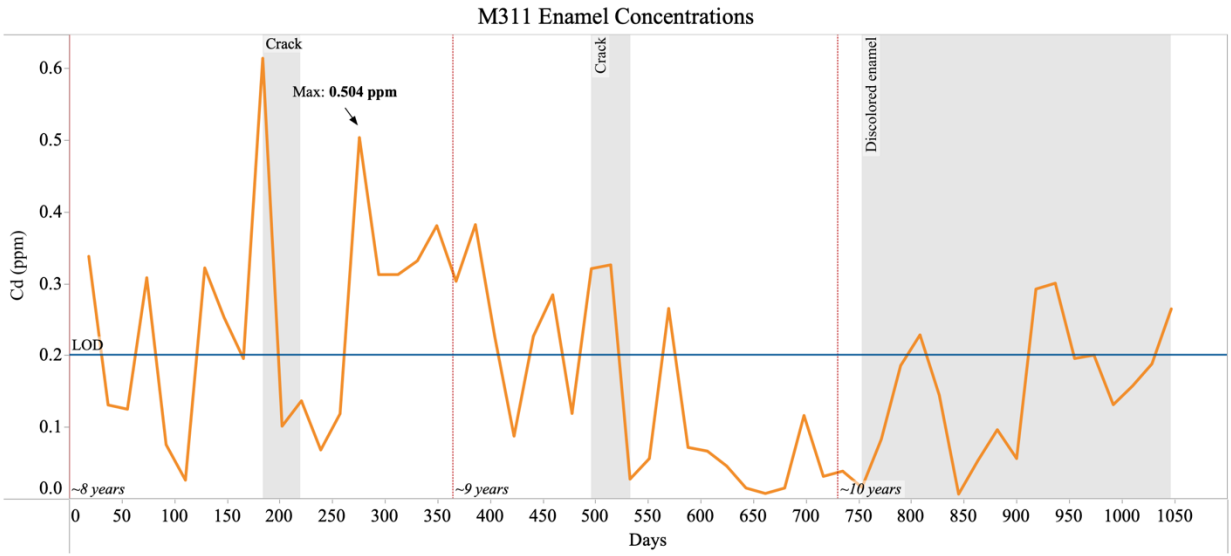


Figure 65 | Concentration of Cd along ablation transect of M311 enamel. LOD indicated by blue line. Areas highlighted in light gray represent potential postmortem alteration and are excluded from analysis.

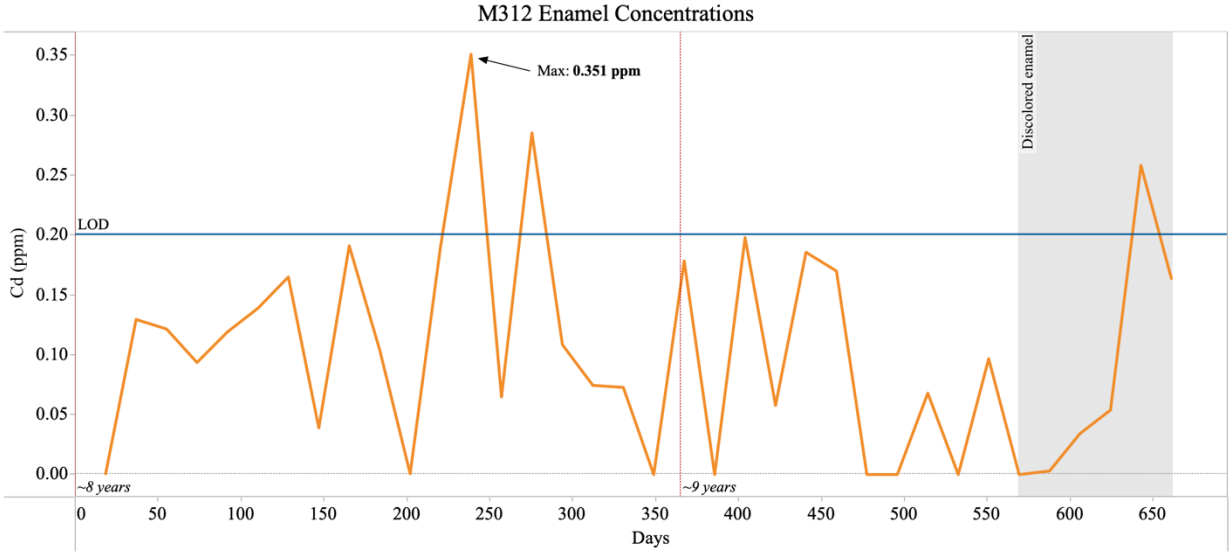


Figure 66 | Concentration of Cd along ablation transect of M312 enamel. LOD indicated by blue line. Areas highlighted in light gray represent potential postmortem alteration and are excluded from analysis.

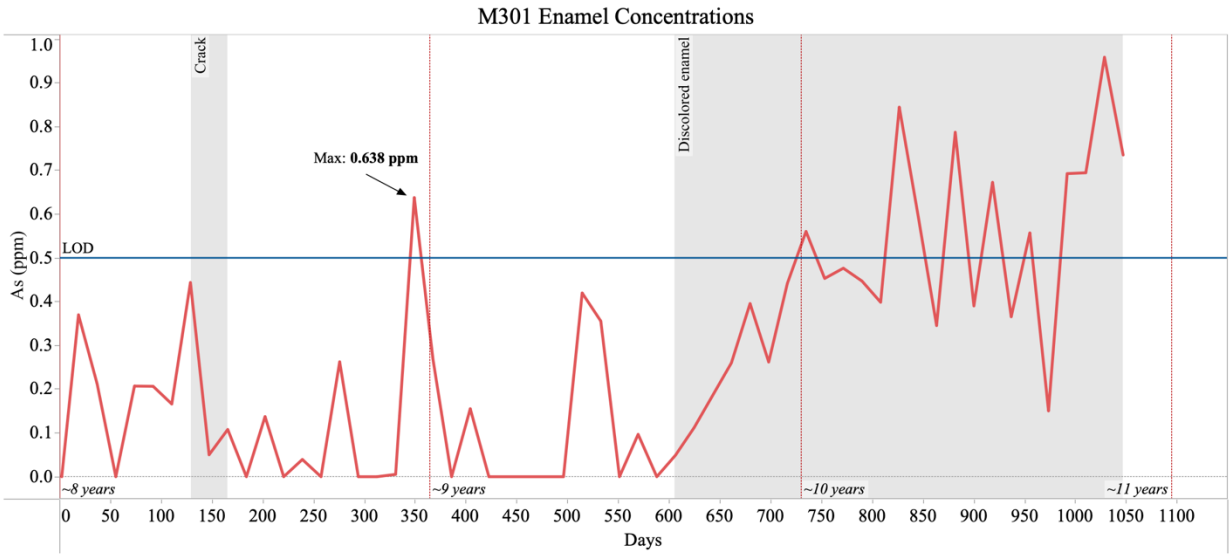


Figure 67 | Concentration of As along ablation transect of M301 enamel. LOD indicated by blue line. Areas highlighted in light gray represent potential postmortem alteration and are excluded from analysis.

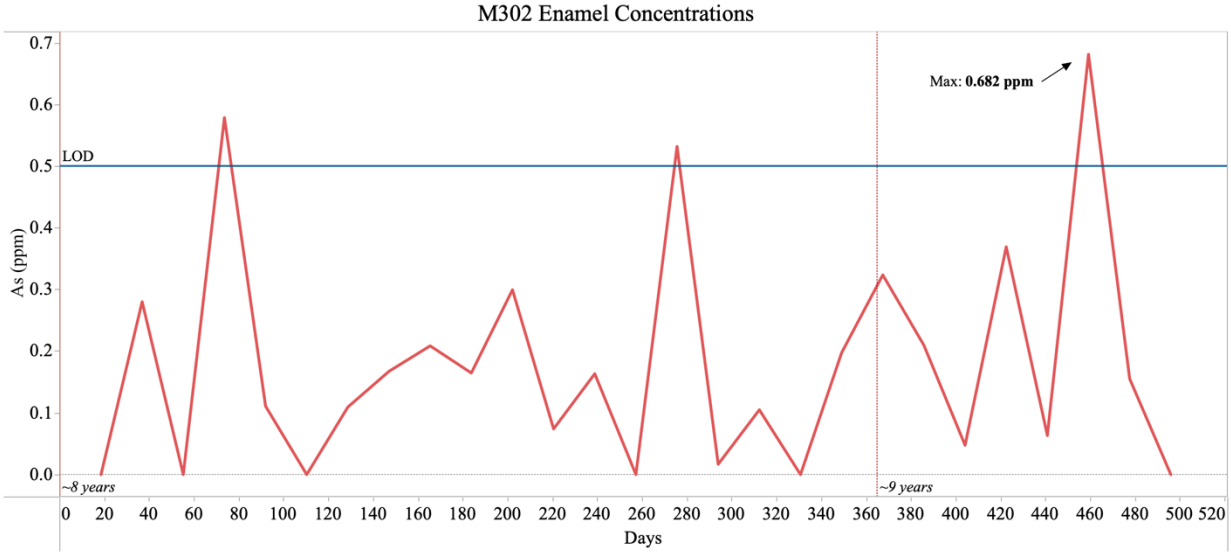


Figure 68 | Concentration of As along ablation transect of M302 enamel. LOD indicated by blue line. Areas highlighted in light gray represent potential postmortem alteration and are excluded from analysis.

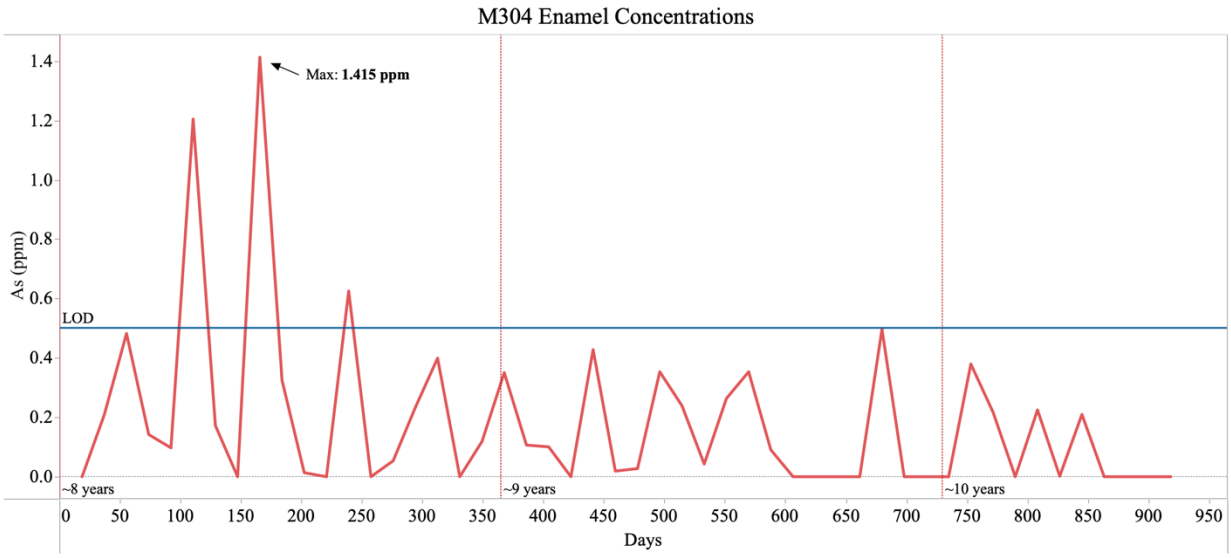


Figure 69 | Concentration of As along ablation transect of M304 enamel. LOD indicated by blue line. Areas highlighted in light gray represent potential postmortem alteration and are excluded from analysis.

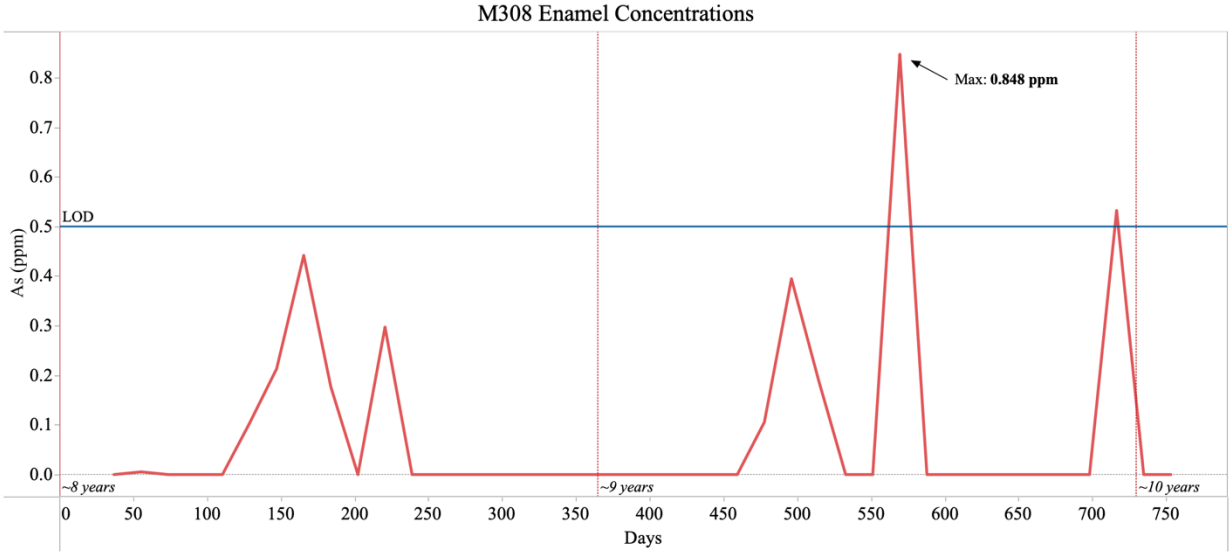


Figure 70 | Concentration of As along ablation transect of M308 enamel. LOD indicated by blue line. Areas highlighted in light gray represent potential postmortem alteration and are excluded from analysis.

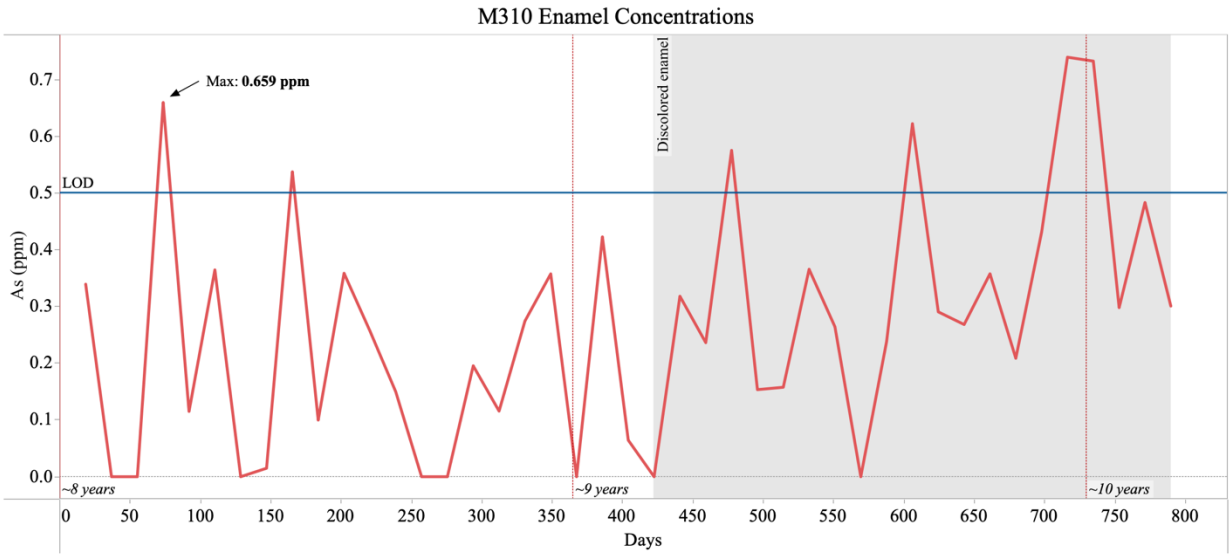


Figure 71 | Concentration of As along ablation transect of M310 enamel. LOD indicated by blue line. Areas highlighted in light gray represent potential postmortem alteration and are excluded from analysis.

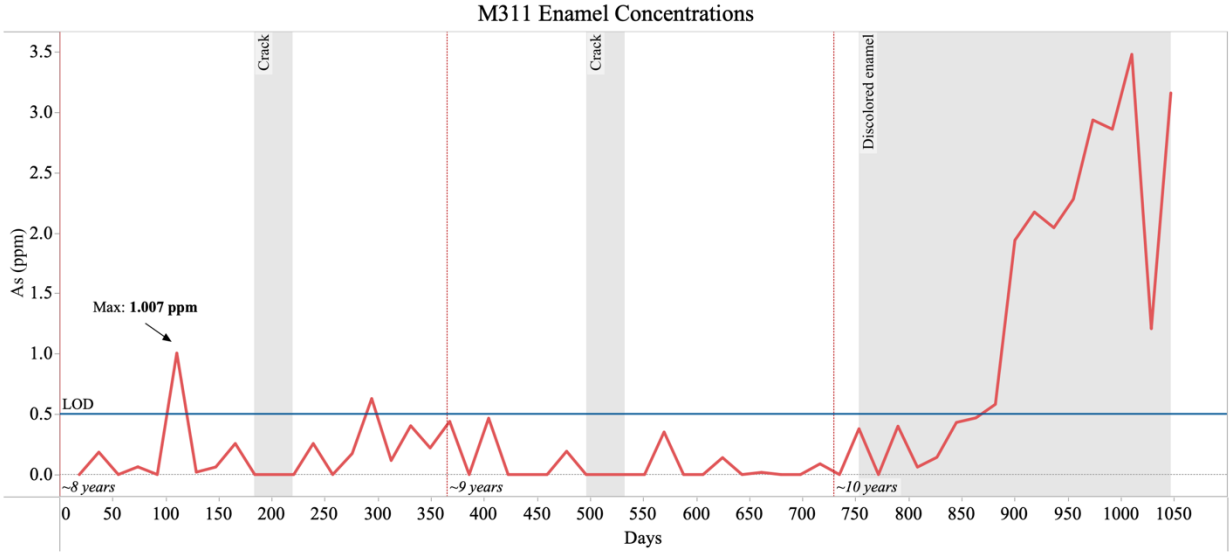


Figure 72 | Concentration of As along ablation transect of M311 enamel. LOD indicated by blue line. Areas highlighted in light gray represent potential postmortem alteration and are excluded from analysis.

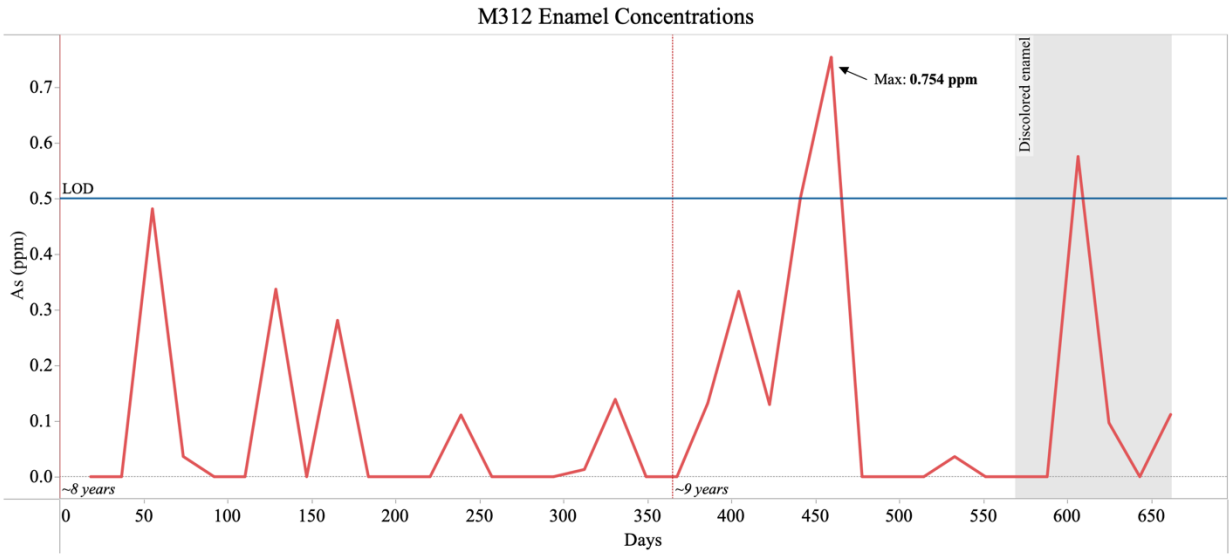


Figure 73 | Concentration of As along ablation transect of M312 enamel. LOD indicated by blue line. Areas highlighted in light gray represent potential postmortem alteration and are excluded from analysis.

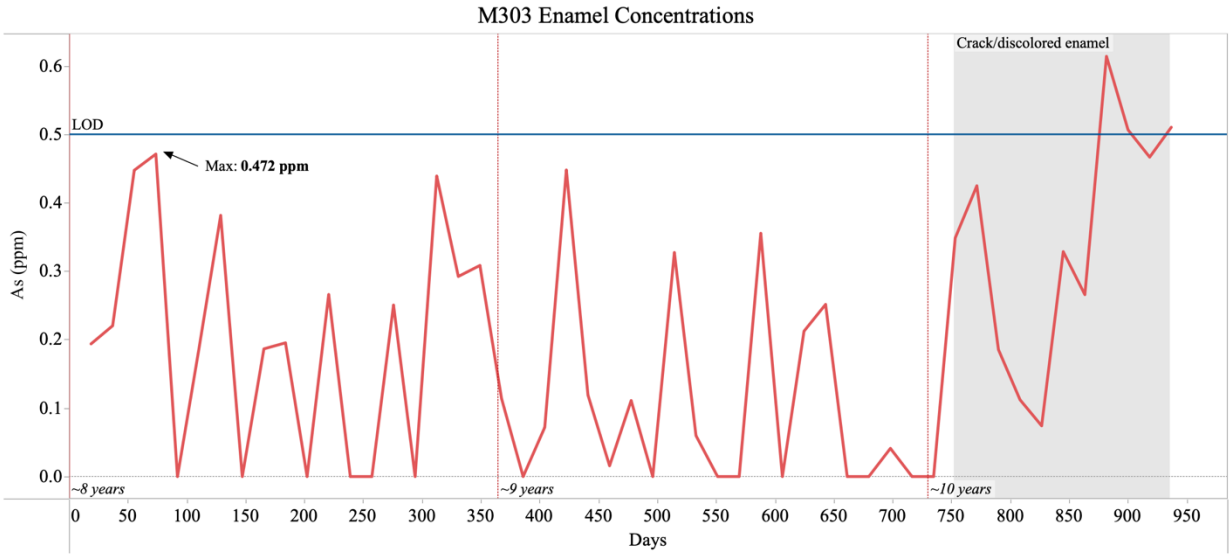


Figure 74 | Concentration of As along ablation transect of M303 enamel. LOD indicated by blue line. Areas highlighted in light gray represent potential postmortem alteration and are excluded from analysis.

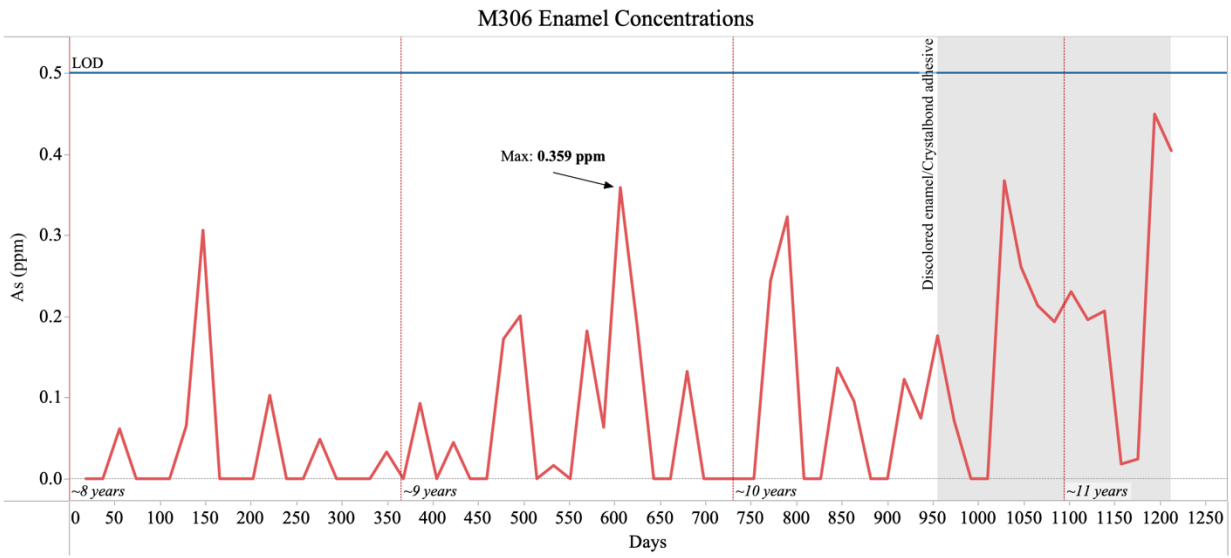


Figure 75 | Concentration of As along ablation transect of M306 enamel. LOD indicated by blue line. Areas highlighted in light gray represent potential postmortem alteration and are excluded from analysis.

Chapter 5: Discussion

Overall concentrations of Pb, Cd, and As are low. In LA-ICP-MS analysis, limits of detection (LOD) are described as the lowest concentration of an element that can be measured or detected. This measure is different from element to element and is also influenced by the matrix being used (Chemnitzer 2019; Pollard et al. 2007). According to Pollard et al. (2007), elemental concentrations measured close to or below their established LOD should be excluded from interpretations. During LA-ICP-MS analysis, the average LOD for Pb, Cd, and As were 0.01 ppm, 0.2 ppm, and 0.5 ppm, respectively. In this thesis, the term "low" is defined as at or below an element's limit of quantification or the value at which the concentration of an element can reliably be determined (10x the LOD) (Dr. Chris Yakymchuk, email communication). This means that the values measured for Pb, Cd, and As close to or below ~1 ppm, ~2 ppm, and ~5 ppm, accordingly, are not reliable values for interpretation and are considered to be low.

5.1 | Patterns of Variation Over Time

Interpretations of the results for Pb are based on the temporal trends or patterns reflecting the uptake of the heavy metal along the ablation transect, which has more meaning than the actual values (Dolphin et al. 2012; Limbeck et al. 2015). Examination of Pb revealed that all individuals included in the main analysis exhibit: (1) stable; (2) variable; (3) increasing; or (4) decreasing patterns of exposure over time.

5.1.1 | Stable Exposure Over Time

Examination of Pb signatures across ablation transects revealed stable patterns of exposure in one first molar (M111), one premolar (PM01), and four third molars (M301, M303, M306, and M311). The teeth in this grouping also have lower concentrations of Pb with M111,

M306, and M311 maxima falling below 0.1 ppm and PM01, M301, and M303 maxima falling between 0.1 ppm and 0.250 ppm.

5.1.2 | Variable Exposure Over Time

Three first molars (M101, M102, and M103) and three third molars (M304, M308, and M310) exhibited variable patterns of Pb exposure over time with at least two peaks in concentration. M101, M102, and M310 had the highest concentrations of Pb throughout the entire sample at 1.318 ppm, 0.839 ppm, and 0.987 ppm, respectively. Samples M103, M304, and M308 had lower maxima of 0.271 ppm, 0.144 ppm, and 0.190 ppm, respectively.

5.1.3 | Increasing Exposure Over Time

Increasing exposure over time was the least prevalent pattern throughout the entire sample and only occurred in premolars. Examination of heavy metal concentrations revealed two premolars (PM01 and PM03) with increasing Pb exposure.

5.1.4 | Decreasing Exposure Over Time

Finally, four of the eight first molars (M104, M106, M108, and M109) exhibited patterns of decreasing Pb exposure over time. Three premolars (PM02, PM05, and PM06), and two third molars (M302 and M312) also exhibited this pattern. Interestingly, there are no trends across tooth groups indicating a specific exposure pattern is more prevalent than another. Additionally, there is no tooth group that has remarkably higher maxima than the others, suggesting there are no notable differences in the uptake of Pb between age groups. Across graves, the two first molars excavated from Grave 6 (M101 and M102) have the highest concentrations of Pb at 1.318 ppm and 0.839 ppm, respectively. However, the premolars (PM01 and PM02) and third molars

(M302, M303, and M304) from Grave 6 have concentrations all below 0.2 ppm. The other two teeth with some of the highest concentrations of Pb (M310 and PM05) at 0.987 ppm and 1.074 ppm, respectively, were both recovered from Grave 3; yet, last two teeth recovered from the same grave (M109 and M311) have concentrations below 0.225 ppm. Hence, there does not seem to be a meaningful pattern or difference in heavy metal uptake between graves.

5.1.5 | Cadmium and Arsenic Exposure Over Time

As previously stated in Chapter 4, the LA-ICP-MS instrument is not as sensitive to Cd and As compared to Pb. This results in noisy data that makes it difficult to identify temporal patterns in the uptake of Cd and As. As such, the four patterns characterizing Pb uptake over time were not used in the examination of Cd and As. Instead, teeth were characterized as being above or below Cd and As's average LODs. The most that can be interpreted from these results is to say that while concentrations are low as defined above, there are some teeth that have a measurable concentration of one or both heavy metals (rising above the average LOD). All individuals included in the main analysis except M108, M109, and M111 had Cd concentrations rising above Cd's LOD (0.2 ppm) and all individuals except M103, M303, and M306 had As concentrations rising above As's LOD (0.5 ppm). Thus, these individuals were exposed to some amount of Cd and As.

5.2 | Previous Studies in Wadi Faynan

As far as this researcher is aware, there are no published studies from Wadi Faynan using LA-ICP-MS to examine individual temporal variation in heavy metal uptake. In 2021, another master's student at the University of Waterloo, Kaithleen Tan, explored a similar question using LA-ICP-MS on teeth recovered from WF100 in 2019. However, her research focused solely on

Pb and is not yet published (Tan 2021). Most trace element analyses of human remains from Wadi Faynan use bulk sampling strategies which entails the dissolution of a whole tooth or large portions of the tooth prior to measurement (Alomary et al. 2006; Beherec et al. 2016; Perry et al. 2011) or they use bone rather than teeth (Grattan et al. 2005; Grattan et al. 2002; Pyatt et al. 2005). Bulk sampling strategies homogenize elemental variation within an individual tooth effectively removing information about the frequency and timing of exposure episodes (Dolphin 2012). Unlike enamel and dentine, bone does not offer a chronological record of heavy metal bioaccumulation. Across the life course, bone undergoes cycles of resorption and formation that are influenced by a variety of factors including sex, age, health, and lifestyle (Simpson et al. 2021). The rates of these cycles are also dependent on the type of bone and skeletal tissue. For instance, cortical bone turnover rates are slower than trabecular bone turnover rates (Hill 2014; Hedges et al. 2007; Simpson et al. 2021). Trace elements are incorporated during bone formation, which occurs throughout an individual's life effectively creating a "mosaic" of trace elements that is representative of several years to decades of environmental exposure (Simpson et al. 2021).

When looking at these previous studies in comparison to this research, it is notable that they have also found inter- and intraindividual variation in their samples. For instance, Grattan et al. (2002) investigated interindividual variation by measuring Pb in the long bones of 36 Byzantine individuals from Khirbet Faynan, finding concentrations ranging from 1.0 to 289.2 μg/g. Grattan et al. (2005) explored inter- and intraindividual variation by examining patterns of heavy metal partitioning in the humeri of 17 individuals revealing differences in concentrations across the long bones: medial epicondyle 4.4-61.8 μg/g; mid-shaft 2.5-56.4 μg/g; and head 3.1-52.5 μg/g. Pyatt et al. (2005) also explored inter- and intraindividual variation by measuring

concentrations of Pb in cortical and trabecular bone of two femurs and a cranium recovered from Bronze Age and Byzantine burial sites. Not only did they find higher concentrations of Pb in the cortical bone (98 mg/kg; 196 mg/kg; 35 mg/kg) than the trabecular bone (74 mg/kg; 170 mg/kg; 24 mg/kg) but they also found that the Byzantine femur had a higher concentration of Pb than the Bronze Age femur.

Beherec et al. (2016) used bulk sampling to measure the concentrations of Pb in enamel and dentine of 36 Iron Age individuals. In addition to reporting their findings in molar ratios (Pb/Ca), they also listed concentrations of Pb in ppb, which can easily be converted into ppm. When possible, they used multiple teeth from the same individual resulting in concentrations indicative of intraindividual variation. For instance, one of the individuals included in their sample ranged from 0.572 – 2.723 ppm and another ranged from 0.221 – 2.875 ppm. Across the sample the range was from 0.192 – 24.534 ppm (Beherec et al. 2016).

Differing from the results of this thesis, some of the studies discussed above reported higher concentrations of Pb. As an example, Grattan et al. (2002) measured a concentration of 289.2 μg/g (289.2 ppm) in a Byzantine long bone and Grattan et al. (2005) measured a concentration of 61.8 μg/g (61.8 ppm) in a Byzantine humerus. These high concentrations could be explained by the choice of sampling from bone rather than teeth, as explained above. An alternative explanation could be that the individuals included in these studies lived during the Roman Period (4^{th}-7^{th} century AD) and were recovered from Khirbet Faynan (Grattan et al. 2005; Grattan et al. 2002). This site is thought to be the Roman industrial and notorious penal mining and smelting center where criminals of the Roman Empire were sentenced to a life of slavery (Pyatt et al. 2005). Evidence for extensive copper production at Khirbet Faynan includes furnaces, ore spoil, shaft mines, and slag heaps that dot the landscape about 10 km north and

south of the site. In addition, Khirbet Faynan has evidence of substantial irrigated agricultural fields that were necessary to feed the population of Phaino and, in turn, support the copper industry (Grattan et al. 2002). The mining and smelting technologies used at Khirbet Faynan (e.g. shaft mines and furnaces) as well as the large work force would have allowed for more intensive, large scale, industrial copper production as compared to the small scale, domestic production practiced during EBA Ib. See Table 8 for a summary of previous trace element studies using human skeletal remains from Wadi Faynan.

Study	Time Period	Location	Method	Sample Number	Sample	Pb Max	Pb Min
Grattan et al. (2002)	Byzantine Period (4th – 7th c. AD)	Khirbet Faynan	Acid digestion; ICP-MS	36	Bone	289.2 µg/g	1.0 µg/g
Grattan et al. (2005)	Byzantine Period (4th – 7th c. AD)	Khirbet Faynan	Acid Digestion; FAAS	25	Bone	~90 µg/g	10 µg/g
	Byzantine Period (4th – 7th c. AD)	Khirbet Faynan	Acid Digestion; FAAS	11	Bone	~62 µg/g	~3 µg/g
	Byzantine Period (4th – 7th c. AD)	Khirbet Faynan	Acid Digestion; FAAS	17	Medial Epidondyle; mid-shaft; head of humerus	61.8 µg/g; 56.4 µg/g; 52.5 µg/g	4.40 µg/g; 2.5 µg/g; 3.1 µg/g
Pyatt et al. (2005)	Bronze Age	Khirbet Faynan	Acid Digestion; FAAS	2	Trabecular bone from femur; cortical bone from femur	74 mg/kg; 98 mg/kg	N/A
	Byzantine Period (4th – 7th c. AD)	Khirbet Faynan	Acid digestion; FAAS	2	Trabecular bone from femur; cortical bone from femur	170 mg/kg; 196 mg/kg	N/A
	Byzatine Period (4th – 7th c. AD)	Khirbet Faynan	Acid digestion; FAAS	2	Trabecular bone from cranium; cortical bone from cranium	24 mg/kg; 35 mg/kg	N/A
	Byzantine Period (4th – 7th c. AD)	Khirbet Faynan	Acid digestion; FAAS	1	Rib	99 mg/kg	N/A
Beherec et al. (2016)	Iron Age II (10th – 9th c. BCE)	Wadi Fidan 40	Acid Digestion; ICP-MS	36	Enamel; dentine	24,534 ppb; 2875 ppb	192 ppb; 221 ppb

Table 8 | Summary of previous trace element studies using human skeletal remains from Wadi Faynan.

5.3 | Inter- and Intraindividual Variation Across Time

The results of this trace element analysis indicate inter- and intraindividual variation in the uptake of heavy metals across the sample population. The three types of teeth included in the sample represent different time periods offering information about variation in exposure across early life for both individuals and across the sample population. First permanent molars begin forming ~30 weeks *in utero* and continue until ~3 years old (Hillson 2024). Public health research has demonstrated that Pb, Cd, and As are transported through the placenta to the fetus and breastmilk to the infant (Arbuckle et al. 2016; Espart et al. 2018; Geng and Wang 2019; Manton et al. 2003; Mohammadi et al. 2022; Navasumrit et al. 2019; Ortiz-Garcia et al. 2023; Needleman and Bellinger 1991; Rebelo and Caldas 2016; Tellez-Rojo et al. 2004; Winterbottom et al. 2019). Assuming completion of natural weaning occurs between 2 and 4 years of age (Grueger 2013), the heavy metals measured in the enamel of first molars provide information about exposure during gestation and breastfeeding (Lee et al. 1999).

Third and fourth premolars begin forming at ~1.8 years and ~2.8 years, respectively, with crown completion by ~5 to 6 years of age (Hillson 2024). Based on their developmental timeframes, concentrations measured in premolars provide insight into exposure during breastfeeding, weaning, and early childhood. Finally, third molars begin forming at ~8 years of age, although this is highly variable, and crown completion occurs around 11 years old. Thus, third molars provide insight into heavy metal exposure during childhood and early adolescence.

The low concentrations seen in the results could be attributed to several factors. EBA Ib represents early copper production. Smelting was likely a long and slow process, relying on the use of ceramic crucibles that were placed on a bed of charcoal and subsequently heated by

human breath through blowpipes from above (Adams 2002). Findings from an EBA Ia site in Faynan, Wadi Fidan 4, indicate that smelting also included a secondary smelting process following the crushing of and selection of initially smelted ore (Adams 2002). Furthermore, EBAI mining was restricted to easily accessible or already exposed ore bodies which were transported to settlements for smelting (Adams 2002; Adams and Genz 1995; Hauptmann 2007).

Based on the archaeological evidence, mining and smelting of copper ore at WF100 was likely practiced on a small-scale and in domestic contexts. It could be that exposure to heavy metal pollution only occurred in individuals directly involved in the mining and smelting of copper ores because there was not yet widespread release of heavy metals into the environment as seen today (Grattan et al. 2005; Grattan et al. 2003a; Grattan et al. 2013; Grattan et al. 2002; Hunt and el-Rishi 2010; Pyatt et al. 2002a; Pyatt et al. 2002b; Pyatt et al. 2000; Pyatt et al. 1999). This is further supported by evidence from Wadi Fidan 4 where the density of metallurgical materials and waste within specific areas of the site indicate that copper production was a craft specialization during EBA Ia with only specific individuals or groups participating (Adams 2002). If this is the case, the results from this thesis could indicate that women and children were not directly involved in copper production activities.

Despite such low concentrations, all individuals included in the main analysis exhibit stable, variable, increasing, or decreasing patterns of exposure to Pb over time; meaning that the individuals included in this sample were exposed to some heavy metal pollution. Low, stable concentrations of Pb over time could indicate that these individuals did not live close to copper production operations during their early lives. When examining the pattern for M111 (Figure 8), the stability of Pb could also indicate that their mother did not live close to and was not directly involved in copper production activities before or during gestation or breastfeeding.

Variable exposure over time could indicate periods of migration to and from WF100. For samples M101 and M102, the fluctuations in Pb concentrations likely reflect an exposure episode for these individual's mothers. For individual M310, their highest peak in Pb occurs ~250 days or between an estimated 8 and 9 years old; thus, reflecting an exposure episode for this individual that could be attributed to a short movement to and from WF100. Similarly, increasing and decreasing trends could indicate movement to or movement from areas impacted by copper production.

Health implications such as those discussed in Chapter 2.1.1.1 cannot be inferred by looking solely at the concentrations measured in this thesis. However, it is important to note that Pb, Cd, and As are considered non-essential trace elements that serve no biological function (Balali-Mood et al. 2021; Jaishankar et al. 2014; Tchounwou et al. 2012). Furthermore, even low dosage exposure to these heavy metals can cause health issues (Balali-Mood et al. 2021; Engwa et al. 2019; Tchounwou et al. 2012; Ufelle and Barchowsky 2019) and simultaneous exposure to two or more can have cumulative deleterious health effects (Balali-Mood et al. 2021).

5.2 | Limitations and Future Directions

One significant limitation of this thesis is that teeth only represent bioaccumulation of heavy metals during early life. If an individual was directly involved in copper production as an adult, their teeth would not provide information about occupational exposure episodes. Another limitation is the lack of demographic information for each individual included in the sample that might provide further insight into life experiences at WF100. Due to the commingled nature of the human remains, there is no easy way to associate teeth or bone together to glean more nuanced demographic information. So, while the low concentrations of heavy metals in first

molars might indicate that the mothers were not directly involved in copper production and, ergo, there is potential gender division in copper production activities, one cannot say for certain that this is the case without further evidence.

One of the benefits of LA-ICP-MS is that there was minimal damage to the teeth allowing future research opportunities with the same samples. The ratios of stable isotopes in teeth can reveal information about past diet and nutrition, geographic origin, and mobility patterns. Thus, stable isotope analysis of this sample could provide insight into dietary choices, breastfeeding and weaning practices, health and disease, and migration at both individual and group levels (White and Longstaffe 2016). Furthermore, histological analysis could uncover evidence of past diseases or developmental conditions that impact tooth formation as well as provide more precise estimates in defining developmental stages in both enamel and dentine (Hillson 2024). These types of analyses coupled with the results from this study could reveal more information about copper production activities and daily life at WF100.

Chapter 6: Conclusion

Wadi Faynan 100 is situated within one of the oldest known industrial landscapes in the world. The individuals recovered from the cemetery revealed some of the earliest evidence of heavy metal exposure, variation across the sample population, and differences in the frequency and timing of exposure episodes. While exposure to Pb, Cd, and As at WF100 is low, even low dosage exposure to heavy metals can cause health issues (Balali-Mood et al. 2021; Engwa et al. 2019; Tchounwou et al. 2012; Ufelle and Barchowsky 2019). Such low concentrations found in this sample align with the likely practice of small-scale, domestic copper production and use of ceramic crucibles and blowpipes as opposed to more extensive operations (Adams 2002; Adams and Genz 1995; Hauptmann 2007). It is possible that there was a gender division in copper production activities based on examination of exposure in first molars and premolars. Additionally, it seems as though children and adolescents were not necessarily directly involved in these activities as one would expect there to be higher concentrations in the enamel that formed during these time periods. Lastly, examination of temporal variation revealed potential movement to and from areas with more heavy metal pollution possibly indicating mobility patterns associated with WF100.

References

Ackerfeld, Dana, Yael Abadi-Reiss, Omri Yagel, Yehudit Harlavan, Talia Abulafia, Dmitry Yegorov, and Erez Ben-Yosef. 2020. "Firing up the Furnace: New insights on metallurgical practices in the Chalcolithic Southern Levant from a recently discovered copper-smelting workshop at Horvat Beter (Israel)." *Journal of Archaeological Science: Reports* 33: 3-14. https://doi.org/10.1016/j.jasrep.2020.102578.

Adams, Dr. Russell, Dr. Alexis Dolphin, Professor John Grattan, Dr. Amy Scott, Mr. Alan Weston, Mr. Michael Boyles, Mr. Jeff Coffin, Ms. Lisa Usman, Ms. Robyn Wood, and Ms. Aparajita Battacharya. "Barqa Landscape Project 2023: Preliminary Report to the Department of Antiquities."

Adams, Dr. Russell, Dr. Alexis Dolphin, Professor John Grattan, Dr. Keith Haylock, Dr. Juan Tebes, Mr. Alan Weston, Jacquie Meijer, Mr. Andrew Lawson, and Alexandra Harris. "Barqa Landscape Project 2019: Preliminary Report to the Department of Antiquities."

Adams, Russell. 2003. "External Influences at Faynan During the Early Bronze Age: A Re-Anlaysis of Building 1 at Barqa El-Hetiye, Jordan." *Palestine Exploration Quarterly* 135: 6-21. https://doi.org/10.1179/peq.2003.135.1.6.

Adams, Russell. 2006. "Copper Trading Networks across the Arabah during the later Early Bronze Age." In *Crossing the Rift: Resources Routes, Settlement Patterns and Interaction in the Wadi Arabah*, edited by P. Bienkwoski and Katharina Galor, 137-144. Council for British Research in the Levant.

Adams, Russell and Hermann Genz. 1995. "Excavation at Wadi Fidan 4: A Chalcolithic Village Complex in the Copper Ore District of Feinan, Southern Jordan." *Palestine Explortation Quarterly* 127: 8-20. https://doi.org/10.1179/peq.1995.127.1.8.

Adams, Russell B. 2002. "From farms to factories: The development of copper production at Faynan, southern Jordan, during the Early Bronze Age." In *Metals and Society,* edited by B. S. Ottaway and E. C. Wager, 21-32. Oxford: Archaeopress.

Adams, Russell B., Hannah A. Friedman, James D. Anderson, Michael M. Homan, J.P. Grattan, and Lynne M. Rouse. 2017. "The Barqa Landscape Project, 2009." In *Walking Through Jordan: Essays in Honor of Burton MacDonald*, edited by Michael Neeley, Geoffrey Clark, and P.M. Michèle Daviau, 247-264. Sheffield, UK: Equinox Publishing Ltd.

Agarwal, Sabrina C. 2016. "Bone Morphologies and Histories: Life Course Approaches in Bioarchaeology." *Yearbook of Physical Anthropology* 159: S130-S149.

Alomary, A., I. F. Al-Momani, and A. M. Massadeh. 2006. "Lead and cadmium in human teeth from Jordan by atomic absorption spectrometry: Some factors influencing their concentrations." *Science of the Total Environment* 369: 69-75. https://doi.org/10.1016/j.scitotenv.2006.04.023.

Arbuckle, Tye E, Chun Lei Liang, Anne-Sophie Morisset, Mandy Fisher, Hope Weiler, Ciprian Mihai Cirtiu, Melissa Legrand, Karelyn Davis, Adrienne S Ettinger, and William D Fraser. 2016. "Maternal and Fetal Exposure to Cadmium, Lead, Manganese and Mercury:

The MIREC Study." *Chemosphere (Oxford)* 163: 270–82. https://doi.org/10.1016/j.chemosphere.2016.08.023.

Arnay-de-la-Rosa, M, E González-Reimers, Y Yanes, C.S Romanek, J.E Noakes, and L Galindo-Martín. 2011. "Paleonutritional and Paleodietary Survey on Prehistoric Humans from Las Cañadas Del Teide (Tenerife, Canary Islands) Based on Chemical and Histological Analysis of Bone." *Journal of Archaeological Science* 38, no. 4: 884–95. https://doi.org/10.1016/j.jas.2010.11.018.

Arruda-Neto, J.D.T., L.P. Geraldo, G.R. Prado, F. Garcia, M.C. Bittencourt-Oliveira, J.E.S. Sarkis, F. Martinez-Lusardo, L. Lima-Cazorla, D. Rosa-Medero, T.E. Rodrigues, and G.C. Genofre. 2010. "Study of metals transfer from environment using teeth as biomonitor." *Environment International* 36: 243-246.

Asaduzzaman, Khandoker, Mayeen Uddin Khandaker, Nurul Atiqah Binti Baharudin, Yusoff Bin Mohd Amin, Mohideen Salihu Farook, D.A. Bradley, and Okba Mahmoud. 2017. "Heavy metals in human teeth dentine: A bio-indicator of metals exposure and environmental pollution." *Chemosphere* 176: 221-230.

Balali-Mood, Mahdi, Kobra Naseri, Zoya Tahergorabi, Mohammad Eza Khazdair, and Mahmood Sadeghi. 2021. "Toxic Mechanisms of Five Heavy Metals: Mercury, Lead, Chromium, Cadmium, and Arsenic." *Frontiers in Pharmacology* 12: 1-19.

Balasse, Marie, Stanley H Ambrose, Andrew B Smith, and T.Douglas Price. 2002. "The Seasonal Mobility Model for Prehistoric Herders in the South-Western Cape of South Africa Assessed by Isotopic Analysis of Sheep Tooth Enamel." *Journal of Archaeological Science* 29, no. 9: 917–32. https://doi.org/10.1006/jasc.2001.0787.

Barker, Graeme, Russell Adams, Oliver Creighton, Hwedi el-Rishi, David Gilbertson, John Grattan, Chris Hunt, Paul Newson, Brian Pyatt, and Tim Reynolds. 2007. "Chalcolithic (c.5000-3600 cal. BC) and Bronze Age (c.3600- 1200 cal. BC) settlement in Wadi Faynan: metallurgy and social complexity." In *Archaeology and Desertification: The Wadi Faynan Landscape Survey, Southern Jordan,* edited by Graeme Barker, David Gilbertson, and D. J. Mattingly, 227-270. Oxford, UK: Oxbow Books.

Barnes, H., M. Flender, I. Ruben, R. Shafiq, and A. McQuitty. 1995. "Wadi Faynan Project, 1994-1995 (Phase 3): Report on March 1995 Season." *British Institute at Amman for Archaeology and History*.

Barton, Henryk J. 2011. "Advantages of the Use of Deciduous Teeth, Hair, and Blood Analysis for Lead and Cadmium Bio-Monitoring in Children. A Study of 6-Year-Old Children from Krakow (Poland)." *Biological Trace Element Research* 143, no. 2: 637-658.

Bataille, Clement P. and Gabriel J. Bowen. 2012. "Mapping $^{87}Sr/^{86}Sr$ variations in bedrock and water for large scale provenance studies." *Chemical Geology* 304-305: 39-52. https://doi.org/10.1016/j.chemgeo.2012.01.028.

Beard, Brian L. and Clark M. Johnson. 2000. "Strontium isotope composition of skeletal material can determine the birth place and geographic mobility of humans and animals." *Journal of Forensic Sciences* 45, no. 5: 1049-61. https://doi.org/10.1520/JFS14829J.

Bech, Jauma, Charlotte Poschenrieder, Merce Llugany, Juan Barcelo, P. Tume, F.J. Tobias, J.L. Barranzuela, and E.R. Vasquez. 1997. "Arsenic and heavy metal contamination of soil and vegetation around a copper mine in Northern Peru." *Science of the Total Environment* 203, no. 1: 83-91. https://doi.org/10.1016/S0048-9697(97)00136-8.

Beherec, Marc A., Thomas E. Levy, Ofir Tirosh, Mohammad Najjar, Kyle A. Knabb, and Yigal Erel. 2016. "Iron Age Nomads and their relation to copper smelting in Faynan (Jordan): Trace metal and Pb and Sr isotopic measurements from the Wadi Fidan 40 cemetery." *Journal of Archaeological Science* 65: 70-83. https://doi.org/10.1016/j.jas.2015.10.006.

Ben-Yosef, E., A. Gidding, L. Tauxe, U. Davidovich, M. Najjar, and T. E. Levy. 2016. "Early Bronze Age copper production systems in the northern Arabah Valley: New insights from archaeomagnetic study of slag deposits in Jordan and Israel." *Journal of Archaeological Science* 72: 71-84. https://doi.org/10.1016/j.jas.2016.05.010.

Bianchi, Nicola, Adriana Moroni, Simone Bonucci, Giulia Capecchi, Stefania Ancora, Stefano Ricci, and Claudio Leonzio. 2017. "Trace Elements in Eneolithic and Late Medieval Human Bones from Two Archaeological Sites in Tuscany: Evaluation of Diagenetic Processes, Diet and Exposure to Heavy Metals." *Journal of Anthropology and Archaeology* 5, no. 2: 31-43. https://doi.org/10.15640/jaa.v5n2a3.

Blakely, Robert L., and Lane A. Beck. 1981. "Trace Elements, Nutritional Status, and Social Stratification at Etowah, Georgia." *Annals of the New York Academy of Sciences* 376, no.1: 417–31. https://doi.org/10.1111/j.1749-6632.1981.tb28183.x.

Bocca, Beatrice, Giovanni Forte, Valentina Giuffra, Rita Maria Serra, Yolande Asara, Cristiano Farace, Marco Milanese, et al. 2018. "Metals in Bones of the Middle-Aged Inhabitants of Sardinia Island (Italy) to Assess Nutrition and Environmental Exposure." *Environmental Science and Pollution Research International* 25, no. 9: 8404–14. https://doi.org/10.1007/s11356-017-1140-6.

Boskabady, Marzie, Vahideh Ghorani, Sima Beigoli, and Mohammad Hossein Boskabady. 2022. "The Effects of Environmental Lead on Teeth and Bone Status and the Mechanisms of These Effects, Animal and Human Evidence, a Review." *Toxin Reviews* 41 (4): 1396–1415. https://doi.org/10.1080/15569543.2022.2026398.

Brown, Catriona J., Simon R.N. Chenery, Barry Smith, Carol Mason, Andrew Tomkins, Graham J. Roberts, Louise Sserunjogi, and John V. Tiberindwa. 2004. "Environmental influences on the trace element content of teeth—implications for disease and nutritional status." *Archives of Oral Biology* 49: 705-717.

Burton, James. 2008. "Bone Chemistry and Trace Element Analysis." In *Biological Anthropology of the Human Skeleton,* edited by M. Anne Katzenberg and Shelley R. Saunders, 443-460. Hoboken, NJ: Wiley & Sons, Inc.

Chemnitzer, Rene. 2019. "Strategies for Achieving the Lowest Possible Detection Limits in ICP-MS." *Spectroscopy* 34, no. 10: 12-17.

Chen, Li, Mingxi Zhou, Jingzhe Wang, Zhiqin Zhang, Chengjiao Duan, Xiangxiang Wang, Shuling Zhao, Xiaohan Bai, Zhijie Li, Zimin Li, and Linchuan Fang. 2022. "A global meta-analysis of heavy metal(loid)s pollution in soils near copper mines: Evaluation of

pollution level and probabilistic health risks." *Science of the Total Environment* 835: 1-11.

Chesson, Meredith S. and Nathan Goodale. 2014. "Population aggregation, residential storage and socioeconomic inequality at Early Bronze Age Numayra, Jordan." *Journal of Anthropological Archaeology* 35: 117-134. https://doi.org/10.1016/j.jaa.2014.02.002.

Christou, Anastasis, Christodoulos P. Theologides, Costas Costa, Ioannis K. Kalavrouziotis, and Soterios P. Varnavas. 2017. "Assessment of Toxic Heavy Metals Concentrations in Soils and Wild and Cultivated Plant Species in Limni Abandoned Copper Mining Site, Cyprus." *Journal of geochemical exploration* 178: 16–22.

Coffin, Jeffrey, Alexis E Dolphin, Mary Jackes, Chris Yakymchuk, and Thomas Perrin. 2022. "Exploring Childhood Mobility in Neolithic Southern France (Roquemissou) Using Incremental Analyses of Sr Isotope Ratios in Tooth Enamel." *Journal of Archaeological Science, Reports* 42: 103417-. https://doi.org/10.1016/j.jasrep.2022.103417.

Cucina, Andrea, Hector Neff, and Vera Tiesler. 2004. "Provenance of African-Born Individuals from the Colonial Cemetery of Campeche (Mexico) by Means of Trace Element Analysis." *Dental Anthropology Journal* 17, no. 3: 65-69. https://doi.org/10.26575/daj.v17i3.148.

Cucina, Andrea, Vera Tiesler, Thelma Sierra Sosa, and Hector Neff. 2011. "Trace-element evidence for foreigners at a Maya port in Northern Yucatan." *Journal of Archaeological Science* 38: 1878-1885. https://doi.org/10.1016/j.jas.2011.03.032.

Dent, Sophia C. 2017. "Interindividual differences in embodied marginalization: Osteological and stable isotope analyses of antebellum enslaved individuals." *American Journal of Human Biology* 29, no. 4: 1-16.

DeWitte, Sharon N. 2015. "Bioarchaeology and the Ethics of Research Using Human Skeletal Remains." *History Compass* 13, no. 1: 10-19. https://doi.org/10.1111/hic3.12213.

Dolphin, Alexis E. and Alan H. Goodman. 2009. "Maternal Diets, Nutritional Status, and Zinc in Contemporary Mexican Infants' Teeth: Implications for Reconstructing Paleodiets." *American Journal of Physical Anthropology* 140: 399-409. https://doi.org/10.1002/ajpa.21068.

Dolphin, Alexis E. and Russell B. Adams. 2023. "Something old, something new: Ongoing revelations within the Faynan Landscape." *Palestine Exploration Quarterly:* 1–17. https://doi.org/10.1080/00310328.2023.2171954.

Dolphin, Alexis E., Siv Hjorth Dundas, Jan Kosler, Helene Meyer, Tvinnereim, and Audrey Geffen. 2012. "A comparison of techniques for measuring the trace element content of human teeth: laser ablation ICP-MS versus solution ICP-MS of micromilled enamel." *International Journal of Analytical and Bioanalytical Chemistry* 2, no. 3: 189-195.

Dudgeon, John V., Monica Tromp, Bryan K. Hanks, and Andrei V. Epimakhov. 2016. "Investigating Biogenic Versus Diagenetic Trace Element Incorporation in Archaeological Mineralized Tissues with LA-ICP-MS." In *Recent Advances in Laser Ablation ICP-MS for Archaeology*, edited by Laure Dussubieux, Mark Golitko, and Bernard Gratuze, 323-341. Berlin: Springer.

Durrant, Steven F. and Neil I. Ward. 2005. “Recent biological and environmental applications of laser ablation inductively coupled plasma mass spectrometry (LA-ICP-MS).” *Journal of Analytical Atomic Spectrometry* 20, no. 9: 821-829. https://doi.org/10.1039/B502206A.

Engwa, Godwill Azeh, Paschaline Udoka Ferdinand, Friday Nweke Nwalo, and Marian N. Unachukwu. 2019. “Mechanism and Health Effects of Heavy Metal Toxicity in Humans.” In *Poisoning in the Modern World,* edited by Ozgur Karcioglu and Banu Arslan, 77-99. London, England: IntechOpen.

Eshel, Tzilla, Naama Yahalom-Mack, Ofir Tirosh, Aren M. Maeir, Yehudit Harlavan, Ayelet Gilboa, and Yigal Erel. 2020. “Pollution and human mobility in the southern Levant during the Iron Age using chemical and isotopic analysis of human tooth enamel.” *Journal of Archaeological Science* 124: 1-13. https://doi.org/10.1016/j.jas.2020.105262.

Espart, Anna, Sebastián Artime, Glòria Tort-Nasarre, and Edinson Yara-Varón. 2018. “Cadmium Exposure during Pregnancy and Lactation: Materno-Fetal and Newborn Repercussions of Cd(Ii), and Cd-Metallothionein Complexes.” *Metallomics* 1 (1): 1359–67. https://doi.org/10.1039/c8mt00174j.

Farell, Jana, Dulasiri Amarasiriwardena, Alan H Goodman, and Bernardo Arriaza. 2013. “Bioimaging of Trace Metals in Ancient Chilean Mummies and Contemporary Egyptian Teeth by Laser Ablation-Inductively Coupled Plasma-Mass Spectrometry (LA-ICP-MS).” *Microchemical Journal* 106: 340–46. https://doi.org/10.1016/j.microc.2012.09.005.

Filimon, Marioara Nicoleta, Ion Valeriu Caraba, Roxana Popescu, Gabi Dumitrescu, Doina Verdes, Liliana Petculescu Ciochina, and Adrian Sinitean. 2021. “Potential Ecological and Human Health Risks of Heavy Metals in Soils in Selected Copper Mining Areas-A Case Study: The Bor Area.” *International Journal of Environmental Research and Public Health* 18, no. 1516: 1-18.

Fraga, Cesar G. 2005. “Relevance, essentiality and toxicity of trace elements in human health.” *Molecular Aspects of Medicine* 26, no. 4: 235-244. https://doi.org/10.1016/j.mam.2005.07.013.

Fricker, Mattias B. and Detlef Gunther. 2016. “Instrumentation, Fundamentals, and Application of Laser Ablation-Inductively Coupled Plasma-Mass Spectrometry.” In *Recent Advances in Laser Ablation ICP-MS for Archaeology*, edited by Laure Dussubieux, Mark Golitko, and Bernard Gratuze, 1-19. Berlin: Springer.

Geng, Hui-Xia, and Lai Wang. 2019. “Cadmium: Toxic Effects on Placental and Embryonic Development.” *Environmental Toxicology and Pharmacology* 67: 102–7. https://doi.org/10.1016/j.etap.2019.02.006.

Ghaderian, S. Majid, and Ali A. Ghotbi Ravandi. 2012. “Accumulation of Copper and Other Heavy Metals by Plants Growing on Sarcheshmeh Copper Mining Area, Iran.” *Journal of Geochemical Exploration* 123: 25–32.

Giffin, K. L., T. Swanston, I. Coulthard, A. R. Murphy, D. M. L. Cooper, and T. L. Varney. 2017. “Skeletal Lead Burden of the British Royal Navy in Colonial Antigua.” *International Journal of Osteoarchaeology* 27, no. 4: 672–82.

Golden, J. 2014. “Who dunnit? New clues concerning the development of Chalcolithic metal technology in the southern Levant.” In *Archaeometallurgy in Global Perspective:*

Methods and Syntheses, edited by B. W. Roberts and C. P. Thornton, 559-578. New York: Springer.

Goodman, Alan H., Alexis E. Dolphin, Dulasiri D. Amarasiriwardena, Rebecca Klein, Jeffrey R. Backstrand, John B. Reid, Jr., and Peter Outridge. 2003. "Tooth Rings: Dental Enamel as a Chronological Biomonitor of Elemental Absorption from Pregnancy to Adolescence." *Journal of Children's Health* 1, no. 2: 203-214.

Grattan, J., L. Abu Karaki, D. Hine, H. Toland, D. Gilbertson, Z. al-Saad, and B. Pyatt. 2005. "Analyses of patterns of copper and lead mineralization in human skeletons excavated from an ancient mining and smelting centre in the Jordanian desert: a reconnaissance study." *Mineralogical Magazine* 69, no. 5: 653-666. https://doi.org/10.1180/0026461056950277.

Grattan, John, Alan Condron, Sharon Taylor, Lotus Sbu Karaki, F. Brian Pyatt, David D. Gilbertson, and Ziad al-Saad. 2003b. "A Legacy of Empires? An Exploration of the Environmental and Medical Consequences of Metal Production in Wadi Faynan, Jordan." In *Geology and Health: Closing the Gap*, edited by H. Catherine W. Skinner and Antony R. Berger, 99-103. Oxford: Oxford University Press.

Grattan, John P., David D. Gilbertson, and Martin Kent. 2013. "Sedimentary metal-pollution signatures adjacent to the ancient centre of copper metallurgy at Khirbet Faynan in the desert of southern Jordan." *Journal of Archaeological Science* 40, no. 11: 3834-3853. https://doi.org/10.1016/j.jas.2012.12.022.

Grattan, John, Steven Huxley, Lotus Abu Karaki, Harry Toland, David Gilbertson, Brian Pyatt, and Ziad al Saad. 2002. "'Death…more desirable than life'? The human skeletal record and toxicological implications of ancient copper mining and smelting in Wadi Faynan, southwestern Jordan." *Toxicology and Industrial Health* 18: 297-307. https://doi.org/10.1191/0748233702th153oa.

Grattan, J. P., R. B. Adams, H. Friedman, D. D. Gilbertson, K. I. Haylock, C. O. Hunt, and M. Kent. 2016. "The first polluted river? Repeated copper contamination of fluvial sediments associated with Late Neolithic human activity in southern Jordan." *Science of the Total Environment* 573: 247-257. https://doi.org/10.1016/j.scitotenv.2016.08.106.

Grattan, J. P., S. I. Huxley, and F. B. Pyatt. 2003a. "Modern Bedouin exposures to copper contamination: an imperial legacy?" *Ecotoxicology and Environmental Safety* 55: 108-115. https://doi.org/10.1016/S0147-6513(02)00135-5.

Gregoricka, Lesley A. 2014. "Assessing Life History from Commingled Assemblages: The Biogeochemistry of Inter-Tooth Variability in Bronze Age Arabia." *Journal of Archaeological Science* 47: 10–21. https://doi.org/10.1016/j.jas.2014.04.004.

Gregoricka, Lesley A. 2023. "The ethics of excavating: bioarchaeology and the case for rehabilitating legacy human skeletal collections in the Near East." *Levant: The Journal of the Council for British Research in the Levant* 55, no. 3: 294-303. https://doi.org/10.1080/00758914.2023.2278287.

Grimstead, Deanna N, Amy E Clark, and Adam Rezac. 2018. "Uranium and Vanadium Concentrations as a Trace Element Method for Identifying Diagenetically Altered Bone

in the Inorganic Phase." *Journal of Archaeological Method and Theory* 25, no. 3: 689–704. https://doi.org/10.1007/s10816-017-9353-z.

Grueger, Barbara. 2013. "Weaning from the Breast." *Paediatrics & Child Health* 18, no. 4: 1-5.

Guede, Iranzu, Maria Cruz Zuluaga, Luis Angel Ortega, Ainhoa Alonso-Olazabal, Xabier Murelaga, Miriam Pina, and Francisco Javier Gutierrez. 2017. "Analyses of human dentine and tooth enamel by laser ablation-inductively coupled plasma-mass spectrometry (LA-ICP-MS) to study the diet of medieval Muslim individuals from Tauste (Spain)." *Microchemical Journal* 130: 287-294. https://doi.org/10.1016/j.microc.2016.10.005.

Handler, Jerome S, Arthur C Aufderheide, Robert S Corruccini, Elizabeth M Brandon, and Lorentz E Wittmers. 1986. "Lead Contact and Poisoning in Barbados Slaves: Historical, Chemical, and Biological Evidence." *Social Science History* 10 (4): 399-. https://doi.org/10.2307/1171025.

Hare, Dominic, Christine Austin, and Philip Doble. 2012. "Quantification strategies for elemental imaging of biological samples using laser ablation-inductively coupled plasma-mass spectrometry." *Analyst* 137, no. 7: 1527-1537. https://doi.org/10.1039/C2AN15792F.

Hauptmann, Andreas. 2007. *The Archaeometallurgy of Copper*. Berlin: Springer.

Hauptmann, A. and Weisberger G. 1987. "Archaeometallurgical and Mining-archaeological Investigations in the Area of Feinan, Wadi 'Arabah, Jordan." *Annual of the Department of Antiquities of Jordan / Hashemite Kingdom of Jordan* 31: 419-437.

Hauptmann, Andreas, Sigrid Schmitt-Strecker, Thomas E. Levy, and Friedrich Begemann. 2015. "On Early Bronze Age Copper Bar Ingots from the southern Levant." *Bulletin of the American Schools of Oriental Research* 373: 1-24. https://doi.org/10.5615/bullamerschoorie.373.0001.

Hedges, Sapna, Mukthineni Sridhar, Dinesh Rao Bolar, Shubaha AreHalli Bhaskar, and Mitesh Bharat Sanghavi. 2010. "Relating tooth- and blood-levels in children residing near a zinc-lead smelter in India." *International Journal of Paediatric Dentistry* 20: 186-192.

Hedican, Edward J. 2016. *Public Anthropology: Engaging Social Issues in the Modern World*. North York, Ontario: University of Toronto Press.

Hillson, Simon. 2024. *Dental Anthropology*. Cambridge: Cambridge University Press.

Humphrey, Louise T. 2016. "Chemical and Isotopic Analyses of Dental Tissues." In *A Companion to Dental Anthropology*, edited by Joel D. Irish and G. Richard Scott, 499–513. Hoboken, NJ: John Wiley & Sons, Inc.

Hunt, Chris and Hwedi el-Rishi. 2010. "Human Paleoecology in the Ancient Metal-Smelting and Farming COmplex in the Wadi Faynan, SW Jordan, at the Desert Margin in the Middle East." In *Landscapes and Societies: Selected Cases,* edited by I. Peter Martini and Ward Chesworth, 121-134. Dordrecht: Springer.

Hunt, Chris O., David D. Gilbertson, and Hwedi A. El-Rishi. 2007. "An 8000-year history of landscape, climate, and copper exploitation in the Middle East: the Wadi Faynan and the

Wadi Dana National Reserve in southern Jordan." *Journal of Archaeological Science* 34, no. 8: 1306-1338. https://doi.org/10.1016/j.jas.2006.10.022.

Hutton, M. 1987. "Human Health Concenrs of Lead, Mercury, Cadmium and Arsenic." In *Lead, Mercury, Cadmium and Arsenic in the Environment*, edited by T. C> Hutchinson and K. M. Meema, 53-68. John Wiley & Sons, Inc.

Jaishankar, Monisha, Tenzin Tseten, Naresh Anbalagan, Blessy B Mathew, and Krishnamurthy N Beeregowda. 2014. "Toxicity, Mechanism and Health Effects of Some Heavy Metals." *Interdisciplinary Toxicology* 7 (2): 60–72. https://doi.org/10.2478/intox-2014-0009.

Jayamurali, Dheepthi, Krishnapriya Madhu Varier, Wuling Liu, Jegadeesh Raman, Yaacov Ben-David, Xiangchun Shen, and Babu Gajendran. 2021. "An Overview of Heavy Metal Toxicity." In *Metal, Metal Oxides and Metal Sulphides for Biomedical Applications*, edited by Saravanan Rajendran, Mu. Naushad, D. Durgalakshmi, and Eric Lichtfouse, 323-342. Cham, Switzerland: Springer Nature.

Kamenov, George D, Ellen M Lofaro, Gennifer Goad, and John Krigbaum. 2018. "Trace Elements in Modern and Archaeological Human Teeth: Implications for Human Metal Exposure and Enamel Diagenetic Changes." *Journal of Archaeological Science* 99: 27–34. https://doi.org/10.1016/j.jas.2018.09.002.

Kang, Daniel, Dulasiri Amarasiriwardena, and Alan H. Goodman. 2004. "Application of laser ablation-inductively coupled plasma-mass spectrometry (LA-ICP-MS) to investigate trace metal spatial distributions in human tooth enamel and dentine growth layers and pulp." *Analytical Bioanalytical Chemistry* 378, no. 6: 1608-1615. https://doi.org/10.1007/s00216-004-2504-6.

Kennedy, Melissa A. 2015. "Life and Death at Tell Umm Hammad, Jordan: A Village Landscape of the Southern Levantine Early Bronze Age IV / Intermediate Bronze Age." *Zeitschrift des Deutschen Palastina-Vereins (1953-)* 131, no. 1: 1-28.

Kerfoot, Charles W., Noel R. Urban, Cory P. McDonald, Ronald Rossmann, and Huanxin Zhang. 2016. "Legacy Mercury Releases during Copper Mining near Lake Superior." *Journal of Great Lakes Research* 42, no. 1: 50–61.

Knabb, Kyle A. 2019. "Human and Environmental Impacts of Ancient Copper Metallurgy." *Current Anthropology* 60, no. 6: 840-848. https://doi.org/10.1086/706543.

Knabb, Kyle A., Yigal Erel, Ofir Tirosh, Tammy Rittenour, Sofia Laparidou, Mohammad Najjar, and Thomas E. Levy. 2016. "Environmental impacts of ancient copper mining and metallurgy: Multi-proxy investigation of human-landscape dynamics in the Faynan valley, southern Jordan." *Journal of Archaeological Science* 74: 85-101. https://doi.org/10.1016/j.jas.2016.09.003.

Kohn, Matthew J, Jennifer Morris, and Paul Olin. 2013. "Trace Element Concentrations in Teeth – a Modern Idaho Baseline with Implications for Archeometry, Forensics, and Palaeontology." *Journal of Archaeological Science* 40 (4): 1689–99. https://doi.org/10.1016/j.jas.2012.11.012.

Lamas, Gervasio A, Francisco Ujueta, and Ana Navas-Acien. 2021. “Lead and Cadmium as Cardiovascular Risk Factors: The Burden of Proof Has Been Met.” *Journal of the American Heart Association* 10 (10): e018692-. https://doi.org/10.1161/JAHA.120.018692.

Lee, K. M., J. Appleton, M. Cooke, F. Keenan, and K. Sawicka-Kapusta. 1999. “Use of laser ablation inductively coupled plasma mass spectrometry to provide element versus time profiles in teeth.” *Analytica Chimica Acta* 395: 179-185. https://doi.org/10.1016/S0003-2670(99)00319-0.

Levy, Thomas E., Russell B. Adams, Andreas Hauptmann, Michael Prange, Sigrid Schmitt-Strecker, and Mohammad Najjar. 2002. “Early Bronze Age metallurgy: a newly discovered copper manufactory in southern Jordan.” *Antiquity* 76: 425-437. https://doi.org/10.1017/S0003598X00090530.

Limbeck, Andreas, Patrick Geller, Maximilian Bonta, Gerald Bauer, Winfried Nischkauer, and Frank Vanhaecke. 2015. “Recent advances in quantitative LA-ICP-MS analysis: challenges and solutions in the life sciences and environmental chemistry.” *Analytical and Bioanalytical Chemistry* 407, no. 22: 6593-6617. https://doi.org/10.1007/s00216-015-8858-0.

Linge, Kathryn L. and Kym E. Jarvis. 2009. “Quadrupole ICP-MS: Introduction to Instrumentation, Measurement Techniques and Analytical Capabilities.” *Geostandards and Geoanalytical Research* 33, no. 4: 445-467. https://doi.org/10.1111/j.1751-908X.2009.00039.x.

Lopez-Costas, Olalla, Malin Kylander, Nadine Mattielli, Noemi Alvarez-Fernandez, Marta Pérez-Rodríguez, Tim Mighall, Richard Bindler, and Antonio Martínez Cortizas. 2020. “Human bones tell the story of atmospheric mercury and lead exposure at the edge of Roman World.” *Science of the Total Environment* 710: 1-7.

Malara, Piotr, Agnieszka Fischer, and Beata Malara. 2016. “Selected Toxic and Essential Heavy Metals in Impacted Teeth and the Surrounding Mandibular Bones of People Exposed to Heavy Metals in the Environment.” *Journal of Occupational Medicine and Toxicology (London, England)* 11, no. 1: 56–56. https://doi.org/10.1186/s12995-016-0146-1.

Manton, W.I, C.R Angle, K.L Stanek, D Kuntzelman, Y.R Reese, and T.J Kuehnemann. 2003. “Release of Lead from Bone in Pregnancy and Lactation.” *Environmental Research* 92, no. 2: 139–51. https://doi.org/10.1016/S0013-9351(03)00020-3.

Martin, Debra L., Ryan P. Harrod, and Ventura R. Perez. 2013. *Bioarchaeology: An Integrated Approach to Working with Human Remains.* New York: Springer.

Meijer, Jacqueline, Alexis E Dolphin, Chris Yakymchuk, and Michael Gervers. 2019. “Interpreting Medieval Mobility from Burials at the Rock-hewn Church of St. Georges, Gurat (France): Insights from Strontium Isotope Analysis of Bones and Teeth.” *International Journal of Osteoarchaeology* 29, no. 4: 574–83. https://doi.org/10.1002/oa.2753.

Mohammadi, Salman, Maryam Shafiee, Seyed Nooreddin Faraji, Mohsen Rezaeian, and Ali Ghaffarian-Bahraman. 2022. “Contamination of Breast Milk with Lead, Mercury,

Arsenic, and Cadmium in Iran: A Systematic Review and Meta-Analysis." *Biometals* 35, no. 4: 711–28. https://doi.org/10.1007/s10534-022-00395-4.

Montgomery, J., J. A. Evans, S. R. Chenery, V. Pashley, and K. Killgrove. 2010. "'Gleaming, white and deadly': using lead to track human exposure and geographic origins in the Roman period in Britain." *Journal of Roman Archaeology* 78: 199-226.

Müller, Wolfgang, Alessia Nava, David Evans, Paola F Rossi, Kurt W Alt, and Luca Bondioli. 2019. "Enamel Mineralization and Compositional Time-Resolution in Human Teeth Evaluated via Histologically-Defined LA-ICPMS Profiles." *Geochimica et Cosmochimica Acta* 255: 105–26. https://doi.org/10.1016/j.gca.2019.03.005.

Nassiri, Oumayma, Ali Rhoujjati, Eduardo Moreno-Jimenez, and Moulay Lâarabi E. L. Hachimi. 2023. "Environmental and Geochemical Characteristics of Heavy Metals in Soils Around the Former Mining Area of Zeïda (High Moulouya, Morocco)." *Water, Air, and Soil Pollution* 234, no. 110: 1-21.

Navasumrit, Panida, Krittinee Chaisatra, Jeerawan Promvijit, Varabhorn Parnlob, Somchamai Waraprasit, Chalida Chompoobut, Ta Thi Binh, et al. 2019. "Exposure to Arsenic in Utero Is Associated with Various Types of DNA Damage and Micronuclei in Newborns: A Birth Cohort Study." *Environmental Health* 18, no. 1: 51–16. https://doi.org/10.1186/s12940-019-0481-7.

Needleman, H L, and D Bellinger. 1991. "The Health Effects of Low Level Exposure to Lead." *Annual Review of Public Health* 12 (1): 111–40. https://doi.org/10.1146/annurev.pu.12.050191.000551.

Nriagu, Jerome O. 1996. "A history of global metal pollution." *Science* 272, no. 5259: 223-225.

Ortiz-Garcia, Nancy Y, Anayansi Ixchel Cipriano Ramírez, Karen Juarez, Jazmin Brand Galindo, Gabriela Briceño, and Ernesto Calderon Martinez. 2023. "Maternal Exposure to Arsenic and Its Impact on Maternal and Fetal Health: A Review." *Curēus (Palo Alto, CA)* 15, no. 11: e49177–e49177. https://doi.org/10.7759/cureus.49177.

Palmer, Carol, David Gilbertson, Hwedi el-Rishi, Chris Hunt, John Grattan, Sue McLaren, and Brian Pyatt. 2007. "The Wadi Faynan today: landscape, environment, people." In *Archaeology and Desertification: The Wadi Faynan Landscape Survey, Southern Jordan*, edited by Graeme Barker, David Gilbertson, and D. J. Mattingly, 227-270. Oxford, UK: Oxbow Books.

Palumbo, Gaetano. 2008. "The Early Bronze Age IV." In *Jordan: An Archaeological Reader*, edited by Russell B. Adams, 227-262. London: Equinox Pub.

Philip, Graham. 2008. "The Early Bronze Age I-III." In *Jordan: An Archaeological Reader*, edited by Russell B. Adams, 161-226. London: Equinox Pub.

Pollard, A. M. 2007. *Analytical Chemistry in Archaeology*. 1st ed. Cambridge: Cambridge University Press.

Punshon, T., Julia A. Bauer, Margaret R. Karagas, Modupe O. Coker, Marc G. Weisskopf, Joseph J. Mangano, Felicitas B. Bidlack, Matthew N. Barr, and Brian P. Jackson. 2024. "Quantified retrospective biomonitoring of fetal and infant elemental exposure using LA-

ICP-MS analysis of deciduous dentin in three contrasting human cohorts." *Journal of Exposure Science & Environmental Epidemiology*: 1-12. https://doi.org/10.1038/s41370-024-00652-3.

Pyatt, F. B., A. J. Pyatt, and J. P. Grattan. 2002a. "A public health problem? Aspects and implications of the ingestion of copper and lead contaminated food by Bedouin." *Environmental Management and Health* 13, no. 5: 467-470. https://doi.org/10.1108/09566160210441771.

Pyatt, F. B., A. J. Pyatt, C. Walker, T. Sheen, and J. P. Grattan. 2005. "The heavy metal content of skeletons from an ancient metalliferous polluted area in southern Jordan with particular reference to bioaccumulation and human health." *Ecotoxicology and Environmental Safety* 60: 295-300. https://doi.org/10.1016/j.ecoenv.2004.05.002.

Pyatt, F. B. and J. P. Grattan. 2001. "Some consequences of ancient mining activities on the health of ancient and modern human populations." *Journal of Public Health* 23, no. 3: 235-236. https://doi.org/10.1093/pubmed/23.3.235.

Pyatt, F. B., D. Amos, J. P. Grattan, A. J. Pyatt, and C. E. Terrell-Nield. 2002b. "Invertebrates of ancient heavy metal spoil and smelting tip sites in southern Jordan: Their distribution and use as bioindicators of metalliferous pollution derived from ancient sources." *Journal of Arid Environments* 52: 53-62. https://doi.org/10.1006/jare.2002.0982.

Pyatt, F. B., G. Gilmore, J. P. Grattan, C. O. Hunt, and S. McLaren. 2000. "An Imperial Legacy? An Exploration of the Environmental Impact of Ancient Metal Mining and Smelting in Southern Jordan." *Journal of Archaeological Science* 27: 771-778. https://doi.org/10.1006/jasc.1999.0580.

Pyatt, F. B., G. W. Barker, P. Birch, D. D. Gilbertson, J. P. Grattan, and D. J. Mattingly. 1999. "King Solomon's Miners—Starvation and Bioaccumulation? An Environmental Archaeological Investigation in Southern Jordan." *Ecotoxicology and Environmental Safety* 43, no. 3: 305-308. https://doi.org/10.1006/eesa.1999.1795.

Quansah, Reginald, Frederick Ato Armah, David Kofi Essumang, Isaac Luginaah, Edith Clarke, Kissinger Marfoh, Samuel Jerry Cobbina, et al. 2015. "Association of Arsenic with Adverse Pregnancy Outcomes/Infant Mortality: A Systematic Review and Meta-Analysis." *Environmental Health Perspectives* 123, no. 5: 412–412. https://doi.org/10.1289/ehp.1307894.

Rasmussen, Kaare Lund, Jesper Lier Boldsen, Hans Krongaard Kristensen, Lilian Skytte, Katrine Lykke Hansen, Louise Mølholm, Pieter M Grootes, Marie-Josée Nadeau, and Karen Marie Flöche Eriksen. 2008. "Mercury Levels in Danish Medieval Human Bones." *Journal of Archaeological Science* 35, no. 8: 2295–2306. https://doi.org/10.1016/j.jas.2008.03.003.

Rebelo, Fernanda Maciel, and Eloisa Dutra Caldas. 2016. "Arsenic, Lead, Mercury and Cadmium: Toxicity, Levels in Breast Milk and the Risks for Breastfed Infants." *Environmental Research* 151: 671–88. https://doi.org/10.1016/j.envres.2016.08.027.

Reinhard, K. J. and A. M. Ghazi. 1992. “Evaluation of lead concentrations in 18th-century Omaha Indian skeletons using ICP-MS.” *American Journal of Physical Anthropology* 89, no. 2: 183-195. https://doi.org/10.1002/ajpa.1330890205.

Rodríguez, Juliana, and Patricia Mónica Mandalunis. 2018. “A Review of Metal Exposure and Its Effects on Bone Health.” *Journal of Toxicology* 2018 (2018): 1–11. https://doi.org/10.1155/2018/4854152.

Sandford, Mary K. 1993. “Understanding the Biogenic-Diagenetic Continuum: Interpreting Elemental Concentrations of Archaeological Bone.” In *Investigations of Ancient Human Tissue: Chemical Analyses in Anthropology*, edited by Mary K. Sandford, 3-57. Langhorne, PA: Gordon and Breach Science Publishers.

Scheper-Hughes, Nancy. 2009. “Making Anthropology Public.” *Anthropology Today* 25, no. 4: 1–3. https://doi.org/10.1111/j.1467-8322.2009.00674.x.

Schrader, Sarah A. and Christina Torres-Rouff. 2021. “Embodying Bioarchaeology: Theory and Practice.” In *Theoretical Approaches in Bioarchaeology,* edited by Colleen M. Cheverko, Julia R. Prince-Buitenhuys, and Mark Hubbe: 15-27. New York: Routledge.

Schroeder, Hannes, Kristrina A Shuler, and Simon R Chenery. 2013. “Childhood Lead Exposure in an Enslaved African Community in Barbados: Implications for Birthplace and Health Status.” *American Journal of Physical Anthropology* 150 (2): 203–9. https://doi.org/10.1002/ajpa.22193.

Simpson, Rachel, David M. L. Cooper, Treena Swanston, Ian Coulthard, and Tamara L. Varney. 2021. “Historical Overview and New Directions in Bioarchaeological Trace Element Analysis: A Review.” *Archaeological and Anthropological Sciences* 13, no. 24: 1-27. https://doi.org/10.1007/s12520-020-01262-4.

Squires, Kirsty, Thomas Booth, and Charlotte A. Roberts. 2019. “The Ethics of Sampling Human Skeletal Remains for Destructive Analyses.” In *Ethical Approaches to Human Remains: A Global Challenge in Bioarchaeology and Forensic* Anthropology, edited by Kirsty Squires, David Errickson, and Nicholas Marquez-Grant, 265-297. Cham, Switzerland: Springer.

Stojanowski, Christopher M. and William N. Duncan. 2015. “Engaging Bodies in the Public Imagination: Bioarchaeology as Social Science, Science, and Humanities.” *American Journal of Human Biology* 27: 51-60.

Tan, Kaithleen. 2021. *A Trace Element Analysis of Lead in Human Tooth Enamel from Wadi Faynan 100, Jordan*. University of Waterloo, Master’s Thesis.

Tchounwou, Paul B., Clement G. Yedjou, Anita K. Patlolla, and Dwayne J. Sutton. 2012. “Heavy Metals Toxicity and the Environment.” In *Molecular, Clinical and Environmental Toxicology*, edited by Andreas Luch, 133-164. Springer.

Téllez-Rojo, Martha María, Mauricio Hernández-Avila, Héctor Lamadrid-Figueroa, Donald Smith, Leticia Hernández-Cadena, Adriana Mercado, Antonio Aro, Joel Schwartz, and Howard Hu. 2004. “Impact of Bone Lead and Bone Resorption on Plasma and Whole Blood Lead Levels during Pregnancy.” *American Journal of Epidemiology* 160 (7): 668–78. https://doi.org/10.1093/aje/kwh271.

Ufelle, Alexander C. and Aaron Barchowsky. 2019. “Toxic Effects of Metals.” In *Casarett & Doull’s Toxicology: The Basic Science of Poisons, 9th edition,* edited by Curtis D. Klaassen. McGraw-Hill Education.

United Nations Executive Body for the Convention on Long-range Transboundary Air Pollution. “1998 Protocol on Heavy Metals, as amended on 13 December 2012”. ECE/ED.AIR/115. UN Economic Commission of Europe, October 16, 2014. https://unece.org/sites/default/files/2021-10/ECE.EB_.AIR_.115_ENG.pdf.

Uryu, Tsutomu, Jun Yoshinaga, Yukio Yanagisawa, Masahiko Endo, and Junichi Takahashi. 2003. “Analysis of Lead in Tooth Enamel by Laser Ablation-Inductively Coupled Plasma-Mass Spectrometry.” *Analytical Sciences* 19, no. 10: 1413- 1416. https://doi.org/10.2116/analsci.19.1413.

Walker, Phillip L. 2008. "Bioarchaeological ethics: a historical perspective on the value of human remains." In *Biological Anthropology of the Human Skeleton, Second Edition,* edited by Mary Anne Katzenberg and Shelley Rae Saunders, 3-40. Hoboken, NJ: John Wiley & Sons, Inc.

Webb, Ellen, Dulasiri Amarasiriwardena, Socheata Tauch, Ethan F. Green, Joseph Jones, and Alan H. Goodman. 2005. “Inductively coupled plasma-mass (ICP-MS) and atomic emission spectrometry (ICP-AES): Versatile analytical techniques to identify the archived elemental information in human teeth.” *Microchemical Journal* 81, no. 2: 201-208. https://doi.org/10.1016/j.microc.2005.04.002.

Weisberger, G. and A. Hauptmann. 1988. “Early copper mining and smelting in Palestine.” In *The Beginning of the Use of Metals and Alloys: Papers from the Second International Conference on the Beginning of the Use of Metals and Alloys, Zhengzhou, China, 21–26 October 1986,* edited by R. Maddin, 52-62. Cambridge, MA: MIT Press.

Wesp, Julia K. 2017. “Embodying Sex/Gender Systems in Bioarchaeological Research.” In *Exploring Sex and Gender in Bioarchaeology*, edited by Sabrina C. Agarwal and Julie K. Wesp, 99-126. Albuquerque: University of New Mexico Press.

White, Christine D. and Fred J. Longstaffe. 2016. “Stable isotopes and selective forces: examples in biocultural and environmental anthropology.” In *New Directions in Biocultural Anthropology,* edited by Molly K. Zuckerman and Debra L. Martin, 7-26. Hoboken: John Wiley & Sons, Inc.

Wilson, B., and F.B. Pyatt. 2007. “Heavy Metal Dispersion, Persistance, and Bioccumulation around an Ancient Copper Mine Situated in Anglesey, UK.” *Ecotoxicology and Environmental Safety* 66, no. 2: 224–231.

Winterbottom, Emily F, Yuka Moroishi, Yuliya Halchenko, David A Armstrong, Paul J Beach, Quang P Nguyen, Anthony J Capobianco, et al. 2019. “Prenatal Arsenic Exposure Alters the Placental Expression of Multiple Epigenetic Regulators in a Sex-Dependent Manner.” *Environmental Health* 18 (1): 18–8. https://doi.org/10.1186/s12940-019-0455-9.

Wright, Katherine, Mohammed Najjar, Jonathan Last, Norah Moloney, Matthias Flender, Jonathan Gower, Nicholas Jackson, Amanda Kennedy, and Rula Shafiq. 1998. “The Wadi Faynan Fourth and Third Millennia Project, 1997: Report on the First Season of

Test Excavations at Wadi Faynan 100." *The Journal of the Council for British Research in the Levant* 30, no. 1: 33-20. https://doi.org/10.1179/007589198790217142.

Zhang, Shudi, Miaohong He, Zhibin Yin, Eryi Zhu, Wei Hang, and Benli Huang. 2016. "Elemental fractionation and matrix effects in laser sampling based spectrometry." *Journal of Analytical Atomic Spectrometry* 31, no. 2: 358-382. https://doi.org/10.1039/C5JA00273G.

Zuckerman, Molly K. and Debra L. Martin. 2016. "Introduction: the development of biocultural perspectives in anthropology." In *New Directions in Biocultural Anthropology,* edited by Molly K. Zuckerman and Debra L. Martin, 7-26. Hoboken: John Wiley & Sons, Inc.

Zuckerman, Molly K., Kelly R. Kamnikar, and Sarah A. Mathena. 2014. "Recovering the 'Body Politic': a Relational Ethics of Meaning for Bioarchaeology." *Cambridge Archaeological Journal* 24, no. 3: 513-522.

Appendix A: Heavy Metals and the Body

A.1 | Lead and the Body

Lead (Pb) is a highly toxic metal that affects multiple organ systems (Needleman and Bellinger 1991), including the kidneys, liver, central nervous system (CNS), and hematopoietic, endocrine, and reproductive systems (Tchounwou et al. 2012). Additionally, 90-95% of the body's lead burden accumulates in skeletal tissue (Hutton 1987; Jaishankar et al. 2014). After exposure, Pb is distributed throughout the body via red blood cells (Boskabady et al. 2022; Tchounwou et al. 2012). One of the reasons for Pb's high toxicity is its ability to inhibit or mimic calcium, which causes Pb to interfere with calcium dependent processes. Calcium is a significant constituent in the mineral phase of skeletal tissue, hydroxyapatite, and Pb can incorporate into hydroxyapatite in place of calcium (Tchounwou et al. 2012). Long- and short-term exposure to Pb can affect the skeletal system leading to decreased bone mineral content, imbalances in the bone remodeling process, and the manifestation of bone pathologies (Boskabady et al. 2022). Acute Pb exposure can lead to a wide range of symptoms including headaches, hypertension, abdominal pain, kidney dysfunction, loss of appetite, fatigue, hallucinations (Jaishankar et al. 2014), brain damage, and gastrointestinal disease (Tchounwou et al. 2012). Chronic Pb exposure can also lead to brain damage, kidney dysfunction, and hypertension as well as mental disorders, paralysis, muscular damage, issues with vitamin D metabolism, and death (Jaishankar et al. 2014; Tchounwou et al. 2012). Additionally, exposure to Pb can affect the reproductive system leading to decreased sperm count and spontaneous abortions (Tchounwou et al. 2012). Furthermore, Pb is thought to be carcinogenic through inhibition of DNA synthesis and repair, oxidative damage, and interactions with tumor suppressing proteins (Tchounwou et al. 2012).

In pregnant persons, umbilical cord blood Pb levels reflect maternal blood Pb levels due to its ability to pass through the placenta (Needleman and Bellinger 1991). Ergo, if the mother is exposed to Pb during pregnancy and lactation, the fetus or infant is also at risk of Pb exposure. Compounding this, throughout pregnancy and lactation, there is a high demand for Ca causing physiological changes in the mother increasing rates of bone turnover, releasing Ca from their bones into the blood. The mobilized Ca transfers to the fetus via the umbilical cord or the infant via lactation (Tellez-Rojo et al. 2004; Manton et al. 2003). Maternal Pb follows the same pattern of mobilization as Ca; thus, if the mother has high bone Pb levels, the bone resorption process will also release Pb into the bloodstream putting the fetus and infant at risk of lead toxicity (Tellez-Rojo et al. 2004; Manton et al. 2003). Various studies have shown that maternal bone Pb levels could result in low birth weight, reduced stature, impairment of cognitive abilities, digestive disorders, and decreased hearing acuity among others (Boskabady et al. 2022; Needleman and Bellinger 1991; Tchounwou et al. 2012).

A.2 | Cadmium and the Body

Cadmium (Cd) is distributed to the soft tissues of the body via the circulatory system by binding to primarily albumin and other proteins in the blood stream (Lamas et al. 2021; Tchounwou et al. 2012; Ufelle and Barchowsky 2019). This heavy metal predominately accumulates in the liver and kidneys and absorption can be exacerbated by deficiencies of essential trace elements such as Zn, Ca, and Fe (Lamas et al. 2021; Ufelle and Barchowsky 2019). Because Cd mimics such essential trace elements, it can replace them or follow their pathways within the body effectively disrupting their biological functions (Balali-Mood et al. 2021; Jaishankar et al. 2014). For instance, Cd is transported to cells via Ca channels and replaces Zn in antioxidant enzymes (Lamas et al. 2021; Ufelle and Barchowsky 2019). Some

acute side effects include nausea, abdominal pain, vertigo, muscle cramping, shock, loss of consciousness, convulsions, and acute pneumonitis with pulmonary edema (Jaishankar et al. 2014; Ufelle and Barchowsky 2019). Chronic exposure to Cd can result in kidney dysfunction, lung injuries, liver damage, cardiovascular disease, and osteoporosis (Balali-Mood et al. 2021; Lamas et al. 2021; Ufelle and Barchowsky 2019) as well as imbalances in the neurotransmitters norepinephrine, serotonin, and acetylcholine (Jaishankar et al. 2014).

Cd is thought to both directly affect bone cells by stimulating osteoclast activity and indirectly affect skeletal tissues through renal dysfunction, which increases Ca and phosphorous (P) excretion, impairs vitamin D synthesis, and decreases the Ca absorption during digestion (Rodriguez and Mandalunis 2018; Ufelle and Barchowsky 2019). At the cellular level, Cd causes cellular damage and death, mitochondrial and DNA damage, and disrupts protein and nucleic acid synthesis (Lamas et al. 2021; Tchounwou et al. 2012). Cd is considered a carcinogen by the International Agency for Research on Cancer (IARC) causing prostate, kidney, liver, lung, gastrointestinal, breast, and hematopoietic system cancers (Balali-Mood et al. 2021; Tchounwou et al. 2012). Lastly, there are strong correlations in epidemiological studies of increased exposure to Cd and preeclampsia during pregnancy as well as premature birth, reduced birth weight and length, adverse effects on childhood health, and the development of epigenetic changes (Jaishankar et al. 2014; Lamas et al. 2021; Tchounwou et al. 2012; Ufelle and Barchowsky 2019).

A.3 | Arsenic and the Body

Ancient and contemporary smelting practices have been shown to release As into the air, soil, and water systems (Jaishankar et al. 2014). Ingestion is the primary route of exposure to As;

however, exposure also occurs via inhalation and dermal contact. This heavy metal affects almost all organ systems, distributing to many different tissues and organs including the heart, lungs, liver, and kidneys, and throughout the nervous and gastro-intestinal systems (Balali-Mood et al. 2021; Tchounwou et al. 2012). As's pervasive effects are attributed to its capability to bind to proteins and inhibit over 200 enzymes and its ability to replace phosphorous in several biochemical reactions. As exposure can impair cellular respiration, inhibit DNA repair, and cause chromosomal aberrations (Tchounwou et al. 2012).

Acute As exposure has been shown to cause nausea and vomiting, abnormal heartbeat, damage to blood vessels, and a pricking sensation in extremities. Chronic exposure has been shown to cause skin lesions, neurological problems, pulmonary disease, peripheral vascular disease, hypertension, cardiovascular disease and diabetes (Jaishankar et al. 2014). As is considered carcinogenic causing cancers in the bladder, lungs, kidneys, liver, and prostate (Tchounwou et al. 2012; Tolins et al 2014). Furthermore, As's toxicity disrupts cell-to-cell signaling of neurotransmitters and animal studies indicate that it causes reductions in body and brain weight. As's ability to induce oxidative stress is the mechanism by which this heavy metal's neurotoxicity and carcinogenicity is attributed (Tchounwou et al. 2012; Tolins et al. 2014).

In pregnant persons, As can transfer through the placenta to the fetus causing spontaneous abortions, stillbirths, preterm births and low birth weight (Balali-Mood et al. 2021; Quanash et al. 2015). With the ability to cross the blood brain barrier in the fetus, As also negatively affects the central nervous system of the fetus (Tolins et al. 2014). Lastly, the male reproductive system can be affected by As exposure leading to impairment of testes function and production of sperm (Balali-Mood et al. 2021).

Appendix B: Dentine Development and Chemical Composition

Odontoblasts secrete predentine, an organic collagen matrix, in a regular, layering manner similarly to the way that enamel is deposited. Layers are added on the inside of the tooth, grow towards the root, and form the pulp chamber floor and roots (Hillson 2024). Dentine also has incremental structures that represent shorter and longer periods of development that are equivalent to striations and striae of Retzius, and prisms, although they are not as well-defined as the markings found in enamel (Hillson 2024; Humphrey 2016). Several days after odontoblasts secrete the predentine matrix, they begin the mineralization process that results in mature dentine that is about 72% inorganic and 20% organic. Unlike ameloblasts, odontoblasts are thought to remain active throughout the life of the tooth. With increasing tooth wear and age, formation of dentine continues around the pulp chamber. Thus, dentine development can be divided into different phases: primary dentine, secondary or regular secondary dentine, and tertiary or irregular secondary dentine. Primary dentine represents initial tooth formation that occurs in early life. Secondary or regular secondary dentine is slowly deposited around the pulp chamber after adolescence. Lastly, tertiary or irregular dentine forms to seal off the pulp chamber when the overlying primary dentine is exposed due to dental caries or extensive tooth wear (Hillson 2024).

Like enamel, dentine is also a composite material consisting of an inorganic or mineral component and an organic component. The inorganic component of dentine consists of hydroxyapatite crystallites that are significantly smaller than those found in enamel, about 20-100 nm long, as well as less densely packed throughout (Humphrey 2016; Webb et al. 2005). The hydroxyapatite component of dentine also undergoes elemental substitutions (Humphrey 2016); however, elemental concentrations found in dentine are less studied (Hillson 2024). Generally,

there are higher concentrations of fluoride found in dentine than enamel and higher concentrations of Zn and Pb than the deeper layers of enamel with all three elements increasing towards the pulp chamber. Sr is found at lower concentrations in dentine but similarly follows uniform distribution throughout (Hillson 2024).

Unlike enamel, dentine is biologically more active, with odontoblasts active throughout the tooth's life, resulting in continued dentine production deposited as secondary and tertiary dentine. Element substitutions in dentine continue throughout the life of the tooth (Asaduzzaman et al. 2017). This thesis sampled the dentine of each tooth (n=29) down the root, with the intention of obtaining elemental exposure later in life. All dentine samples had significantly elevated concentrations of U and La surpassing their respective MTCs, indicating that, like bone, dentine is more susceptible to postmortem alteration. As such, all dentine samples were excluded from the main analysis and interpretations. See Table 7 for maximum and minimum concentrations found in the dentine samples.

Tooth ID	Pb Min-Max (ppm)	Cd Min-Max (ppm)	As Min-Max (ppm)	U Min-Max (ppm)	La Min-Max (ppm)
M101	4.642-43.052	0.496-15.639	0.975-71.893	1.123-2.203	0.017-0.315
M102	0.240-2.118	0.138-2.477	0.017-1.628	0.012-2.327	0.003-0.152
M103	1.018-2.311	0.144-0.824	1.679-4.376	0.611-2.175	0.129-3.290
M104	1.500-4.817	0.011-2.455	1.426-10.216	0.457-1.857	0.090-1.871
M105	0.236-0.537	2.405-4.551	6.644-8.763	0.309-0.715	0.002-0.079
M106	0.552-2.654	0.633-9.943	8.647-15.769	2.759-5.057	0-0.081
M107	0.321-0.613	0.269-0.986	0.900-1.794	0.285-0.436	0.002-0.089
M108	0.755-3.109	0.315-1.230	2.167-58.511	0.901-5.883	0-0.757
M109	0.127-1.289	0.017-5.059	0-2.772	0-1.635	0-0.751
M110	0.072-291.263	0-395.061	0-574.410	0.005-97.734	0-13.266
M111	0.245-4.413	0.048-1.381	0.091-25.178	0.178-20.364	0-2.244
M301	1.068-2.491	0.261-1.851	0.936-3.839	0.259-3.190	0.039-1.230
M302	2.396-111.772	0.241-219.553	0-638.169	0.187-33.934	0.049-16.368
M303	0.814-10.699	0.776-6.331	0-45.628	1.051-6.115	0.026-5.526
M304	1.423-61.428	0.823-182.697	4.734-574.177	0.183-65.428	0.002-9.802
M305	3.156-4.304	0.540-1.677	1.127-2.627	0.515-0.845	0.109-1.966
M306	0.150-6.500	0.058-2.216	0-2.975	0.015-2.105	0-0.713
M307	0.360-3.839	1.084-3.487	1.842-10.494	0.268-9.208	0-0.811
M308	1.328-4.570	0.746-3.122	0.975-3.951	0.334-0.531	0.002-0.322
M309	1.165-5.734	1.135-11.077	7.335-16.395	4.295-10.420	0.002-0.724
M310	3.063-58.311	0.579-204.410	0-95.926	3.493-93.992	0.037-7.520
M311	0.678-1.531	0.778-2.675	4.265-11.823	4.544-8.333	0.003-0.266
M312	2.654-5.048	0.261-1.900	1.522-4.278	5.908-10.064	0.017-0.687
PM01	0.327-54.981	0-4.045	0-914.059	0.792-31.240	0.020-8.934
PM02	1.192-2.471	1.426-4.599	5.728-9.069	3.080-4.646	0.024-0.177
PM03	0.059-2.567	0.084-1.632	0-3.722	0.001-2.242	0-5.405
PM04	1.559-7.501	1.122-3.330	15.993-23.146	3.818-9.496	0.002-2.667
PM05	1.484-133.638	0.177-49.292	0-18.753	0.672-12.128	0.025-102.933
PM06	1.561-10.360	0.365-3.733	1.247-2.796	6.189-10.688	0.144-4.716

Table 9 | Minimum and maximum concentrations of Pb, Cd, As, U, and La found along ablation transect of dentine for all samples.

Appendix C: Dental Pathology and Non-Metrics

C.1 | Dental Pathology

Tooth ID	Tooth Type	Caries	Enamel Hypoplasia	Calculus
M101	Lower Left 1st Molar	Absent	Absent	Present
M102	Lower Left 1st Molar	Absent	Present	Present
M103	Upper Left 1st Molar	Absent	Absent	Present
M104	Upper Left 1st Molar	Present	Absent	Present
M105	Lower Left 1st Molar	Absent	Present	Present
M106	Upper Right 1st Molar	Absent	Unobservable	Present
M107	Lower Right 1st Molar	Absent	Absent	Present
M108	Lower Right 1st Molar	Absent	Absent	Present
M109	Lower Left 1st Molar	Absent	Absent	Present
M110	Lower Left 1st Molar	Absent	Present	Present
M111	Upper Right 1st Molar	Absent	Present	Present
M301	Upper Left 3rd Molar	Present	Absent	Present
M302	Upper Left 3rd Molar	Absent	Present	Present
M303	Upper Left 3rd Molar	Present	Present	Present
M304	Upper Left 3rd Molar	Present	Absent	Present
M305	Upper Left 3rd Molar	Absent	Present	Present
M306	Upper Left 3rd Molar	Absent	Present	Absent
M307	Upper Left 3rd Molar	Absent	Unobservable	Absent
M308	Lower Left 3rd Molar	Present	Present	Present
M309	Upper Left 3rd Molar	Absent	Unobservable	Absent
M310	Upper Right 3rd Molar	Absent	Present	Present
M311	Upper Right 3rd Molar	Absent	Present	Present
M312	Upper Left 3rd Molar	Absent	Absent	Present
PM01	Lower Left 3rd Premolar	Absent	Present	Present
PM02	Lower Left 3rd Premolar	Absent	Present	Present
PM03	Lower Left 4th Premolar	Absent	Absent	Present
PM04	Lower Left 4th Premolar	Absent	Absent	Present
PM05	Upper Right 3rd Premolar	Absent	Present	Present
PM06	Upper Left 3rd Premolar	Absent	Absent	Present

Table 10 | Dental pathology for all samples. All pathology was evaluated macroscopically and recorded as present or absent.

C.1 | Non-Metric Traits

Tooth ID	Tooth Type	Accessory Cusps	Distosagittal Ridge	Mesial Accessory Ridge	Distal Accessory Ridge	Root Number
PM05	Right 3rd Premolar	0	0	0	1	2
PM06	Left 3rd Premolar	0	0	0	0	1

Table 11 | Dental non-metric traits for maxillary premolars.

Tooth ID	Tooth Type	Lingual Cusp Number	Root Number	Lingual Cusp Complexity	Elongated Form
PM01	Left 3rd Premolar	1	1	1	0
PM02	Left 3rd Premolar	1	1	1	0
PM03	Left 4th Premolar	2	Unobservable	3	0
PM04	Left 4th Premolar	1	Unobservable	1	0

Table 12 | Dental non-metric traits for mandibular premolars.

Table 13 | Dental non-metric traits for maxillary molars.

Tooth ID	Tooth Type	Hypocone	Carabelli's Trait	Cusp 5 (Metacone)	Mesial Marginal Accessory Tubercles	Enamel Extensions	Upper Molar Root Number	Metacone	Parastyle	3rd Molar Peg or Reduction Trait
M103	Left M1	3	1	1	1	Unobservable	Unobservable	5	Unobservable	N/A
M104	Left M1	3	0	0	0	0	Unobservable	4	0	N/A
M106	Right M1	4	5	0	0	Unobservable	3	4	0	N/A
M111	Right M1	4	0	0	1; 1	0	Unobservable	3	0	N/A
M301	Left M3	2	2	0	1; 1	Unobservable	Unobservable	3	0	0
M302	Left M3	4	6	5	1; 1	1	3	4	0	0
M303	Left M3	3	0	1	1; 1	0	3	4	0	0
M304	Left M3	1	0	0	1	0	3	4	0	0
M305	Left M3	0	0	0	1	0	Unobservable	3	0	0
M306	Left M3	1	0	0	0	Unobservable	Unobservable	4	0	0
M307	Left M3	0	0	0	0	0	Unobservable	3	0	0
M309	Left M3	0	0	0	0	0	3	3	0	0
M310	Right M3	3	0	0	1	0	3	3	0	0
M311	Right M3	1	0	0	0	Unobservable	Unobservable	3	0	0
M312	Left M3	0	0	0	1	0	1	3	0	1

Table 14 | Dental non-metric traits for mandibular molars.

Tooth ID	Tooth Type	Hypoconulid	Groove Pattern	Cusp 6	Cusp 7	Protostylid	Deflecting Wrinkle	Root Number	Anterior Fovea	Trigonid Crest	Cusp Number
M101	Left M1	3	0	0	0	0	0	2	0	0	5
M102	Left M1	3	0	1	0	0	2	Unobservable	2	0	6
M105	Left M1	3	1	0	0	3	2	Unobservable	3	0	5
M107	Right M1	4	2	0	0	0	0	Unobservable	0	0	5
M108	Right M1	3	1	0	0	1	0	Unobservable	0	0	5
M109	Left M1	2	1	0	0	Unobservable	2	Unobservable	1	0	5
M110	Left M1	4	0	0	0	1	1	Unobservable	3	0	5
M308	Left M3	3	1	1	0	0	0	Unobservable	2	0	6

Appendix D: Early Bronze Age Society and Copper Production

Investigations into ancient copper production in Faynan began in the 1980s by Hauptmann and Weisberger (1987) through the German Mining Museum (Deutsches Bergbau Museum [DBM]) Early Metallurgy Project (Adams 2002; Adams et al. 2017). Focusing on the technological evolution of prehistoric copper production in Faynan, they investigated mines and smelting sites throughout Faynan forming the foundation for subsequent archaeological projects (Adams 2002; Adams et al. 2017; Hauptmann 2007). This includes the Faynan Landscape Survey, which conducted detailed surveys and collected surface archaeological material across Faynan to further understandings about the landscape (Barker et al. 2007), and the Jabal Hamrat Fidan Archaeological Project, which investigated the relationships between early metallurgy and social change from the Neolithic to the Iron Age (Levy et al. 1999). Due to the extent of archaeological work conducted here, Faynan is one of the most studied regions in Jordan (Adams et al. 2017).

It is suggested that the Neolithic societies in the southern Levant were village-based (Barker et al. 2007) and saw the rise of food production and animal husbandry as well as the introduction of pottery (Hauptmann 2007; Levy et al. 1999). While the earliest indications of copper exploitation in Faynan dates to the Neolithic, there is no evidence of intentional prospecting or smelting of copper ores. Rather, it is suggested that they locally gathered copper ores for beads and pigments on a small-scale (Hauptmann 2007; Hunt and el-Rishi 2010; Hunt et al. 2007).

Archaeological evidence throughout the southern Levant suggests that the Chalcolithic period (4500-3500 BCE) saw remarkable population growth and the development of local social hierarchies. With evidence including prestige objects, formal cemeteries, religious buildings, and

specialized craft workshops, it has been suggested that larger sites from this period represent political centers that controlled economic and religious activities (Barker et al. 2007). Evidence of Chalcolithic copper production in the southern Levant mainly comes from sites uncovered in modern-day Israel's Negev Desert (Levy et al. 2002), such as Shiqmim, Arad, Meser (Hauptmann 2007), Abu Mater (Golden 2014), and Horvat Beter (Ackerfeld et al. 2020). Hauptmann (2007) asserts that Chalcolithic smelting was conducted using crucibles with no evidence of smelting furnaces at sites dating prior to EBII; however, some archaeological work suggests there is evidence for the possible use of furnaces, though these are less common than crucibles (Ackerfeld et al. 2020; Golden 2014). In Faynan, the Chalcolithic period saw the first instances of mining for copper ores that were then transported to the sites in the Negev desert and Egypt (Adams 2006; Golden 2014; Hauptmann 2007; Weisberger and Hauptmann 1988). For instance, lead isotope analysis conducted on slag and crucibles recovered from Horvat Beter, a site more than 100 km away from Faynan in Beersheva, indicated that copper ore brought to the site originated in Faynan (Ackerfeld et al. 2020).

Generally, during the Early Bronze Age, the southern Levant saw the development of more complex hierarchical societies characterized by many urbanism attributes including, "densely nucleated populations; a distinct settlement hierarchy; a stable and productive agricultural system; a differentiated social system; centralized political administration; advanced technology; monumental art and architecture; and long-distance trade" (Barker et al. 2007, 232). Philip (2008) suggests an alternative interpretation for the structure of EBA society in southern Jordan that deviates from the traditional city-state model previously accepted. He argues that EBA social organization was not hierarchical but heterarchical, a system in which, relative to each other, elements go unranked or have the potential to be ranked in various ways. In other

words, EBA social organization was flexible. Philip (2008) also maintains that communities were organized into corporate villages, in which land was communally owned and labor obligations were communal responsibilities. In contrast to the Chalcolithic period, it appears that wealth was understood in terms of land and productive facilities and that kin-based households and groups of households were the basis for social organization (Philip 2008).

The EBA in Jordan was a ~1500 period marked by significant social and economic change (Adams 2002), specifically a transition towards urbanization, construction of fortified communities, and increased population density (Chesson and Goodale 2014; Kennedy 2015); advancements in subsistence practices including use of irrigation, wide use of pack animals, cultivation via ox-drawn ploughs, and wider availability of metal tools (Philip 2008); and transformation from small-scale, community-level, low intensity copper production to large-scale, highly developed, intensive copper production (Adams 2002; Adams et al. 2017). EBI (3600-3000 BCE) marked the beginning of local copper production in Faynan, representing a transition from long-distance transport of copper ores to smelting centers in the Negev (Ben-Yosef et al. 2016; Levy et al. 2002). Importantly, Faynan copper was still widely traded throughout the EBA (Adams et al. 2017; Barker et al. 2007; Hauptmann 2007; Wright et al. 1997) and Adams (2006) asserts that despite geographic location away from 'mainstream' cultural developments, Faynan's "central role of copper production and trade…played a significant role in technological and social developments in the broader region during this period" (137).

According to data collected during the DBM project, EBI mining was restricted to easily accessible or already exposed ore bodies (Adams 2002). Following veins or ore, irregular, rounded open gallery mines were constructed in Umm Ishrin Sandstone (also known as Massive

Brown Sandstone [MBS]) using rudimentary stone hammers or were gathered from erosion debris originating in the Burj Dolomite Shale Formation (also known as Dolomite Limestone Shales [DLS]) (Adams 2002; Hauptmann 2007). The beginning of metallurgy in Faynan during EBI relied on the use of ceramic crucibles for smelting copper ores, which were transported from the mining locations to the settlement for smelting. These were placed on a bed of charcoal and likely covered by more charcoal and subsequently heated by human breath through blowpipes from above (Adams 2002; Adams and Genz 1995; Hauptmann 2007). While there is evidence for the possible use of furnaces in the Negev during the Chalcolithic, there is no indication that furnaces were used for smelting in Faynan prior to EBII (3000-2750 BCE) (Hauptmann 2007).

Wadi Fidan 4 (WF4) provides the earliest evidence of metallurgy in Faynan, dating to EBIa (3600-3300 BCE), and is situated on a plateau on the south bank of Wadi Fidan. Evidence of metallurgy within the settlement include slag, crucible fragments, and secondary copper ores and it is suggested that the crucibles found in WF4 were used for both smelting and casting metal (Adams and Genz 1995). Additionally, Adams (2002) suggests that smelting included multiple steps with initial smelting followed by crushing of and subsequent selection of the smelted ore for secondary smelting. Based on the density of metallurgical materials and waste within specific areas of the site, Adams (2002) also propounds that copper production was a craft specialization at WF4 with only specific individuals or groups participating. Lastly, while Hauptmann (2007) asserts that the amount of copper produced at WF4 was limited in quantity, Adams (2002) maintains that there is evidence the site's inhabitants produced a significant amount of copper.

EBII (3000-2700 BCE) witnessed a significant transition into urban communities as well as increased craft specialization in ceramics, flint tool, and copper production. Metallurgical development progressed from small-volume crucible smelting to large smelting furnaces

indicating a movement toward large scale production (Adams 2002). These furnaces were located on wind-exposed hills catching natural drafts to operate (Ben-Yosef et al. 2016). Additionally, EBII smelting sites were located near mining activities, which had also progressed past restriction to easily accessible or already exposed ore bodies. EBII mining involved the construction of vertical shafts excavated several meters into the DLS before expanding into gallery mines with supporting chamber and pillar systems (Adams 2002). Based on the notable number of mines and advanced mine construction, Adams (2002) suggests that a certain amount of social organization and centralization of resources and labor was required. This possibly contributed to the transition into urban communities and increase in craft specialization. Located in southern Faynan, one of the largest and most remarkable EBII copper production sites is Barqa el-Hetiye (Adams et al. 2017). Here, remnants of wind-operated furnaces, slag, copper prills, and other by-products dot the slopes of nearby hills (Ben-Yosef et al. 2016; Adams 2003). Evidence of copper production at this site indicate that copper ores were smelted in furnaces prior to being processed into metal ingots and other final products (Ben-Yosef et al. 2016; Hauptmann 2007).

Throughout EBIII (2700-2200 BCE) and into EBIV (2200-2000 BCE), craft specialization and the scale of copper production continued to increase. Extensive evidence of the production of metal ingots and final copper objects indicates that this period saw highly specialized metallurgical operations before distribution through trade networks (Adams 2002). Khirbet Hamra Ifdan (KHI), a site dating to EBIII-IV and located approximately 2 km up wadi from Wadi Fidan 4 (Hauptmann 2007; Hauptmann et al. 2015), was a densely packed settlement in which thousands of objects relating to metallurgy have been recovered (Hauptmann et al. 2015). This includes copper prills, slag, ores, furnace remains, casting molds, and copper axes

and chisels (Levy et al. 2002). This site housed the largest EBA metal workshop in which they produced crescent-shaped metal ingots known to be an intermediary product used in transportation of copper (Hauptmann et al. 2015; Levy et al. 2002). Ingots recovered from Hebron Hills and Har Yeruham, contemporaneous sites located in the Negev Desert 100 km north of and 60 km northwest of Faynan respectively, underwent lead isotope analysis with signatures indicating that they were indistinguishable from the ingots found at KHI. This suggests that KHI was involved in the exchange of copper products and likely supplied these far away sites (Hauptmann et al. 2015).

Lastly, EBIV represents social change from urban to non-urban with simpler subsistence practices and dispersed rural settlements. The economy was largely based on household production and local trade with little to no evidence of international trade networks (Palumbo 2008). Palumbo (2008) asserts that this "ruralization" could have been caused by a myriad of factors including drought conditions, interruption of trade routes, or competition between sites or any combination thereof. Regardless, whatever sparked the crisis led to the needs of urban centers surpassing the capacity of supporting rural villages (Palumbo 2008).